AN APPRAISAL AND DEVELOPMENTS OF LASER HOLOGRAPHY FOR INTERFEROMETRIC ENGINEERING MEASUREMENT

by

DAVID DENBY

A Doctoral Thesis

Submitted in partial fulfilment of the requirements for the award of

Doctor of Philosophy
of the
Loughborough University of Technology

November 1973

Supervisor: Professor J. N. BUTTERS, Ph.D, C.Eng, F.Inst.P, M.I.Mech.E.
Department of Mechanical Engineering.

Frontispiece

Opposite is a time averaged focused image hologram recorded on film, showing, by reconstruction, the resonant vibration mode at 1647 Hz of a small turbine blade. This may be viewed by arranging a white light beam (e.g. sunlight or a table lamp as source) to illuminate the hologram from the right. View the hologram squarely from about reading distance (8 to 10 inches), in the manner indicated by the sketch.

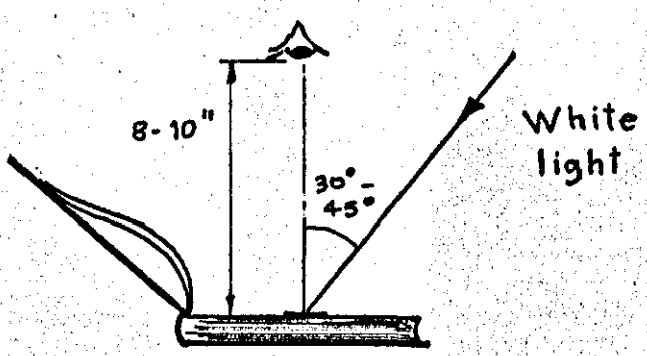

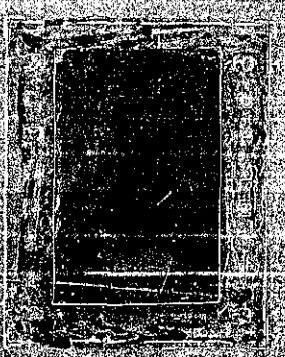

SYNOPSIS

Holography is a two-stage method of imagery in which both amplitude and phase information characterizing a wavefront are recorded, and subsequently reconstructed. Only with the advent of laser light sources in the early 1960's did the method become practical, motivating research into applications. One of these, holographic interferometry, was based on the fact that a reconstructed wavefront from a hologram could be used as a reference for interferometric comparison. This enabled interferometry to be extended to objects having scattering surfaces of any shape, and the potential of the method in engineering measurement was considered to be high.

A literature survey carried out at the start of this project (1967 to 1968), and reported in Chapter 2, revealed that many potential applications in the fields of stress analysis, vibration analysis, fault detection in materials and structures, and dimensional inspection, had been proposed but were not quickly materializing. This was seen to be partly due to practical difficulties necessitating laboratory procedures, and partly due to difficulties in analysing interferograms to obtain specific measurements. Accordingly, the aims of this project were:-

(i) to develop apparatus and methods that would simplify and improve the practice of holographic interferometry and the interpretation of results;

(ii) to investigate fringe interpretation, and to assess the accuracy and general feasibility, in relation to practical measurements of surface deformation.

Chapter 3 describes the design of basic apparatus and technique used in this work, taking account of holographic principles and the performance of the available continuous wave gas lasers and photographic recording materials. Practical techniques which improved the performance of real time holographic interferometry are reported.

The interpretation of holographic interferograms and the practical accuracy in making measurements form the subject of Chapter 4. It was established that in the relatively simple case, for which the direction of surface displacement is independently known, analysis is reasonably simple and quick, while in the general case the procedure for quantitative analysis becomes elaborate, laborious and subject to appreciable computational error. The qualitative interpretation of interferograms is also examined and shown to be an important means of analysis. Accuracy was considered in two parts: practical imperfections which were found by experiment to limit accuracy to $\pm$ ¼ fringe in real time work; and accountable error in measuring the geometry of the optical arrangement and in determining fringe order numbers.

Following this general treatment, the feasibility of applying holography in a specific engineering situation was examined: Chapter 5. As part of an experimental stress analysis programme, surface strain in a model of an engine casing was measured by holography and the results assessed against those obtained by conventional strain gauging. In this particular case, holography was found to be laborious

and inaccurate, and consequently strain gauging was considered to be more appropriate. However, holography was seen to be generally valuable as a non-contacting method providing over-all information.

By the method of focused image holography, sharp images with interferograms may be formed by white light reconstruction. It was thought that techniques using this principle would be beneficial in holographic interferometry, by simplifying the procedures of reconstruction and analysis. Chapter 6 sets out the principles relevant to holographic interferometry, justified by supporting experiments, and describes the design of a projector for viewing focused image holograms. This projector was constructed to aid research in this topic, and to realize fully the benefits of the method. Proposals are made for a standardized rig and procedure for using the method in envisaged applications, especially in non-destructive testing.

It is concluded that measurements of surface displacement can in principle be made by holographic interferometry, though in the general case the procedure is laborious and results are subject to appreciable error. Consequently holography is generally more suited to measurements requiring only qualitative analysis, as in non-destructive testing applications. Despite simplifications of procedure and improved technique, holography remains a laboratory method at the recording stage. Industrial applications are unlikely to become common until significant practical developments occur, especially in pulsed lasers and means of recording. Effort should also be directed into instrumentation that will scan interferograms and compute the data according to

prepared programmes. There are however already developments taking place based on speckle pattern interferometry which is much more practical due to electronic detection, processing and display. Also an electrically controlled plastic recording material has recently reached a prototype form having acceptable characteristics for holography, with the great advantages over photographic emulsions of 'instant' processing and repeated use.

Acknowledgements

I wish to acknowledge the considerable help received in undertaking this work, from :-

Professor Butters, for his encouragement and guidance as supervisor of the project ;

Mr. Leendertz, Mr. Wall, Mr. Cassells, and Mr. Hockley for many stimulating technical discussions ;

Technician staff in this Department, in particular ;
Mr. Norton, who manufactured much of the apparatus,
Mr. Topley, who undertook much of the photographic work,
Mr. Petty, who constructed the projector for viewing focused image holograms ;

Staff of the University library, for assistance in obtaining literature ;

Ruston and Hornsby Ltd., who enabled a collaborative study of an industrial problem to be undertaken.

Contents

Notation of frequently used Symbols

Abbreviations and Units

Symbols

a	Amplitude of a (light) wave; amplitude of vibration
d	Displacement
$f/$	"f" number (in optical imaging)
n	Fringe order number
v	Image distance
x, y, z	Cartesian co-ordinate directions
D	Diameter; lens aperture
I	Intensity (of light)
M	Lateral magnification
V	Visibility (of fringes)
α, β	Angles relating the directions of surface displacement, viewing and illumination.
δ	Phase or phase change
λ	Wavelength
μ	Refractive index
ϵ	Direct strain
ϕ	Shear strain

Abbreviations

HI	Holographic interferometry
FI	Focused image (holography or hologram)
ESPI	Electronic speckle pattern interferometry
CCTV	Closed circuit television

Note on Units used :

It was natural at the time to use British units for this work, since most materials, components, and apparatus manufactured in the Department, were made to Imperial dimensions. Accordingly the actual (British) units have been stated in this thesis, but to comply with University regulations concerning thesis presentation, quantities have also been expressed in corresponding SI units.

Chapter 1

BACKGROUND TO INTERFEROMETRIC MEASUREMENT.

Measurement has several definitions being a term used in many contexts. Fundamentally it is the act of establishing the extent or quantity of some thing by comparison with a predefined standard. This often implies a numerical result. Much less specifically it can be merely a judgement of extent or degree. In the case of optical interferometry, measurements are made of length and separation, surface displacement, surface shape and finish. Such measurements are usually precise numerical quantities. However, the nature of an interferogram is such that useful information is also conveyed without necessarily assigning numerical values. For example the irregularity of the fringes observed in examining a polished surface may reveal scratches and their directions. This may be the only information required, but is within the field of measurement. In this thesis the term "interferometric engineering measurements" includes measurements that are either quantitative or qualitative.

Optical interferometry is well established in the optics laboratory as a means of measuring length and surface movement and shape with high accuracy. It's beginnings can be traced to 1801 when Young was the first person to demonstrate optical interference thereby providing strong evidence for the wave theory of light. Within thirty years it was suggested by Babinet that the wavelength of light be used as a unit of length. In 1892 Michelson measured the metre in terms of the cadmium red line wavelength.

Following his work the metre was defined in terms of this wavelength. The present day ultimate standard of length is the orange line wavelength of radiation emitted by Krypton -86, following international agreement in 1960 that the metre be defined in terms of this wavelength. The accuracy of reproducing this wavelength is a few parts in 10^9, which exceeds the accuracy required of practical measurements. For example, even in the absolute measurement of slip gauges accuracy is limited to one part in 10^6, as a result of spurious inputs, principally due to temperature variation.

The principle of interferometry

Interference is a phenomenon in which radiation from a source travels by separate paths to recombine at a detector. This separation may be in space or in time. As the point of detection moves, the resultant intensity fluctuates about the sum of the separate intensities in each path. Visually the effect is a pattern of alternate bright and dark bands called interference fringes. The phenomenon is explained by considering light as a wave motion. The wave motion concept was demonstrated convincingly by Young in 1801, and later corroborated by Fresnel. Subsequently Maxwell formulated the electromagnetic theory of light, now universally accepted, proposing that light is propogated by transverse vibrations of electric and magnetic fields. Two light waves will interfere with maximum effect when the electric field vibrations of both are in the same direction. No interference occurs when they are mutually perpendicular.

For the understanding of optical interference the nature of the electromagnetic vibrations need not be pursued.

It is sufficient to regard light as a wave motion of the form:

$$a \sin 2\pi/\lambda \,.\, (ct - x)$$

in which a is the amplitude, λ is the wavelength, c is the velocity, t is time and x is the single direction of propogation. (This simple form assumes a plane wavefront.) The intensity, being the quantity detected by eye and other photo-detectors, is proportional to the square of the amplitude. By the principle of superposition, the resultant disturbance at a point is the (vector) sum of the disturbances due to each wave separately. For two light waves of the same amplitude and wavelength, propogating along the same line, the resultant intensity I at a point on the line is

$$I \propto 4a^2 . \cos^2(\delta/2) \qquad \ldots . (1.1)$$

in which δ is the phase difference between the two waves (JENKINS and WHITE, 1957). For this ideal case of equal amplitudes the fringes have a $(\cos)^2$ fluctuation of intensity. Their visibility is then a maximum, using the usual definition:

$$\text{visibility} \quad V = \frac{I_{max} - I_{min}}{I_{max} + I_{min}}$$

where I_{max} and I_{min} are respectively the intensities at the maximum and minimum of the fringe pattern. Thus relative phase between the two light waves can be identified with the detected intensity; this is the basis of interferometry.

In any interferometer the fringes are due to a difference in optical path length of the two (or more) beams. As seen from equation (1.1), the fringe intensity varies by one cycle per wavelength change in the optical path length difference. Thus in order to interpret an interferogram the geometry of the optical paths must first be established.

In order to produce a stable interferogram the recombining

beams must maintain a constant phase relationship. This implies that the wavelength spectrum in the light source must be limited in width so that after travelling different optical path lengths the recombining beams are still in phase. The difference in path length which causes the fringe visibility to drop from unity to a prescribed value which is barely tolerable is commonly termed the coherence length of the light source. In the case of an interferometer in which light from different regions of the source wavefront interferes, spatial coherence is also required.

Light Sources

In choosing a light source for interferometry a principal governing factor is the differential optical path length within the interferometer. White light sources permit path differences of only a few wavelengths, though this is used to advantage for accurate path length matching and the examination of thin films. Discharge lamps with spectral line outputs produce interference with path differences ranging from a few millimetres to a few centimetres. These path differences can be increased to nearly half a metre with low pressure isotope discharge lamps. A general characteristic of hot filament and discharge lamps is a broadening of the spectral line width as the temperature and pressure increase, for greater radiance output. Thus, conversely, long coherence length is gained at the expense of intensity. Furthermore the intensity available for interference is severely reduced in order to obtain spatial coherence from such sources, by means of pinhole filtering. Traditionally light sources for interferometry have been of limited coherence and intensity, with the possibility of

gaining one characteristic only at the expense of the other. Consequently applications of interferometry were limited generally to surfaces of small area, involving small path differences, and working in darkened laboratories.

This situation changed remarkably in the mid 1960's when continuously emitting gas laser sources became available. These can provide a well-defined beam of light whose entire output is spatially coherent. Although the radiant flux of conventional discharge lamps for interferometry is typically greater than laser outputs, the intensity of the light available for interference is greater from the laser by a few orders of magnitude. The coherence length of laser light varies, according to the design of the laser oscillator, from several centimetres to a few kilometres. Thus the laser equals or betters, in combination, the properties of intensity and both temporal and spatial coherence of the best conventional sources. Furthermore a laser beam is more manageable. The effect of lasers on interferometry has been to simplify methods and to bring about new applications, through vastly improved coherence and intensity. In particular, greater coherence length has extended the range over which path differences can be continuously varied. Higher intensity has made possible fringe counting at megacycle rates in daylight conditions.

Applications: merits and limitations.

Since the wavelength of light is now the standard unit of length it is logical that it should be used for certain measurements of length requiring the ultimate accuracy. Thus in Standards Laboratories interferometry is used for

the absolute measurement of end standards, with an accuracy of a few parts in 10^8 (HUME, 1970), and for the measurement of Calibration and Reference Grade slip gauges. Interferometry has similarly been used in special purpose measurements involving length, such as the determination of the acceleration due to gravity, and the density of mercury, both to one part in 10^6 (BARRELL, 1959). A valuable feature of interferometric measurements is the reproducibility of the standard wavelength in any Standards Laboratory: it is non-destructible. However these highly accurate measurements of length are mainly confined to the Standards Laboratory because the atmosphere must be controlled, and precise apparatus and elaborate procedures are necessary. Thus for general dimensional measurement of high accuracy, comparators are commonly used, being more convenient. They incorporate transducer elements of high sensitivity such that variations of a few microinches (about 100 nm) can be detected.

More widespread applications of interferometry have traditionally been in the field of surface evaluation. In these cases the highest order of accuracy is not generally required, and the path difference within the interferometer is relatively small. Consequently control of the atmosphere is often unnecessary and sources of less precise wavelength are acceptable, such as a sodium discharge lamp. Typical applications are the measurement of flatness, curvature and parallelism of the surfaces of optical components, and other surfaces which are optically smooth. Variations in dimension of less than a wavelength (which is nominally 500 nm) are easily measured, with virtually no contact. The most common of alternative surface measuring instruments are those employing a surface-following stylus coupled to an electrical

transducer. While such instruments can be equally sensitive as interferometers, they contact the surface, sometimes even damage it, and make point by point measurements, covering only a small fraction of the surface. In comparison interferometry can map out the entire surface instantaneously, indicating positions where measurements should be made from the fringe pattern.

Interferometry has always been potentially applicable to high accuracy displacement measurement, though its use has traditionally been limited due to poor light sources and stability requirements. However, since the introduction of gas laser sources, having far superior coherence and intensity, such applications have been remarkably extended. For example laser interferometers are being developed to measure and control the displacement of machine tool carriages. In this they offer resolution and accuracy equal to or better than that of moire gratings, which are well established as a means of accurate control of linear (and angular) displacements. For displacement measurements over small ranges, from zero to a few millimetres, requiring a resolution of less than a wavelength, displacement transducers are commonly used. These can be capacitive, inductive and piezoelectric types, and their main merits are convenience and high sensitivity. However, being transducers they have inherent non-linearities, and can exhibit a significant instrument-insertion effect, i.e. taking energy from the quantity being measured. These particular instrument defects do not exist (at a practical level) in interferometers. For this class of measurement classical interferometers were inconvenient because the output was not easily read; this was mainly a consequence of low light levels.

However, lasers have stimulated automatic fringe counting, thereby developing this class of interferometer into a readable instrument with a very fast response.

For a long time interferometry was used relatively little in engineering measurement, for several reasons:-

(i) The required stability could not be maintained in an engineering environment, such as that created by running machinery.

(ii) Interferometers required components of high accuracy in terms of surface finish and dimensions. This in turn implied precision adjustment and stability to be provided by the interferometer.

(iii) An optically smooth reference surface was needed in order to perform a measurement on the surface under examination. This limited such surfaces to regular shapes such as flats, cylinders and spheres, and to materials that could be optically worked.

(iv) Practical procedures were generally elaborate. The fringe information was not readily processed, and in some situations the analysis was laborious, with calculated corrections to be made for the atmospheric conditions.

(v) Sensitivity was so high, inherently, as to be unsuitable for common engineering tolerances.

As explained above lasers had considerable impact for engineering interferometry, by reducing the limitations of stability requirements and of elaborate practical procedures, and by extending the path difference range of interferometers. However, lasers have additionally made possible a radically new method: holographic interferomtry. A description of one

particular form of this method was first published by HORMAN (1965); other forms of the method were apparently discovered independently by several other researchers (POWELL and STETSON, 1965; BURCH, 1965; REID and WALL, 1965; BROOKS, HEFLINGER, and WUERKER, 1965). This method overcomes two main obstacles in the path of classical interferometry, namely the need for a reference surface, and the need for highly accurate optical components.

Thus holography was seen to offer an extension to the range of applications of interferometry by removing some of the former limitations, while retaining the merits. An initial examination of the use of holographic interferometry in engineering measurement was the starting point of the work of this thesis.

Chapter 2

THE ROLE OF HOLOGRAPHIC INTERFEROMETRY IN ENGINEERING

Firstly, major early developments and relevant principles of holography are established for subsequent assumption. The main section of this chapter presents an appraisal of published work up to 1968 on H I (holographic interferometry). From this, conclusions are drawn forming the basis of the ensuing programme of this project, commencing in 1968.

2.1 THE EARLY DEVELOPMENT, AND PRINCIPLES OF HOLOGRAPHY.

Holography quietly entered the scientific world in 1948, with the first recognised publication on the subject by GABOR (1948). That short paper described the basic principle, though his original proposal for electron microscopy has not been realised. Although an accepted definition of holography still does not exist, it is regarded (optically) as a two-step method of imagery in which both amplitude and phase characteristics of a wavefront are recorded for subsequent reconstruction. The principle applies to any propagating energy field characterized by a wave equation.

The principle of holography can be considered in terms of interference and diffraction. In the recording stage of an (optical) hologram, monochromatic light illuminates an object to be recorded. The wavefront emitted by the object, whether by transmission, specular reflection or scattering, interferes with a coherent reference beam, producing a

stationary interference pattern. Thus, the point to point amplitude and phase of the object wavefront are coded with respect to that of the reference beam as variations of intensity. By recording this spatial distribution of intensity as corresponding variations of a physical quantity, the object wavefront is effectively recorded. Usually the recording is achieved photographically, and when processed the emulsion becomes the hologram. For the second stage, reconstruction, the hologram acts as a diffracting medium. When illuminated at the appropriate inclination by either of the two original wavefronts which produced it, it diffracts light into the direction of the other. If this illuminating beam is identical to that used for the recording, the diffracted wavefront is an exact duplicate of its original wavefront, in the hologram plane. Usually the reference beam has a simple wavefront, easily duplicated, to enable a relatively complex object wavefront to be faithfully reconstructed. Thus, the light propagating as the reconstructed wavefront effectively emanates from a virtual image (the "primary image") of the original object, and ideally the two are indistinguishable by optical tests, (ignoring a uniform phase difference).

The crucial feature of holographic recording lies in preserving the phase information in a wavefront. The idea can be seen as a logical step, applied by Gabor, from Bragg's method of forming an image of a crystal lattice. This was by diffraction from an initial diffraction pattern produced by the lattice. However, Bragg was limited to forming images of simple (lattice) structures for which phases in the diffracted field could be predicted because the integrating

property of the conventional photographic recording procedure lost the phase information.

The holographic principle of preserving the phase information in the form of an interference pattern has important implications. In the recording stage, the light in both the reference and object beams must be mutually coherent at the recording plane in order to produce interference. For this interference pattern to be recorded, it must normally remain stationary for the duration of the recording period, demanding continued coherence from the light source, and stability of the optical paths to a tolerance of the order of a quarter-wavelength. Whatever the recording medium it must be capable of resolving the interference pattern, whose maxima and minima of intensity may be spaced by the order of a wavelength. Since the reconstruction stage operates by diffraction, the strict coherence requirements for recording no longer apply for the reconstructing reference beam. However, any departure from its original wavelength and geometry causes degradation of the reconstructed wavefront.

Although Gabor had presented the basic theory and demonstrated the recording and reconstructing processes, his was a limited form of holography, in the early years. His holograms were incomplete recordings because the incident phase at the object was largely lost. In fact the original recording arrangement was suitable only for objects having small opaque areas such as lettering set in a transparent medium. Reconstruction was imperfect due to background noise, caused by conjugate diffracted waves

forming an in-line out of focus "twin" image. Furthermore the photographic processing was critical in order to obtain an image of the correct contrast. During the fifties no major practical developments in holography occurred, though theory and concepts progressed. In particular ROGERS (1950, 1952) likened the hologram to the classical zone plate, introducing the concept of a focal length property of holograms. His zone plate concept also explained the higher orders of diffraction in reconstruction, beyond the first order, which result from nonlinear recording of the hologram.

The first significant practical development was made by LEITH and UPATNIEKS (1962), who pioneered off-axis reference beam holography. This automatically separated the troublesome "conjugate" image from the primary image. Also the photographic processing at once became less critical because nonlinearities in the recording now caused noise in reconstruction at higher orders of diffraction, rather than in-line with the primary image. Furthermore the off-axis reference beam provided the means to record all the phase information in the object wavefront, and this led to the recording of objects having continuous tone (LEITH and UPATNIEKS, 1963). At the same time Leith and Upatnieks introduced lasers for recording holograms demonstrating the enormous advantages in terms of greater intensity and coherence over conventional light sources used hitherto. The improved coherence permitted the illumination of the object (transparency) to be diffuse. Subsequently holograms of three-dimensional objects were recorded by scattered reflection from the object (LEITH and UPATNIEKS, 1964). A benefit of scattered light was the elimination of degradations previously caused by dust and

scratches on optical surfaces in the recording apparatus. Another important property they demonstrated was the recording of several objects on the same emulsion by sequential exposures, the holograms of all objects overlapping one another. These developments greatly simplified the practice of holography and opened up potential applications, energetically pursued in the following years.

Holographic interferometry relies on the property of a hologram to reconstruct a wavefront faithfully duplicating the original recorded one, when certain conditions are fulfilled. Ideally the recorded and reconstructed wavefronts are identical, apart from a uniform phase difference, when compared interferometrically. As a corollary, if the object is distorted so as to cause variations of phase in one of these wavefronts, when compared with the other wavefront an interferogram is produced representing the distortion of the object. It is appropriate to list here other basic properties of holograms, to be assumed in following chapters :-

i) In the common case of recording scattered object light, all regions of the hologram effectively record the entire object. Thus in reconstruction different views of the image may be obtained by using different regions of the hologram. Also image quality remains virtually unaffected should the emulsion become scratched.

ii) Brightness variations across the object are faithfully rendered in the image by reconstruction over an enormous range. Intensity ratios of up to 10^6 have been observed in an image (LEITH and UPATNIEKS, 1964).

iii) The reversibility of light applies, such that if the reference beam wavefront for reconstruction is precisely reversed, a real image is formed in the position of the original object.

iv) Reconstruction is possible using a reference beam of different wavelength or different curvature of wavefront from that which recorded the hologram. However the reconstructed wavefront will no longer duplicate its original form, causing a distorted image of the original object. Ray directions for the reconstructed wavefront may be determined by treating the hologram as a two-dimensional diffraction grating.

v) Several wavefronts (of the same or different objects) may be recorded by one emulsion, each using the entire area. They may be reconstructed simultaneously or separately depending on the reference beam configuration for each.

2.2 APPRAISAL OF HOLOGRAPHIC INTERFEROMETRY TO 1968.

The generally recognised first publication on H I was by HORMAN (1965), who explained how a reconstructed wavefront of a transmission scene could be used in various optical tests including interferometry. He established that a record of some particular initial state of the test scene could be preserved and used at any later time for interferometric comparison. An extension of this principle to the case of diffusely reflecting surfaces was reported soon afterwards by several researchers. In particular BURCH (1965) emphasized the value of obtaining interference in this way directly from a rough surface, to obtain fringes representing

the change in shape of an object due to some load. COLLIER et al (1965) demonstrated the two basic methods of producing holographic interferograms, namely real time and double exposure, and derived expressions for the intensity variation of the interferogram for the two cases. H I was not limited to comparing two static shapes of an object surface. POWELL and STETSON (1965) demonstrated time-average holograms of the steady state vibration of objects, and presented their analysis for interpreting the interferogram. In another paper (STETSON and POWELL, 1965) they demonstrated real time examination of object vibration, and discussed the respective merits of live-fringe and frozen-fringe holography. HEFLINGER et al (1966) demonstrated that by using a pulsed laser two momentary states from a continuously and rapidly changing sequence could be recorded and compared by HI.

Methods

Following these early publications which established basic concepts in HI there followed numerous others, proposing methods, application, and theories on the interpretation of interferograms. There were two basic methods :- live-fringe (in real time), and frozen-fringe holography, and from these stemmed all the variations. Undoubtedly the main merit of live-fringe work has been its versatility to adjust the reference state of the object (ARCHBOLD et al, 1967), to examine changes in the object as they happen, and the capability of obtaining many interferograms from a single hologram. Extra information has been obtained by this method. For example the sign of the fringes could be deduced by suitably prodding the object during real time observation (ENNOS, 1968), and the stability of the apparatus and

photographic emulsion could be assessed (STETSON and POWELL, 1965). However, certain difficulties were encountered, notably concerning the relocation of the hologram in the interferometer after its processing, and the visibility of the live fringes. These problems have been reduced by improved experimental technique. Satisfactory component relocation has been achieved by kinematic mounts (ARCHBOLD et al,1967), and fringe visibility made acceptable by beam attenuation using filters (STETSON and POWELL, 1965; ALEKSANDROV and BONCH-BRUEVICH, 1967). In these respects frozen-fringe holography has been advantageous, by eliminating the problems of:- hologram relocation, poor fringe visibility due to unequal beam intensity, and long-term stability. Moreover, a permanent record of an interferogram was obtained without dependence on the other parts of the original interferometer.

Vibration analysis as originally proposed (POWELL and STETSON, 1965), was a frozen-fringe method (time-averaged). Subsequently it has been demonstrated in real time (STETSON and POWELL, 1965) and has gained versatility by stroboscopic illumination (ARCHBOLD and ENNOS,1968; WATRASIEWICZ et al, 1968). Frozen-fringe holography was usually a double exposure procedure but there have been extensions. Multiple exposure methods with equal increments of load, or displacement, to the object have had the effect of fringe sharpening and suppression, thereby detecting non-linearities in deformation (BURCH et al, 1966).

So far considered have been those methods in which fringes were produced by change in position of an object surface.

STETSON and POWELL (1966) established that two other distinct causes of fringe formation existed, which have lent themselves to other interference methods using holography. One was a change of refractive index in the medium transmitting the light. Under controlled conditions this has been applied to form fringes representing constant depth contours of an object(TSURUTA et al, 1967). The other cause was a change in wavelength in the source of the interferometer, or the simultaneous presence of two different wavelengths. This also has been applied, for generating constant range contours over an object (HILDEBRAND and HAINES, 1967).

Fringe Interpretation

As in all interferometers, holographic interferograms are due to phase differences in two (or more) interfering beams. In the case of surface displacement the following assumption is made. For any surface point of interest, the effective optical paths are from the source of illumination via the two (or more) positions of that point to the point of detection. This was incorporated in the earliest of POWELL and STETSON'S analyses (1965) for the form of time-average vibration fringes, and subsequently for the additional cases of double exposure and real time vibration HI (STETSON and POWELL,1966). They related the displacement of an object point to its intensity in the resulting interferogram in terms of the angular relationships of the directions of displacement, illumination and observation. Thus by identifying the fringe order number from an interferogram, the magnitude of displacement could be calculated. However, difficulties could arise in determining the fringe order number especially when the zero order fringe (i.e. for no optical path change) could not be identified.

In any case there remained ambiguity about the sign of the fringes, and whether the fringe adjacent to that numbered n was $n+1$ or $n-1$. In order to resolve uncertainties of this kind ENNOS (1968) proposed live-fringe experiments in order to deduce fringe senses by controlled additional displacement of the object.

In the most general case, in which the direction of object displacement is unknown, the approach discussed above is inadequate, because the relevant geometry cannot be established. According to the analysis of HAINES and HILDEBRAND (1966A), such displacements could be determined from measurements of the position of localization of the fringes and their spacing. An apparent advantage was that fringe order numbers did not need to be determined. However the analysis was restricted to rigid body translations or rotations of the object, or combinations of both. In a subsequent paper (HAINES and HILDEBRAND, 1966B) the analysis was extended to cases in which one part of the surface undergoes a displacement and rotation independent of other parts. In contrast, ALEKSANDROV and BONCH-BRUEVICH (1967) proposed a quite different approach, based on determining the change in fringe order number as the direction of observation was altered. Although they recognized the dependence of the localization of the fringes on the nature of the surface displacement and its illumination, this information was not used. For a case of engineering interest, that of determining in-plane surface strain (in one particular direction), ENNOS (1968) demonstrated that the general problem could be simplified by reducing it to two dimensions. Again the analysis depended on determining fringe order numbers; in this case two separate interferograms had to be

(numerically) subtracted in order to calculate the required component of displacement, and hence strains.

Thus there were different proposed approaches to the interpretation of interferograms, but in fact little indication of their feasibility in practical situations. Little experimental support for the theories was reported, particularly with regard to the accuracy of measurements. No conclusions about accuracy could be drawn from HAINES and HILDEBRAND'S paper (1966A), because their experimental error was large, often as high as ±60%. ALEKSANDROV and BONCH-BRUEVICH (1967) gave no numerical results to support their analysis. Another aspect of accuracy that had received inadequate attention was the effect on measurements of practical imperfections, such as emulsion instability, change in air temperature, and a change of laser output frequency, although there was awareness of such problems (STETSON and POWELL, 1965, 1966; CARCEL et al, 1966).

Applications

In these early years when various possible applications were explored, there were numerous publications demonstrating the potential of HI. Many of these illustrated the extension of interferometry to optically rough surfaces of three-dimensional form. There were proposals to measure small displacements and deformations of engineering components and structures due to the action of load, heat, creep or fatigue, with the usual merits associated with interferometry:- high sensitivity, non-contact, and full-field information. In some circumstances holography was found to be a unique method of obtaining such information. As an example, WOLFE and DOHERTY (1966) used

holography as an experimental method of investigating the distortion of electric cooling modules, requiring high sensitivity and non-contact, over the entire area. Besides making some specific measurements from the interferograms obtained, the irregularities of the fringes readily revealed unsymmetrical distortion of the assembly, and independent deformation of the elements.

In the case of vibration holography, pioneered by POWELL and STETSON (1965), holographic interferometry was soon recognised to have tremendous potential in the analysis of engineering components vibrating at resonant frequencies. At that time the method was unique, in providing the nodal position, the mode of vibration, and amplitude of vibration for a component of any shape - all from a single interferogram. (Strictly, of course, the calculation of amplitudes assumes the direction of vibration to be known. For thin plate-shaped objects this is usually perpendicular to the surface.) The high sensitivity of interferometry enabled holography to detect small amplitudes, when other methods would fail. Subsequent developments were real time / time-average examination, and stroboscopic illumination allowing the phase of the vibration across the object to be studied.

Not surprisingly the early demonstrations using holography to measure surface displacements were mainly cases for which the fringe interpretation was relatively simple. These tended to be situations in which the direction of displacement could be assumed from the nature of the object and its loading, for example diaphragms and other thin discs and plates loaded normally. However measurements of displacement normal to a surface are not always meaningful. In engineering stress and strain analysis the in-plane surface strain is significant.

A holographic method for separating the in-plane displacement component from the complex surface distortion, and thence of deriving the in-plane strain, was devised by ENNOS (1968). By effectively reducing the problem to two dimensions, the fringe interpretation became simpler than the general analyses of HAINES and HILDEBRAND (1966) and ALEKSANDROV and BONCH-BRUEVICH (1967). This method for determining in-plane strain served to illustrate some advantages of HI over other conventional methods of experimental stress analysis. It was more sensitive than moire methods; there was no contact with the surface in contrast to strain gauges, other extensometers, and coatings; full-field information was provided in contrast to point measurements made by strain gauges and transducer probes; and whereas models were essential for photoelasticity, holography could deal directly with engineering surfaces and components.

Difficulties of quantitative fringe analysis were often entirely avoided in such applications as detecting and locating weak spots in an engineering component(BURCH et al, 1966), and detecting separations in aircraft honeycomb-sandwich structures and motor tyres (GRANT, 1968). In such cases the extra deformation at a 'fault' relative to surrounding parts of the object was sufficient to cause an irregularity in the fringe pattern that could be identified by an observer with only little experience. Again the high sensitivity of interferometry was indispensable to enable 'faults' inside the material to be detected by deformation at the surface. Also of course information over the full field of view was essential. This sort of 'fault' finding, and vibration analysis, represented the first industrial applications of HI, in the field of non-destructive testing.

These applications discussed so far have involved the interferometric comparison of two different shapes, or positions, of the same surface. As distinct from this, efforts were made to compare interferometrically two different surfaces of nominally the same shape, with the aim of inspecting component shape against that of a master, recorded holographically. ARCHBOLD et al, (1967) demonstrated this was possible for the special case of a cylinder bore, but only by using extremely oblique illumination in order to eliminate the random surface roughness differences from one cylinder to another. Thus there was little prospect for comparing general engineering components, that would inevitably have unique surface structure due to machining. In this respect the optical interferometer was too sensitive. This problem did not apply in the case of comparing optical surfaces, as proposed by HILDEBRAND et al (1967). As demonstrated, large aperture optics could be inspected for shape in their working environment, revealing for example sag for various positions. Although the surfaces were optically finished, holography still had an important advantage over classical interferometry, in that the arrangement was a common path interferometer.

An alternative method using HI of inspecting the shape of engineering components was proposed by TSURUTA et al (1967). By immersing the component in a contained gas or liquid and changing the refractive index, interference fringes were obtained representing distance contours from the container window to the component surface. Component shape could then be inspected by comparing respective contour patterns. Because the change in refractive index could be adjusted, there was some control over the contour interval. Thus the method had

controlled sensitivity, over a range better suited to engineering tolerances than that of direct interferometry used by ARCHBOLD et al (1967). However the procedure was inconvenient, and the reliability of obtaining an accurate refractive index change was uncertain. Working at this reduced sensitivity, the method could face competition from moire fringe and photogrammetry methods.

There were other applications of holography which also used interference effects, but based on different principles or requiring special equipment. Firstly, was another method for inspecting the shape of scattering surfaces by the generation of contour type fringes, (HILDEBRAND and HAINES, 1967). A laser source producing two discrete wavelengths λ_1 and λ_2 was used, causing constant range fringes at path length differences of $\lambda_1\lambda_2/|\lambda_1-\lambda_2|$. Again the contour interval could be varied to some degree, by choice of wavelengths, and typically represented a considerable reduction in sensitivity compared with direct interferometry. Unfortunately the two wavelengths introduced a problem of image matching, so that accurate positioning of reference sources was necessary. Consequently the angular extent of the object that could be contoured was limited. Secondly, HI could be applied to photoelasticity (FOURNEY, 1968) with the advantage that isopachic fringes could be obtained without special models or interferometers, Thirdly, HEFLINGER et al (1966) demonstrated the potential of pulsed laser HI for examining the difference between two states of a rapidly changing event. It was well-known that stability of the entire apparatus severely limited the use of holography, and thus pulsed lasers had the potential for greatly extending holography. However considerable development was required as pulsed ruby lasers

had a coherence performance much inferior to that of gas lasers. Consequently Heflinger et al were restricted to objects having the form of a transmission path through a fluid.

Conclusions.

The particular advantage of holographic interferometry was seen to be the extension of classical interferometry, with all its inherent merits, to optically rough surfaces of any shape. This was possible because holography provided the means for a common-path interferometer, with effective beam separation in time. This removed some of the major limitations associated with traditional interferometry;- highly accurate optics and a reference surface for comparison were no longer necessary. Moreover there was no accurate alignment procedure, because interference effects were achieved by a difference along the common optical path as set up. Thus the potential for engineering measurement was high, and this prompted the many proposals which appeared in the literature. Yet after two to three years' research and development, few industrial applications of HI were materialising. In fact this was partly to be expected since a high proportion of the proposals were seen to be hypothetical demonstrations rather than practical examples.

In order to conclude why this should have been so, the limitations of HI must be examined. Firstly, holography was a laboratory procedure, both at the recording and reconstruction stages. In particular, stability traditionally associated with interferometry was required at the recording stage. Live-fringe work, virtually indispensable in some instances, required special technique in overcoming difficulties of long-term instability, component relocation and poor fringe

visibility. There were two notable exceptions to the laboratory restriction. The non-destructive testing apparatus, using gas lasers, developed by GC Optronics Inc. was claimed to work in a factory, but at the expense of a servo-controlled pneumatic cushioning device to isolate the work surface from the factory environment. The other exception was the use of a pulsed ruby laser, as demonstrated by Heflinger et al, though the coherence performance was poor. Overall, developments were most needed in lasers and recording materials, for a dramatic reduction in recording and processing time.

Secondly the interpretation of holographic interferograms to obtain a specific measurement was seldom straightforward. Even in cases of simple geometry there could be ambiguity, and for general three-dimensional distortion the analysis appeared laborious, and had not been properly assessed. Thus those applications, in which a qualitative interpretation was adequate, such as vibration analysis and non-destructive testing, had better prospects.

Thirdly the sensitivity was too high for some proposed applications. In particular the comparison of components whose surfaces were produced by the common manufacturing processes, was virtually ruled out, because of random variations in surface structure. (Of course in applications such as detecting stress concentrations and material faults, high sensitivity was a merit.)

2.3 AIMS OF THE PROJECT

The early guidance of this project was influenced by interests in this Department in engineering components, in

particular the performance of instrument diaphragms, (BUTTERS, 1968). Accordingly the field of holographic interferometry that was entered was the measurement of surface deformations. Initially, modest equipment was available centred around an 8 mW He-Ne laser, so restricting experimental work to scattering surfaces of relatively small area. Following a literature survey the project proceeded with the following aims, based on the conclusions reached in the preceding section concerning laboratory procedure and difficulties of fringe interpretation;-

(i) An investigation of fringe interpretation, and assessments of the accuracy and general feasibility, in relation to practical engineering measurements.

(ii) The development of apparatus and methods that would simplify and improve the practice of HI and the interpretation of results.

The project was confined to holographic interferometry concerned with object displacement and deformation; those applications depending on a change in refractive index or a change in wavelength to produce contour type fringes were not pursued. This was because the interpretation of interferograms and associated topics were considered to be more important. Furthermore, suitable lasers for change of wavelength contouring were not then available in the Department.

Chapter 3

PRACTICAL CONSIDERATIONS AND DEVELOPMENTS.

This chapter describes apparatus and techniques for the experimental work of the project. The practical implications of holographic principles are considered, together with the performance of lasers and photographic emulsions, in the design of apparatus and recording arrangements. Early experimental developments aimed at improving real time HI technique are described.

3.1 CONSIDERATIONS FOR HOLOGRAPHIC PRACTICE

As described in Chapter 2 the principle of holographic recording is the recording of an interference pattern formed between a reference beam and wavefronts from the object ("signal beam"). For this to be achieved the main considerations which arise are the light source and its subsequent ray paths, the stability of the apparatus, and the recording material. Reconstruction is by the principle of diffraction, the hologram being a grating structure. This implies certain requirements of the light source and its illumination of the hologram, and the preservation of the original grating structure forming the hologram. The following discussion is restricted to holography with opaque diffusely reflecting objects, being the specific concern of this thesis.

Holographic recording

Amongst light sources only the laser can be considered for practical holography, offering combined coherence and intensity far superior to that of any other type of source. For the work of this project small He-Ne lasers producing between 5 and 20 mW output at 633 nm wavelength were used (specifications in Appendix 1). With regard to temporal coherence, the Doppler gain curve width of He-Ne lasers is about 1700 MHz (BEESLEY, 1969). Consequently, having cavity lengths ranging from 40 to 75 cm, these lasers operated with a few axial modes simultaneously, and the corresponding coherence length was about 25 cm for each. For holography the laser output needs to be not only spatially coherent, but also of uniphase transverse mode (the TEMoo mode), otherwise the object will be incompletely recorded and the brightness of reconstruction will vary from different parts of the hologram. Each of the He-Ne lasers used gave the TEMoo mode output when properly adjusted. The construction of these lasers included Brewster angle windows within the optical cavity, and therefore the output was (vertically) plane polarized. Consequently, when using an arrangement having ray paths in all three co-ordinate directions, with an object which did not depolarize light, care had to be taken that the polarization directions of the reference and signal beams were not mutually crossed at the recording plane.

From the point of view of a material for recording the interference pattern formed between the reference and signal beams, the main consideration is its spatial frequency content.

This is determined principally by the average angle between the directions of the signal beam and the reference beam at the recording plane (the "design angle"). In a simplified case, taking single directions for both the signal and reference beams, as shown in Fig. 3.1, the fringe spacing AB of the interference pattern in the recording plane is

$$AB = \lambda / (\sin\alpha + \sin\beta)$$

λ is the wavelength, and α, β are the respective angles of incidence.

o o

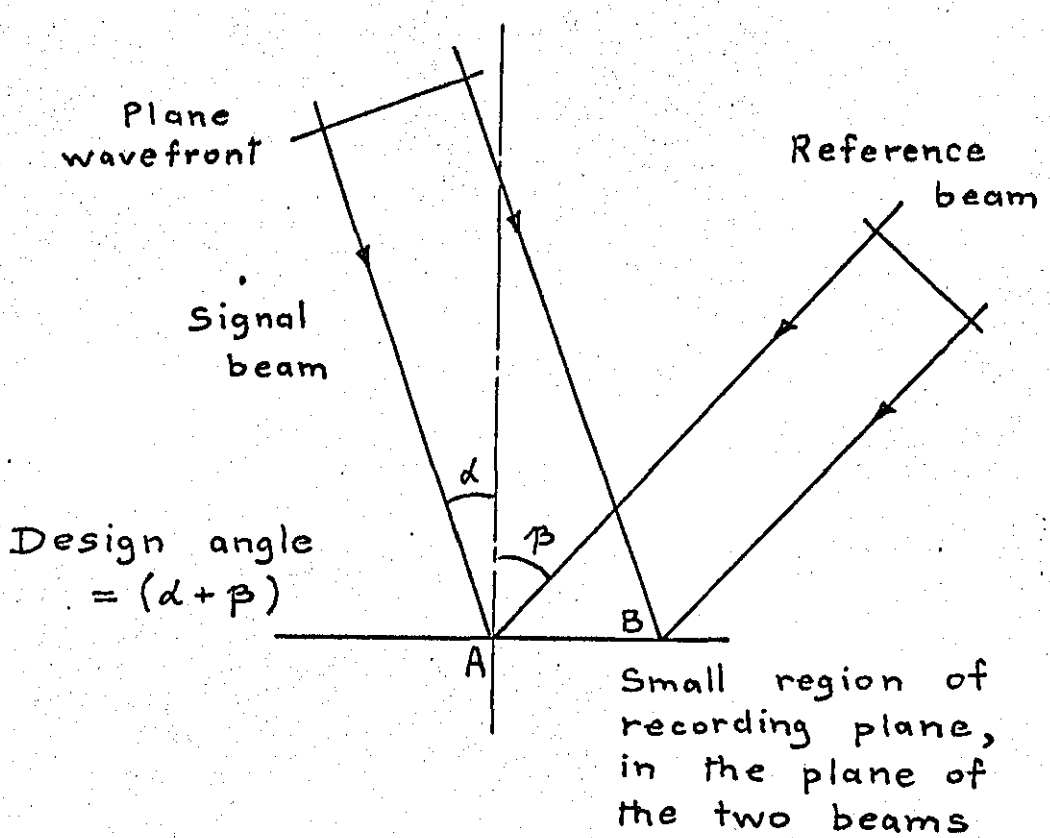

Fig. 3.1 Fringe spacing in the hologram recording plane.

In practice the object is extended and subtends a certain angle at the recording plane. The effect of this is to produce a range of spatial frequencies from zero to a maximum determined by the largest angle subtended from the object. This manifests itself as a speckle pattern at the recording plane. These additional spatial frequencies diffract light in the subsequent reconstruction, producing noise around the reference beam direction. The angular extent of this noise depends on the largest angle subtended from the object. Thus, in order that this noise does not overlap the image of the object, the design angle should be at least three times the semi-angle subtended from the object. For typical engineering components as objects, the design angle needs to be about 30°, giving a predominant fringe spacing in the recording plane of the order 1 μm. Special high resolution photographic emulsions were developed by the main photographic manufacturers for holographic recording. These were used for this project, being the only readily available and convenient-to-use material that was capable of resolving such high spatial frequencies. At first only the Kodak 649F emulsion was available, but by 1968 Agfa was producing emulsions, which were used in preference, being several times more sensitive, with about the same resolution (specifications in Appendix 1). Although holographic emulsions subsequently became available on a film base, plates were used for the majority of the project work because they are far more practical for real time HI, and more convenient for short-run experiments in double exposure HI.

Stability of the entire apparatus is vital, in order to maintain a stable interference pattern at the recording plane

during the photographic exposure. This problem is aggravated by the relative insensitivity of holographic emulsions: even for small scattering objects, exposure times were found to be commonly a few minutes using the Kodak 649F emulsion. Any phase change between the reference and signal beams will alter the intensity at a point in the interference pattern and consequently will reduce the contrast of the recorded pattern. This will result in a dim image by reconstruction. A randomly occuring relative phase change of $\pi/2$ is a considered criterion for failure to record a hologram. This imposes a severe restriction on the random vibratory motion of the photographic material, the object and other components which direct the light. In the worst case (reflection back along the incident path) the restriction is $\lambda/8$, for one component considered alone. Random movement of the apparatus can be caused by vibration transmitted either through the table or the air. The former source can be greatly reduced by use of a massive table of low resonant frequency, supported on a damping medium such as sand, rubber, or pneumatic tubes. Airborne vibration effects can be reduced by special enclosures around the apparatus, and by keeping the optical paths of the reference and signal beams short and close together. The work of this project was done in a building in which much small machinery was in use and occasionally some heavy machinery. Holography was carried out on cast iron tables of a little more than 1000 kg mass, resting on single layers of cross-ribbed rubber with wooden or concrete supports from the floor. In common with other workers (e.g. CARCEL et al, 1966) it was found that satisfactory holograms could be made during

normal working hours, without laboratory temperature control and without special enclosures. Only simple precautions were taken such as switching off laboratory fan heaters and motors. The stability of the table and mounts for mirrors and the beam splitter, could be readily checked by setting up a Michelson interferometer.

Another aspect of stability concerns the laser output. As the cavity warms up the output frequencies of the individual axial modes gradually drift. However, in the case of the He-Ne lasers used, several axial modes operate simultaneously and the frequency spread of this spectrum is virtually unchanged during warming up. Thus, working within the coherence length, holograms could be taken any time after switching on. However it was preferable to wait ½ hour to allow the output power and beam direction to reach a steady state.

For high contrast fringes in an interference pattern the two beam intensities should be roughly balanced. However the conversion from intensity variations in the interference pattern to intensity variations in the photographically processed hologram is then nonlinear. The effect of a 1:1 "beam ratio" (ratio of the intensities of the reference to the signal beams) is to produce noise in the reconstruction process, mainly as higher orders of diffraction above the first (image-forming) order. If this noise overlaps the image, the clarity of the image is degraded. To avoid this effect one beam should be more intense than the other, so reducing the contrast of the fringes and keeping within the reasonably linear part of the emulsion's amplitude transmission/exposure curve. Whereas the reference beam produces

a smooth intensity distribution at the recording plane, that due to the signal beam is modulated by the random, large intensity variations of the speckle pattern. Therefore it is the reference beam that is made more intense to set a bias level on the curve. Holograms can be recorded with widely varying beam ratios, though a ratio of about 4:1 is usual to produce a good compromise between brightness of reconstruction and freedom from noise in reconstruction.

Holographic reconstruction.

Ideally, the spatial structure of the interference pattern forming a hologram would be perfectly preserved during photographic processing, but in fact emulsions are not completely stable. The biggest change arising from processing is shrinkage, a reduction in thickness by 15% being typical. This alters the angle of the fringe "slats" through the thickness of the emulsion and consequently for maximum brightness of reconstruction, it may be necessary to alter the angle of incidence of the reconstructing reference beam (VILKOMERSON et al, 1967). This is undesirable because it causes distortion in the image. If the angle is kept at its original value, i.e. that value for recording the hologram, the image is then undistorted but dimmer in comparison. This effect of shrinkage can be minimised by arranging for the normal to the emulsion plane to bisect the design angle, so that the fringe slats are also normal to the plane. Of greater significance is stability of the emulsion in its own plane. On this depends the preservation of the fringe spacing AB (Fig. 3.1), which governs the angle of diffraction in the reconstruction stage. A discussion of experimental investigations into this aspect

of emulsion stability follows, in section 3.3.

Assuming perfect emulsion stability, precise reconstruction of the signal wavefront is achieved only by precise duplication of the illumination of the hologram by the reference beam. This is required for real time HI. However clear images by reconstruction can be produced by varying both the wavelength and the wavefront shape of the reconstructing reference beam. In these cases distortion to the image, some loss of resolution, and a change in its position occur. Nevertheless these effects may be acceptable in the case of double exposure HI, for the advantage of relaxing the conditions for illuminating the hologram. If the interferogram is to be analysed in such cases, the scale of the degrading effects, especially distortion, needs to be predicted. By regarding the hologram as a two-dimensional diffraction grating and applying Bragg's Law, individual ray directions in reconstruction can be calculated. Thus changes in wavelength and direction of the reconstructing reference beam can be accounted for. The magnification and distortions to the image from such changes in the general case have been worked out by MEIER (1965).

Of particular significance in this project (reconstruction from focused image holograms: Chapter 6) was the effect of a change in the reference beam wavefront shape on the distance of the image from the hologram. For predicting this, Rogers' generalized zone-plate concept of a hologram (ROGERS, 1950; 1952; 1966) is convenient and simple. If s is the distance of an object point from a particular point in the hologram, and r is the distance of the reference beam point source from the same hologram point, then

$$\left[\pm \frac{1}{f} = \frac{1}{s} - \frac{1}{r} \right] \qquad \ldots\ldots (3.1)$$

in which +f is the focal length of the hologram applied to the primary image, and -f applied to the conjugate image. If in reconstruction the reference beam source distance is changed to R, this value is substituted for r in order to find the corresponding image point distance. Thus, using subscripts p and c for the primary and conjugate image point distances respectively for the primary image

$$1/S_p = 1/s - 1/r + 1/R \qquad \ldots\ldots (3.2)$$

and for the conjugate image

$$1/S_c = 1/r - 1/s + 1/R \qquad \ldots\ldots (3.3)$$

r is assumed positive when the reference beam point source is the same side of the hologram as the object. If the point (of divergence or convergence) changes to the opposite side of the hologram in reconstruction, R is then negative. The signs of S_p and S_c indicate whether the images are virtual or real. When in reconstruction the hologram is illuminated on the same side as it was for recording, virtual images are positive and real images negative. When the hologram is illuminated on its other side the signs of the images are reversed. Rogers showed that if λ_1 is the recording wavelength and λ_2 the reconstructing wavelength, the focal length becomes f_2 given by

$$\left[f_2 \lambda_2 = f_1 \lambda_1 \right] \qquad \ldots\ldots (3.4)$$

Certain special cases of interest are simply derived, and are listed here :-

(i) For $r = R = \infty$, $1/S_c = -1/s$

:-for a collimated reference beam, the conjugate image is real on the observation side of the hologram, and is effectively a mirror image of the primary image.

(ii) For $s = r$, $f = \infty$ and $S_p = S_c = R$

:- Fourier holography,

(iii) For $R = r$, $S_c = \frac{rs}{2s - r}$

:- for this condition, the conjugate image is real only if $r > 2s$.

Since this concept of a focal length of a hologram is derived from zone plate theory, strictly it applies to holograms recorded with the object in line with the reference beam. However the error in image positions is only small when small design angles are used. A more rigorous treatment by NEUMANN (1966) applies for general off-axis holograms, restricted to small hologram apertures.

With regard to photographically recording an image, particularly for analysing an interferogram, there is the option of recording a virtual or a real image. However to construct the image without distortion the condition $R = r$ applies, this consideration being important if the image is to be scaled for analysis. Photographing the virtual image with a conventional camera (from the far side of the hologram) can be restrictive, due to the minimum distance the camera can be placed from the image. In this circumstance, the object is preferably positioned before making the hologram at a distance from the recording plane to suit the focal length of the camera lens. Recording a real image has the advantage that no imaging lens is required (providing the image fits within the film or plate). There are two possibilities for producing a precise real image. Firstly, by using a collimated reference beam both for recording and reconstruction, the conjugate image is then real and dimensionally the same as the object. Secondly, by exactly reversing the reference beam in direction and curvature

of wave front, the primary image is real. However this involves a large aperture lens to converge the illuminating beam.

Resolution in the image is directly related to the hologram aperture used, since the size of the speckles of the speckle pattern in the image plane is inversely proportional to the imaging aperture. This is illustrated by the photographs of Figs. 3.3 and 3.4. In each case the image was from the same hologram of cantilever deformation by double exposure HI. In the first case the virtual image was photographed with a 35 mm camera, the lens being set at f/8, whereas for Fig. 3.4 the lens was set at f/22. The difference in speckle size is clear, even though by comparison the print of Fig. 3.3 has been over-exposed. In both cases all 150 odd fringes are resolvable, though a speckle pattern a little more coarse than that of Fig. 3.4 would cause difficulty in resolving the fringes most closely spaced. In a case of HI in which the fringes localize away from the object surface, the aperture can be reduced so as to increase the depth of field, but a compromise must be sought between depth of field and acceptable speckle size.

3.2 DESIGN OF APPARATUS AND INTERFEROMETER LAYOUT.

The experimental work of the project was neither directed towards one specific type of measurement nor an analysis of one specific object. Therefore the underlying thought in the design of apparatus was for versatility. Mounts for optical elements were made small, with convenient means of adjustment to allow easy re-arrangement in another recording layout. As discussed in Chapter 2, HI, as studied here uses

the principle of common path interferometry, and therefore high quality optical elements to produce highly accurate wavefronts are unnecessary. Thus cheap optical elements of no special quality were obtained for the purpose of splitting, directing and expanding the laser beam, and were mounted in mounts designed and manufactured in the Department. A cast iron table was used, having the distinct advantage of enabling components to be magnetically clamped. Its surface was machined, though not optically flat, and measured 2 m by 1.05 m.

The laser was supported on a pair of steel blocks giving a convenient beam height above the table surface of about 9.5 cm. Exposure times ranged from a few seconds to several minutes, and for times up to one minute the beam was conveniently shuttered by a solenoid-actuated arm. This was electronically controlled with remote push-button operation, as described by BUTTERS and MIDDLETON (1970). For occasional exposure times of less than a second a mechanical camera shutter was used, softly supported to reduce vibration transmitted to the table.

Two particular objects of a simple nature were used for experiments in technique and fringe interpretation. One was a vertical steel cantilever displaced by a screw of 40 threads per inch carrying a protractor for crude measurement of the screw's axial displacement: see Fig. 3.2. The other was a 1/16 in 1½ mm thick brass plate 3 in (76 mm) square screwed to a rigid upright pillar and loaded with weights to bend the plate about an axis in its plane, shown in Fig. 4.9. Although holograms can be taken of metal surfaces as machined, this can produce great variations in intensity

between regions which scatter the light and those which specularly reflect to the point of observation. Greater clarity and more uniform fringe contrast in interferograms are obtained using an evenly scattering surface. Therefore the objects were thinly sprayed matt white which gave a nearly uniform scattered intensity with varying angles of illumination and viewing. This paint almost completely depolarized the light. Thus only part of the scattered object light could interfere with the reference beam and the remainder tended to fog the emulsion, but this effect was not serious. Surface points on the object were conveniently identified by marking with black ink.

For splitting the laser beam into reference and object illumination beams, amplitude division was preferable to wavefront division in view of the beam's Gaussian distribution of intensity. A glass flat was used, being more versatile for directing the reflected beam than a split cube. For angles of incidence from a few degrees up to 45°, on an uncoated glass surface, it was found that the reflected beam used as the reference beam produced about the right beam ratio at the recording plane, (using the transmitted beam for object illumination). Thus, uncoated float quality glass of 5 mm or greater thickness was used, this thickness providing complete separation of the two beams reflected from the front and back surfaces of the flat. The beam was split before expansion in the optical path to enable small aperture elements to be used for the splitter and any subsequent beam steering mirrors. Thus a recording arrangement of the form shown in Fig. 3.5 was generally used. By altering the angle of incidence at the beam splitter, the beam ratio could be adjusted by up to a factor of two or three.

Aluminium coated glass flats or float glass were used as front-reflecting beam steering mirrors. Both the beam splitter and mirrors required fine adjustment to direct the beam in the horizontal and vertical planes. Therefore a common design of mount was devised for both, the optical elements being clamped firmly in a channel section wide enough to accommodate thicknesses of glass up to 7 mm. Fine rotational adjustment about one vertical and one horizontal axis was provided by 40 threads per inch screws with knurled heads acting at a nominal radius of 1 cm, backlash being taken up by compression springs. Pot magnets held these mounts firmly, yet were not so strong as to prevent them being eased sideways across the table into position.

For expanding the laser beam single element double concave lenses of 5 to 10 mm focal length were simple and effective. The only built-in adjustment required was for height, a range of about 15 mm being provided by a spindle sliding vertically in a cylinder and clamped by a screw. By attention to keeping optical surfaces clean, such expanded beams were satisfactory both as object illumination and reference beams. In more critical cases, for example the reference beam in focused image holography (Chapter 6) requiring an expanded beam free of dirt or scratch diffraction patterns, a lens/pinhole filter mount was devised. This used interchangeable microscope objectives of different power and a 0.001 in (25 μm) diameter hole filter. One 40 threads per inch screw adjusted the position of the objective lens along the beam axis while two more such screws adjusted the position of the filter in the vertical and

horizontal lateral directions. Each sliding piece was held against its adjustment screw by a compression spring(s). Fig. 3.5 shows the assembled mount.

For the attenuation of either the reference or object illumination beam to obtain the desired beam ratio, a photographic polarizing filter was used, being cheap and convenient. This attenuated all parts of the beam by practically the same factor. Adjustment of the intensity by rotation of the polarizer altered the direction of polarization of the transmitted light, and attention had to be given to the amount by which the polarization directions of the reference and signal beams became crossed. When pinhole filtering the expanded beam the polarizing filter was positioned before the lens, so that diffraction effects caused by the polarizer were also removed. This means of attenuation was satisfactory for double exposure HI. However, for real time work it is usually necessary to adjust one of the beam intensities for the reconstruction stage. For this case the polarizer was unsuitable, and a graded density filter was used, as described in the following section.

The photographic plates for holography were usually cut into quarters for economy. Because these plates were produced in different sizes, a plate holder for various sizes of plate was required. Simple vice action perspex jaws on a pot magnet base were used. The clamping faces of the two perspex jaws were machined flat and relieved by the plate thickness so as to grip the plate firmly without bending it. This plate holder, shown in Fig. 3.5, was entirely satisfactory for double exposure HI, and was convenient in that the hologram was readily accessible for viewing the reconstruction.

For real time HI kinematically relocating and in situ processing plate holders were designed, described in the following section.

Mounts without pot magnet bases were generally held in place with on/off magnets, especially the two objects described which had to be adjusted between exposures in double exposure HI. The arrangement of the components for recording the hologram was generally of the form shown in Fig. 3.5. This allowed easy matching of the path lengths via the object and the reference beam, easy adjustment of the design angle, and arrangement of the two optical paths close together to minimise the effects of any air disturbance. The plate holder and object were arranged reasonably close to the table edge for easy access without risk of disturbing other components. Not shown in Fig. 3.5 were black baffles used to stop the reflection from the second surface of the beam splitter, and to prevent any stray light reaching the plate. Beam intensities at the position of the hologram were compared with a sensitive photographic light meter: model Gossen Lunasix 3.

3.3 DEVELOPMENTS IN EXPERIMENTAL TECHNIQUE

It was found that the practice of double exposure HI required little further technique than that for successful single exposure holography. Particular precautions included delicate adjustment to the object between exposures so as not to disturb the interferometer, and delay after loading an object to allow creep and thermal effects to dissipate before making the second exposure. Furthermore, attention had to be given to the mounting of an object and its preloading to avoid hysteresis effects, otherwise an

interferogram could be obtained representing displacements superimposed on the deformation being investigated.

However, in real time HI particular experimental problems were encountered. These were difficulties of spatially matching the real time and reconstructed wavefronts, and of obtaining high fringe contrast in the interferogram, as experienced by other workers (e.g. ALEKSANDROV and BONCH-BRUEVICH, 1967). If the two wavefronts are inexactly matched, spurious fringes are initially produced and these subsequently modify the form of the fringes due to object deformation. This causes confusion in fringe interpretation, as illustrated by the comparison of the two interferograms shown in Figs. 4.10 and 4.11. In both cases the object deformation was the same, but in the latter case the interferogram was modified by the superposition of secondary fringes. (In this case these fringes were intentionly introduced, as explained in section 4.4, but they illustrate the effect of spurious fringes.) Clearly, extra work in analysis would be required to determine the object's deformation in the second case. Referring to the other problem, poor fringe visibility, fringe centre positions are difficult to locate, and consequently error can arise in analysis. Therefore methods of overcoming these problems were sought.

For real time HI the emulsion bearing the hologram needs to be replaced in its original position to within a wavelength of light, generally. Therefore a mount providing kinematic location of the plate is necessary, of a form described by ARCHBOLD et al (1967). Such a mount, using six location points contacting one face and two edges of the glass plate was evaluated at an early stage of this project.

This permitted sufficiently accurate wavefront matching for real time HI to be carried out, though the performance varied, sometimes producing a few initial mis-match fringes. In case this was due to minute chips of glass wearing off the plate, the plate was then clamped in a perspex frame in which it remained for processing. The frame itself was now kinematically relocated, but this arrangement did not offer any certain improvement. There were the possibilities of thermal expansion (especially high for the perspex), and emulsion shrinkage, both implying that the hologram might in fact need to be minutely adjusted from its original position. Therefore the mount for the perspex frame was modified to incorporate micrometer head controlled adjustments. These provided two translations in the horizontal plane, one in the plane of the hologram and the other perpendicular, and rotation about a vertical axis. It was then found that the initial pattern of mis-match fringes, if present, could usually be reduced but not eliminated. Work in this laboratory by HOCKLEY (1969) showed that a kinematically relocating plate holder with adjustments in <u>five</u> degrees of freedom tended to reduce the pattern of mis-match fringes even further, but still not completely. This indicated that some distortion of the emulsion was likely, in which case simple translations and rotations of the plate would not compensate for this.

An alternative approach, prompted by BOLSTAD (1967), was also under trial, namely processing the plate in situ, thereby eliminating its removal and relocation. A stainless steel frame was machined, having a central window measuring 2 x 2 in (50 x 50 mm), to take a cut plate of size 2½ x 2 in (63 x 50 mm), which was firmly held by four perspex screws

with washers, with the glass in contact with the metal frame. This frame was rigidly suspended to allow 500 ml beakers of solution to be raised so as to immerse the plate for processing:- see photograph of Fig. 3.6. When testing this plate holder, using the recommended processing procedure, one or two initial fringes of mis-match were typically produced, similar to the performance of the kinematic relocating plate holders. However, deliberate straining and release of the stainless steel frame did not produce a net change in the fringes, demonstrating that the plate holder was sufficiently rigid to withstand accidental knocks, for example during processing. Again distortion of the emulsion as a cause of the mis-match fringes was indicated.

In order to try to establish the effect of emulsion movement, and whether such movement could be significantly reduced, a few experiments were carried out, (as published: BUTTERS et al, 1969). A holographic plate was exposed to two point-source beams from a He-Ne laser in the arrangement sketched in Fig. 3.7, effectively forming a hologram of a point source (B).

After processing and repositioning the plate the screen received two wavefronts, one transmitted directly through the plate from B and the other by reconstruction, for which beam A acted as the reference beam. These two wavefronts could interfere, and, having followed the recommended processing procedure, produced the fringes shown in Fig.3.8(a). The presence of these fringes was due to (deliberate) inexact relocation of the plate. However the fringes were noticeably ragged, and this was thought to be due to local distortions of the emulsion in its plane. Such movements would

alter the spacing of the grating structure, thereby locally altering the angle of diffraction in the reconstructed wavefront. Such raggedness of the fringes was likewise diagnosed by STETSON and POWELL (1965).

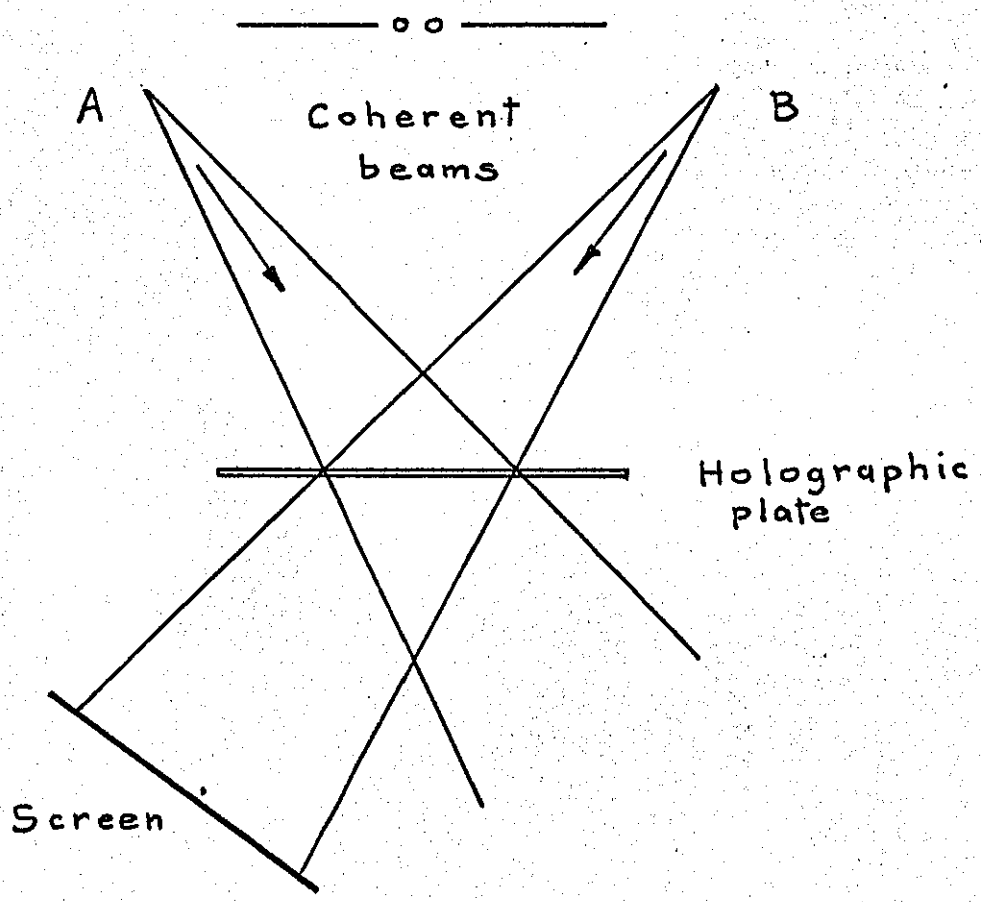

Fig. 3.7 Experimental arrangement to detect emulsion movement.

It was considered that these emulsion movements could result from release, during processing, of production - induced strains 'frozen' in the emulsion. If the strains could be released before exposing and processing the emulsion, the movements resulting from processing would then be reduced.

An initial test of this idea was to expose an emulsion to water vapour for several hours, let it dry, and then use it as in the first case. This resulted in the fringes of Fig. 3.8 (b), in which the degree of raggedness was reduced. Finally another plate from the same batch was immersed in water for two minutes and dried by washing in industrial methylated spirits and leaving in air for ten minutes before exposure. After processing in the usual way it was again rinsed and rapidly dried by the same methylated spirits treatment, so that the emulsion dried out in the same manner. This gave the distinctly smooth fringes shown in Fig. 3.8 (c).

This washing and methylated spirits treatment was then applied to a practical case of real time HI, using the cantilever object. The improvement in the quality of the fringes thus obtained is demonstrated in Fig. 3.9, comparing the two cases: (a) without treatment, and (b) with the methylated spirits treatment. The extra time taken by the pre-exposure treatment was more than compensated for by the fast drying after processing, compared with washing in water followed by drying in air. Thus the overall exposure and processing time was slightly reduced by this treatment, representing a further advantage of the technique for those cases of real time HI in which the object slowly creeps. No adverse effects due to the methylated spirits were detected, even for real time HI over several hours.

It was further thought that emulsion movement could contribute to the initial pattern of one or two 'mis-match' fringes often produced in real time HI. Therefore the methylated spirits treatment was used in conjunction with

Emulsion movements experiments

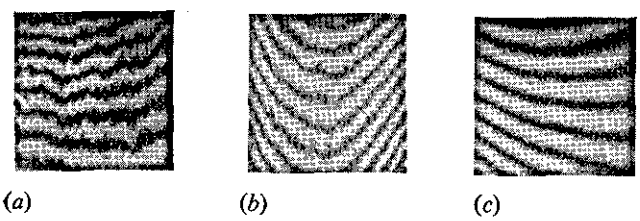

Fig. 3.8 Fringes obtained at the screen of Fig. 3.7,
(a) without pre-exposure treatment;
(b) exposed to water vapour and dried in air before use;
(c) soaked in water, then in methylated spirits, and dried in air before use;

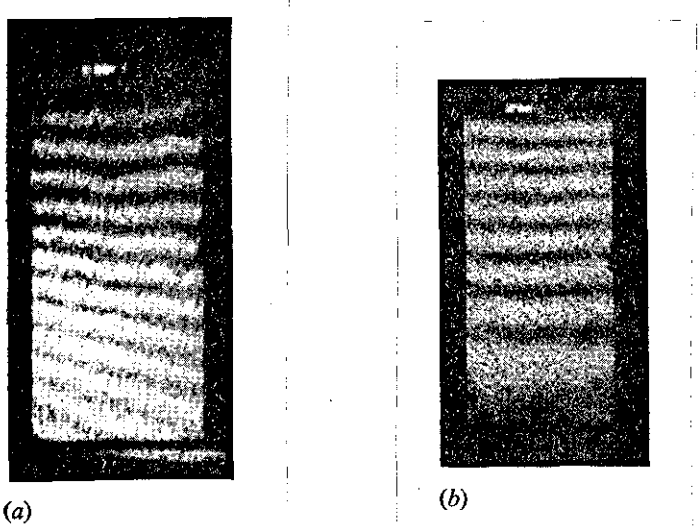

Fig. 3.9 Fringes obtained over a cantilever by real time HI,
(a) without pre-exposure treatment;
(b) treated as for Fig. 3.8 (c) above.

the plate holder for processing in situ. All processing solutions were used at room temperature within 1°C. This gave the best results yet. In a particular test, in which a brass plate as the object subtended an angle of 10° at the hologram, with a spherical wavefront reference beam, the real and reconstructed wavefronts matched so well that not one fringe formed over the object/image field. In fact the fractional fringe order could not be estimated by eye. (After these investigations were carried out, similar work by FRIESEM et al was published (1969), substantiating the idea of stress relief in the emulsion. They also used the remedy of soaking the emulsion before exposure, and obtained consequent improvements in real time HI.)

It was noticed in the above case that the superposition of the reconstructed wavefront slightly brightened the object field, i.e. constructive interference took place. Thus despite the theoretical phase reversal of the reconstructed wavefront, due to the negative action of processing the emulsion (ENNOS, 1968), this does not necessarily happen in practice, probably due to emulsion shrinkage. The fringes of this real time interferometer were monitored over a period of 24 hours, to assess enviromental effects. Over a range of a few degrees Centigrade, the number of fringes changed by about three per degree. Such fringes would be very bothersome when analysing an interferogram of object distortion. Not only would these fringes have to be subtracted from the interferogram, but there could be uncertainty over the number and form of such fringes. The mounting of the table (concrete pillars with single layers of cross-ribbed rubber directly under the table) was found to be adequate most of

the time, but activity within the room by other persons momentarily disturbed the interferometer. (Occasionally, when heavy machinery was running in the building, the disturbance was continuous and disruptive.)

Although the plate holder for processing in situ gave consistently good results, there were still the effects of emulsion shrinkage to consider. Typically the net shrinkage in thickness after normal processing is about 15%. Not only does this alter the position of the hologram's grating structure, but also changes the angle of the fringe "slats" through the emulsion thickness (VILKOMERSON et al, 1967). The effect of the latter is to reduce the intensity of the reconstructed wavefront, this being undesirable in real time HI. Therefore the practice was adopted of arranging the hologram so that the normal to its plane bisected the design angle. For this condition the "slats" were also normal to the emulsion plane and their angle was unchanged by shrinkage. The effect of altering the position of the grating structure is imperfect superposition of the reconstructed wavefront on the real time object wavefront. In order to counteract this, attempts were made to swell the emulsion back to its original thickness, after processing, by the procedure using a solution of triethanolamine recommended by LIN et al (1967). A convenient method of judging the results of this treatment was to make "volume reflection holograms", i.e. holograms for which the emulsion thickness is large compared with the fringe slat spacing, and made by directing the object and reference beams to the emulsion from opposite sides. Such holograms allow reconstruction by a white light source, selecting a narrow band

of wavelengths for the reconstructed wavefront by Bragg's law. Due to emulsion shrinkage such a hologram made with a He-Ne laser produces a green image using white light reconstruction. By re-soaking the emulsion in triethanolamine solution, after processing and drying in air, the emulsion could be swelled to produce a red image, though the solution concentration and temperature, and drying conditions were found to be critical to achieve this. When the treatment was applied to real time HI there was no definite improvement in terms of reducing the initial mis-match fringes, compared with a test plate without the treatment. Therefore the treatment was not pursued, being both inconclusive and time-consuming. However it was deduced that the effect of shrinkage to cause imperfect superposition of the wavefronts would be reduced by using a collimated reference beam as opposed to one with a spherical wavefront. Whereas the collimated beam would produce an image of unit magnification, even though displaced from the object by an amount related to the emulsion shrinkage, the spherical wavefront beam would in addition distort the image.

It was noted, subsequently to this work, that BIEDERMANN and MOLIN (1970), rigorously tackled the problems of rapid processing and fringe-free superposition of the wavefronts in real time HI. They likewise processed the hologram in situ but, in addition, developed a liquid gate around the plate which gave several improvements. Notably, by soaking the emulsion in developer prior to exposure, it was hypersensitized, so reducing the exposure time; reconstruction and observation could commence during the fixing process, only 2 to 3 minutes after exposure; emulsion shrinkage was eliminated;

and intermodulation noise around the reconstructed light was suppressed.

The other main problem initially encountered in real time HI was that of poor fringe contrast in the interferogram. This was mainly due to unequal intensities of the (real time) object and reconstructed wavefronts, the latter usually being considerably dimmer. A straightforward solution was to increase the intensity of the reference beam at the reconstruction stage, until the two interfering wavefronts were of about the same intensity. ALEKSANDROV and BONCH-BRUEVICH (1967) achieved this by replacing the filter in their reference beam by another of higher transmittance, at the reconstruction stage. However this technique implies having a set of filters all of the same optical thickness at corresponding parts of the beam, otherwise the wavefront shape is changed and fringes are introduced. For the work of this project a 6 in by 1½ in (150 x 38 mm) graded neutral density strip filter was used, having an approximately linear distribution of optical density over the range 0 to 2. There was the option of using it in the reference beam, set at low transmittance for exposure and increased for reconstruction, or, in the object illumination beam set high for exposure and decreased for reconstruction. The latter was usually preferred in order to minimise the exposure time. The filter was positioned in the beam before expansion so that the variation of transmittance across the beam was only slight, and also so that the transmitted beam could be spatially filtered. A mount was made having three nylon pegs, two of which slid in a machined and lapped vee groove while the third slid on a flat lapped surface of the same

steel plate. Thus the filter was translated without rotation, within the manufacturing tolerance. In practice the filter operated satisfactorily, without introducing noticeable fringes into the interferogram, and the range of optical density was sufficient. Due to multiple reflections within the filter a few broad fringes were present in the transmitted beam, but their visibility was low, and by arranging the angle of incidence to be about 15° the fringes were displaced to the side of the object being illuminated.

In the case of an object surface which depolarized the light there was an additional problem. Only part of the total intensity of the (real time) object wavefront could interfere with the reconstructed wavefront, the remainder being noise and reducing the fringe visibility. However this noise element was easily removed by means of a standard photographic polarizing filter placed between the hologram and the point of observation.

Bleaching holograms was known to increase the brightness of images in reconstruction, and many researchers had formulated various bleaching solutions and procedures. In principle the consequent brighter image would improve the fringe visibility in real time HI, though there was the possibility that this extra processing would degrade the form of the reconstructed wavefront. Bleaching as a means of improving fringe contrast was not pursued in this project, as the aim was to shorten and simplify procedures rather than extend them.

Conclusions

The making of double exposure holograms was found to be straightforward, whereas successful real time HI required special experimental technique. As discussed in Chapter 2, real time HI is indispensable for certain investigations, and therefore solutions to its particular experimental difficulties were sought. These difficulties were successfully overcome by means of simple and cheap apparatus and materials, and the accompanying procedures were practicable, accepting that holography using continuous-wave lasers and photographic recording is limited in general to being a laboratory procedure. When processing the hologram in the normal manner the plate holder for in situ processing was not necessarily superior to kinematic relocation, but best results for superposition of the real time and reconstructed wavefronts were obtained by combining the pre-exposure wash treatment with in situ processing. With the methylated spirits wash, this procedure was faster than the normal recommended processing. By use of a graded neutral density filter and a polarizing filter, good fringe visibility was obtained.

Thus, real time HI could be successfully undertaken to obtain good quality interferograms free of spurious input. Improvements in clarity, ease of interpretation, and accuracy of analysis were gained from these methods. However, the running of very heavy machinery could not be tolerated, neither during hologram exposure nor during observation of real time fringes (with the existing simple mounting of the table). For real time HI over a period of hours, room temperature control to within would be necessary for accurate fringe analysis.

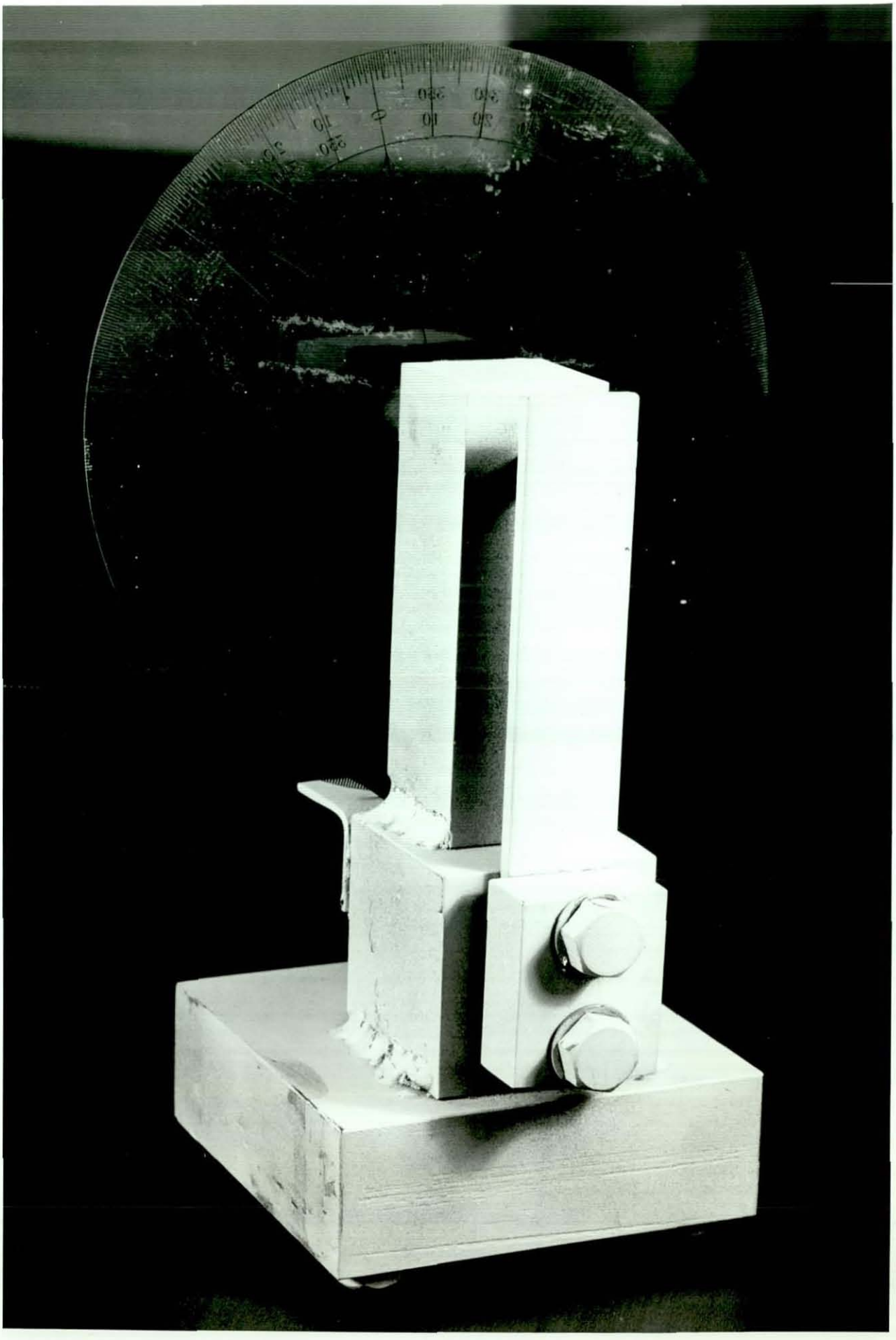

Fig. 3.2. Cantilever object for experiments in HI

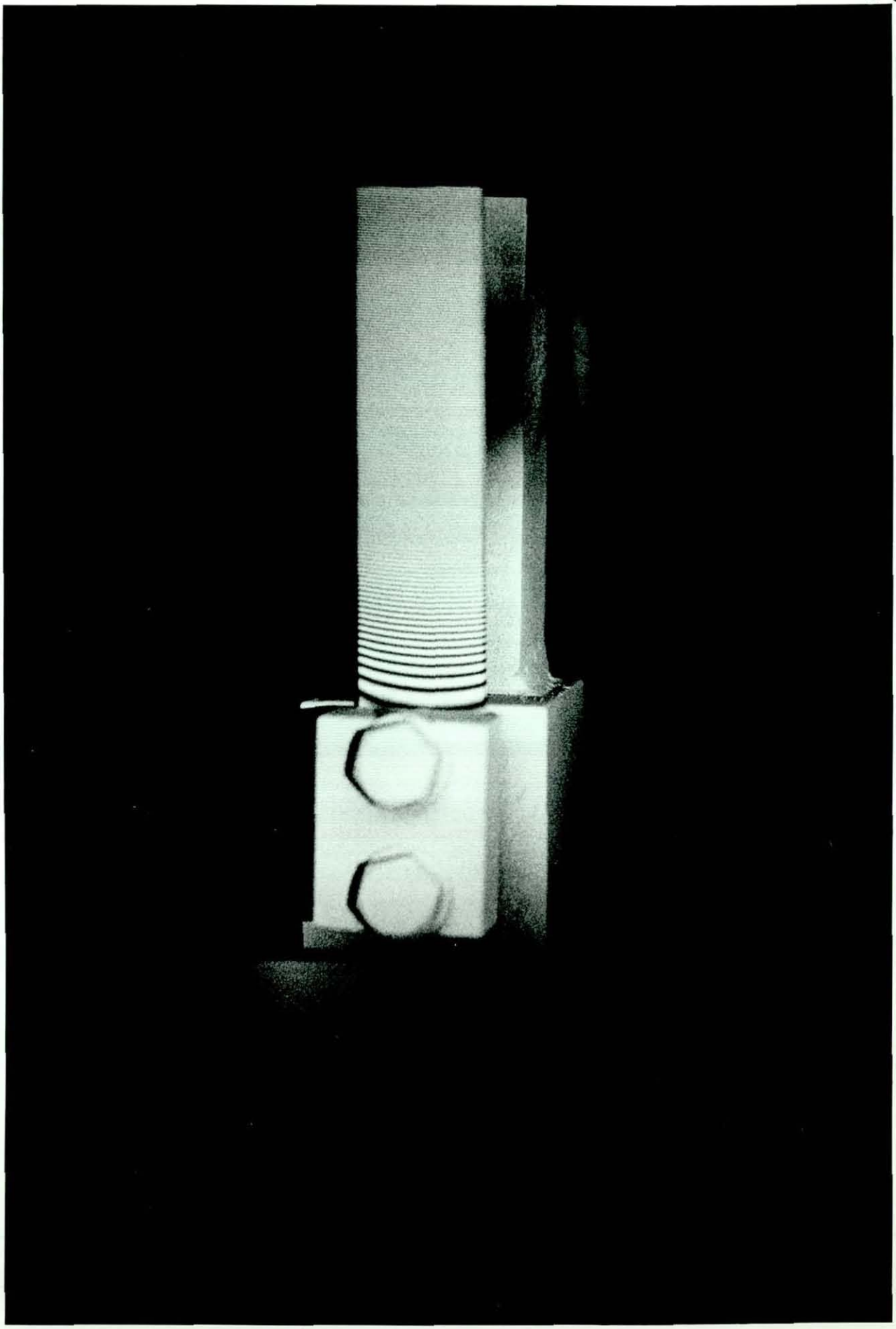

Fig. 3.3 Photograph at f/8 of the virtual image from a hologram of cantilever deformation

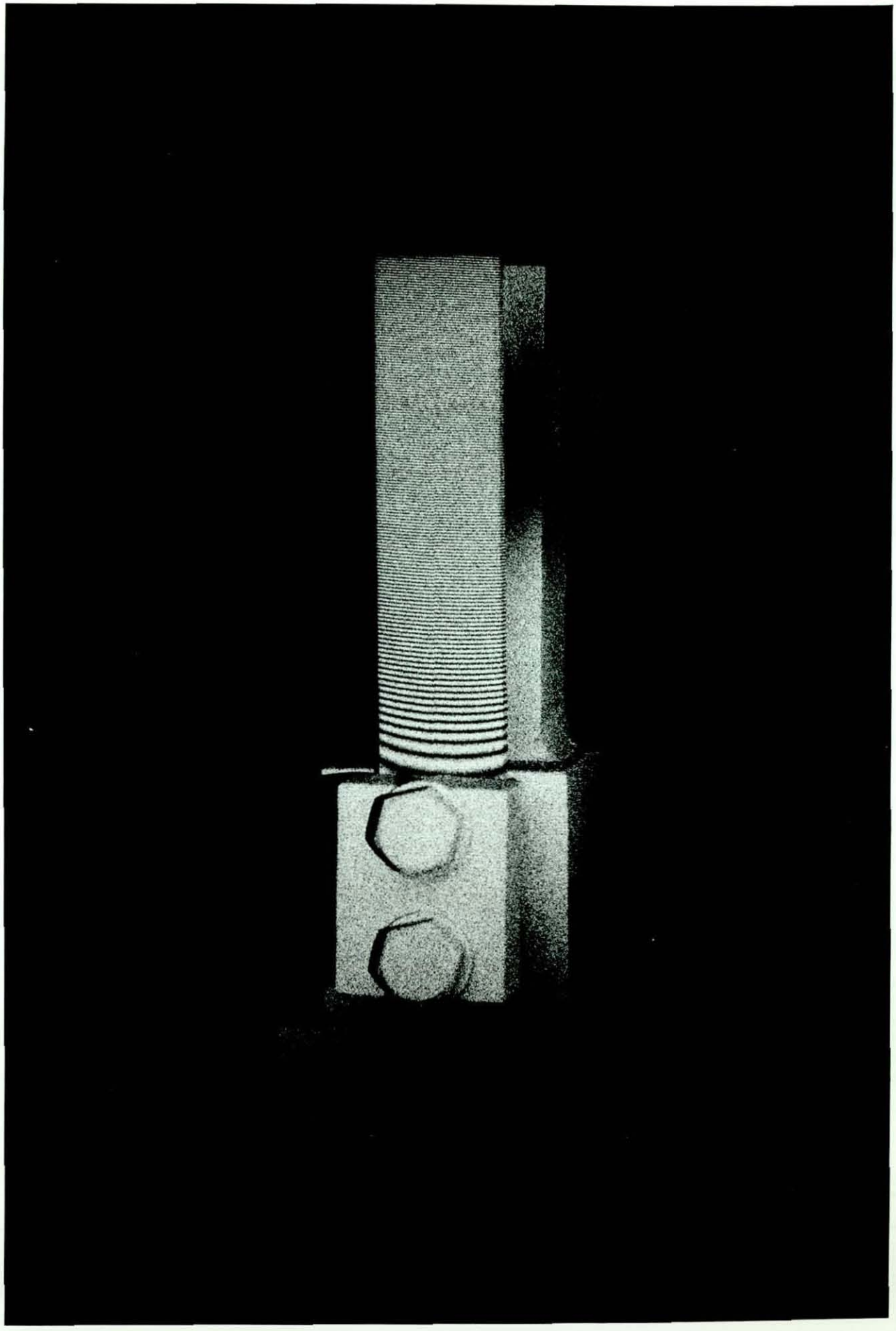

Fig. 3.4 Photograph at f/22 of the image from the same hologram as in Fig. 3.3

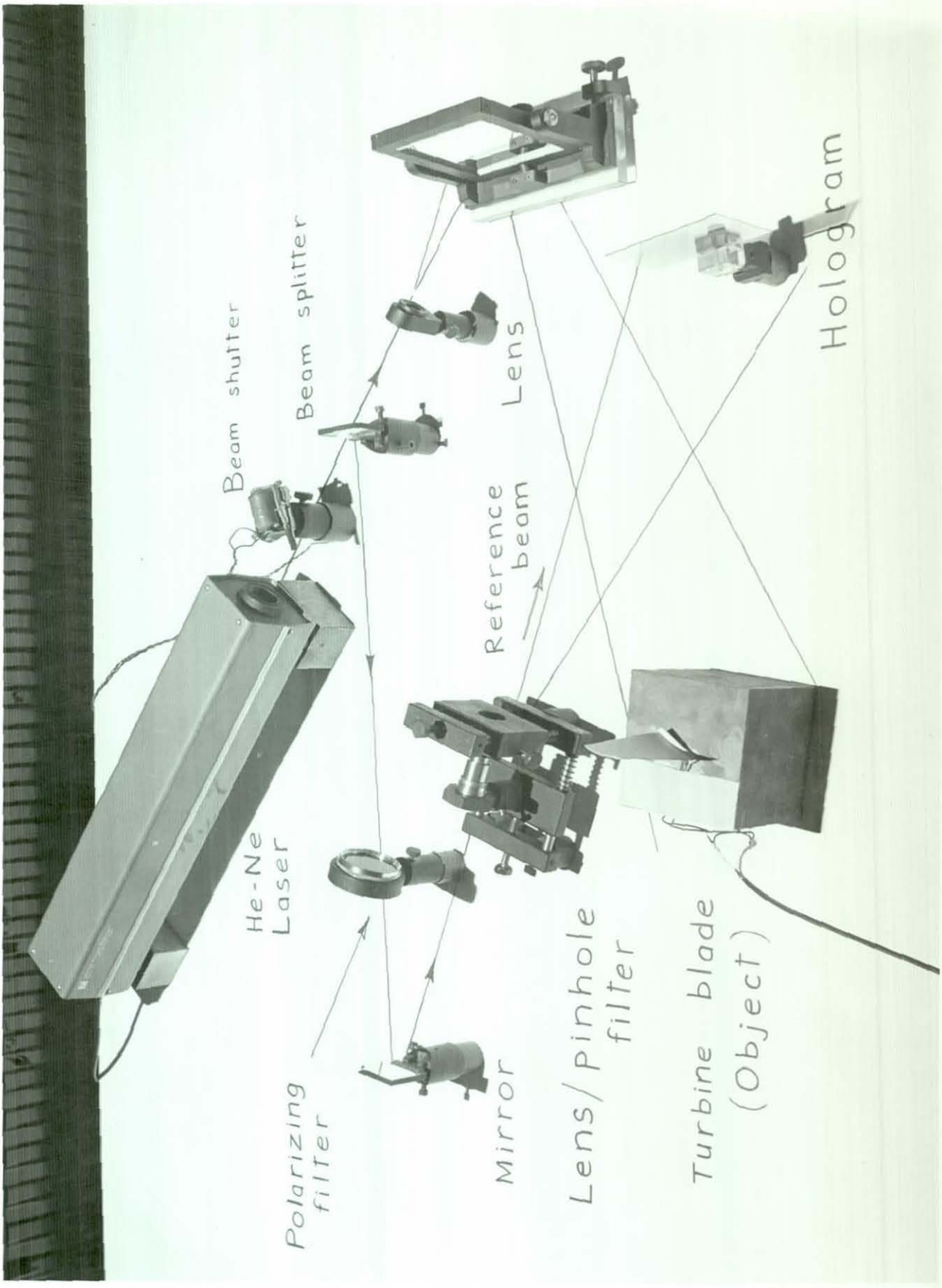

Fig. 3.5 Typical components used and their approximate arrangement for holographic recording

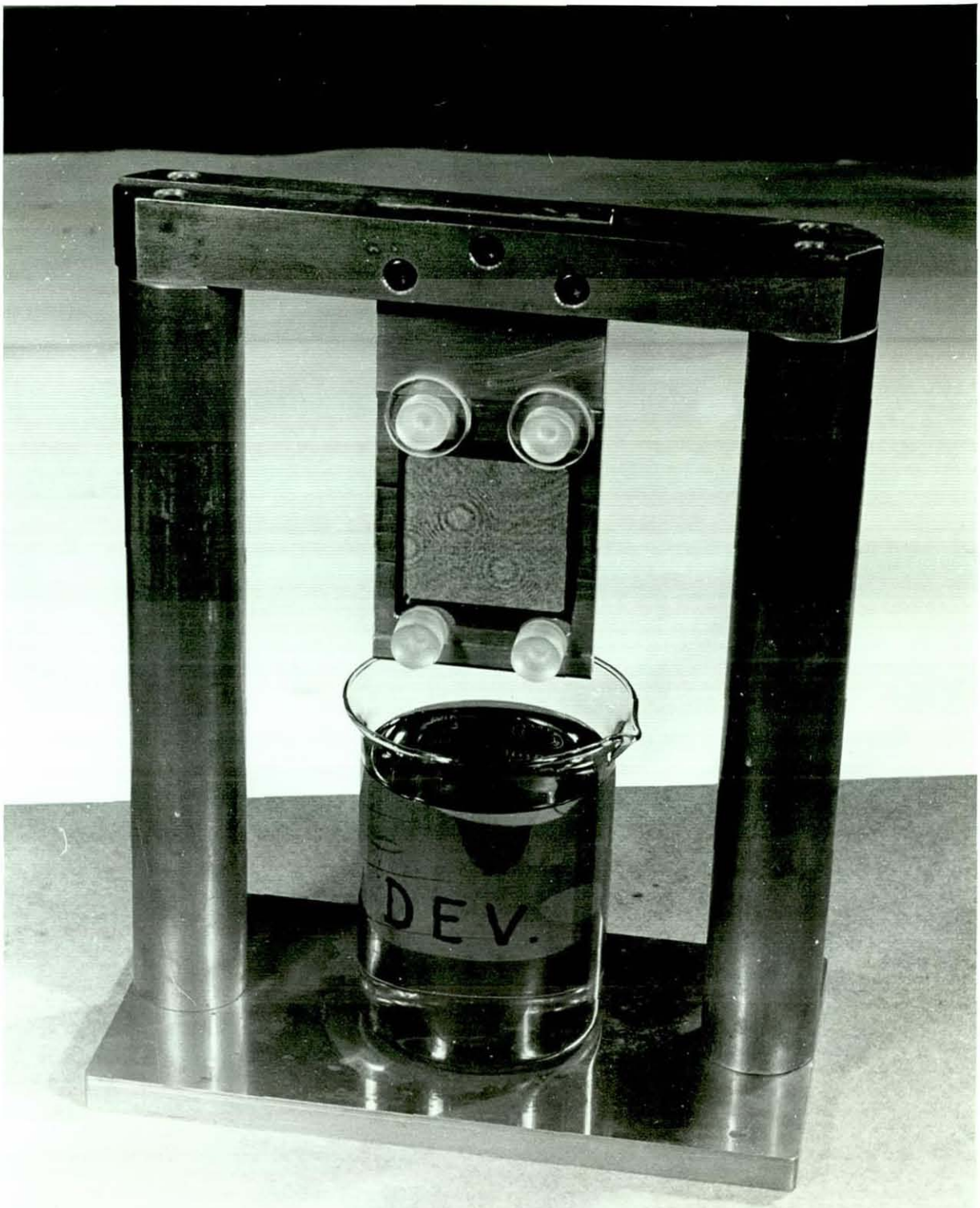

Fig. 3.6 Plate holder for processing holograms in situ, for real time HI

Chapter 4

INTERPRETATION OF HOLOGRAPHIC INTERFEROGRAMS

The purpose of this chapter is to examine the interpretation of holographic interferograms with regard to engineering applications. Also the accuracy of measurements made by HI is investigated.

4.1 THE BASIC RELATION BETWEEN SURFACE DISPLACEMENT AND FRINGE FORMATION.

As in any interferometer, holographic interferograms are due to a difference between one optical path length compared with another. In the case of holography, at least one of the interfering wavefronts is formed by reconstruction from the hologram. The phase of such a wavefront is determined by the wavefront shape of the reconstructing reference beam, and also of course by the grating structure of the hologram. It is known that this grating structure depends on the relative phases of the reference and signal beams incident at the plate when recording the hologram. In turn, these relative phases depend on the respective optical path lengths of the reference and signal beams from the beam splitter to the hologram. In the case of the signal beam this path is via the object surface. Let it be assumed that for reconstruction the reference beam path to the hologram remains identical to that when recording the hologram. Then the phase all across the reconstructed wavefront will be exactly the same as that of the original wavefront of the

signal beam. (This represents an ideal situation for which no phase changes result from processing the photographic emulsion.) This description applies to real time HI, in which the comparison wavefront is provided by continuous illumination of the object surface in its displaced position. In the case of double exposure HI, the two reconstructed wavefronts interfere, and these correspond to two slightly separated positions of the object surface. Thus, in either case, the interference of the two wavefronts may be considered as interference between two sets of paths existing simultaneously. These paths connect the beam splitter with the point of detection, one set via the object surface in its initial position, and the other set via corresponding points of the surface in its displaced position.

From this description it follows that, for real time HI, the same laser beam (prior to beam splitting) must be maintained for the reconstruction stage, otherwise spurious interference effects could arise. This does not apply for reconstruction from a double exposure hologram. In fact the wavelength and the wavefront curvature of the reference beam incident at the hologram may be changed without altering the interference effects of the two reconstructed wavefronts. This is because the relative phases of the two wavefronts, which determine the interference, have already been coded in the hologram, and the reconstructing beam serves only to diffract light from the hologram.

This concept of optical paths via two coexistent object surface positions is convenient for deriving the basic relation between surface displacement and fringe formation. The concept applies for both the real time and double exposure methods.

It is assumed at this stage that only pairs of corresponding points in the two surface positions cause interference. Every point has unique surface structure, and therefore light scattered from two different points will contain different random variations of phase, preventing regular interference. Strictly the paths originate at the beam splitter, but the point of expansion, (at the lens), can be taken as the source since the geometrical path between these two optical elements is common. (This, of course, assumes that no net refractive index change along this path occurs in the time interval between the two beams. Even if it does, it is likely to affect all parts of the beam equally, since the unexpanded beam is only 1 to 2 mm in diameter.)

Consider the displacement d of a surface point from P to Q, shown in Fig. 4.1 (a). Also shown are the two relevant optical paths in the vicinity of this point. By drawing perpendiculars from Q it is seen that the geometrical difference between these two paths is

$$d(\cos\alpha + \cos\beta)$$

(These paths and the displacement direction are not intended to be co-planar; in general the geometry is three-dimensional.) Multiplying this expression by the refractive index of air, μ, converts it to the optical path difference. This may be equated to a multiple of λ, , the wavelength of the light. Thus the basic relationship for a holographic interferometer is:-

$$n\lambda = d(\cos\alpha + \cos\beta) \quad \ldots (4.1)$$

In this equation n is the fringe order number, which in general is a fractional number.

This derivation has assumed perfectly collimated illumination conditions, whereas in practice the simpler

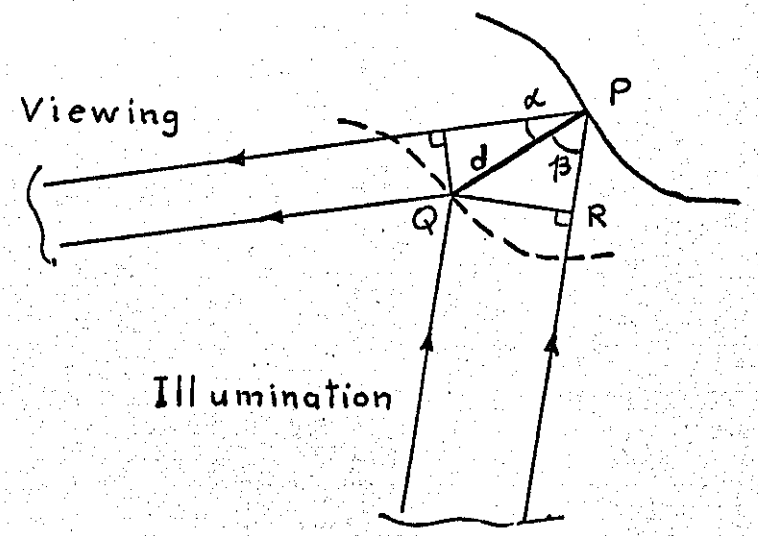

(a)

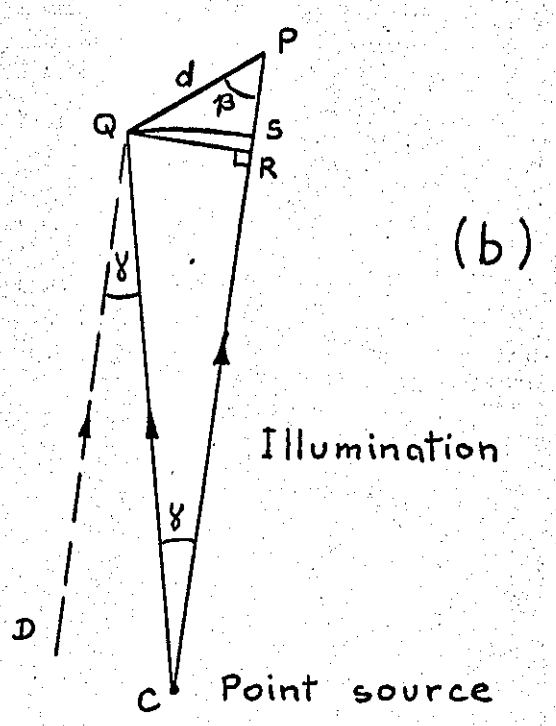

(b)

(d shown greatly exaggerated with respect to CP)

Note :

In the general three-dimensional case, d and β are the true angles in space between the vector $\vec{PQ}$ and the viewing and illumination directions.

Fig. 4.1 (a) The effective optical paths for a surface displacement d.

(b) Diagram to illustrate error in (a) when the illumination is from a point source.

arrangement of a diverging beam is often used to illuminate the object. In this case the wavefront is (approximately) spherical, and, referring to Fig. 4.1 (b) the line of constant phase is the arc QS. Thus the true geometrical path change in illumination is PS, whereas the foregoing analysis assumes it to be PR. However the error is negligible, as shown by calculation for a typical case. Suppose the displacement d is 10 μm and the effective point source of illumination is 35 cm from the surface, with an angle β of 45°. Then, the error, expressed as a fraction of the true path change, is only 10^{-5}. A similar situation exists in the viewing path, since the viewing aperture is usually finite, allowing a small cone angle of ray paths to be accepted from all points such as P. Thus, strictly, α in equation (4.1) is not a single value but a very small range of values. However in practice the range is usually made to be so small that α can be regarded as a single value. (When the viewing aperture becomes large, noticeable effects arise, as is discussed and demonstrated in Chapter 6.)

Equation (4.1) applies both for real time and double exposure methods, though there is a difference when relating intensity in the interferogram to the fringe order number. Assuming the wavefronts are of equal amplitude and are free of noise, the fringe visibility is unity, and the intensity I is then proportional to $\cos^2(n\pi + \delta)$.

In the case of double exposure HI the phase constant δ is zero, and the zero order fringe is always bright. However, in real time HI the value of δ depends on the emulsion processing and shrinkage, and the intensity of the zero order fringe can be anywhere between the maximum and minimum intensities.

The earliest experiments of this project were verifications of the form of equation (4.1) using the cantilever object shown in Fig. 3.2. The displacement direction of each point on the cantilever surface was taken to be parallel to the displacement screw axis. Thus angles α and β could be measured. (For the small deformations produced, the effective error in the approximation for the displacement direction was quite negligible.) Fringes were counted, relative to the base, at a line across the cantilever level with the displacement screw (acting on the rear surface). Thus the displacement at this position could be checked from the measured rotation of the displacement screw. For differing sensitivities to object displacement, arranged by varying the angles α and β, the displacement calculated using equation (4.1) was compared with that measured from the amount of screw rotation. Agreement was obtained, though the possible experimental error was in the region of $\pm 5\%$ because the resolution in measuring the screw displacement was only 15 micro-inches (0.38μm). (Subsequent experiments specifically aimed at assessing the accuracy of HI are described in the next section.

The form of equation (4.1) was further verified by using more than one illumination (and viewing) direction. When the cantilever object was illuminated via a ground screen, positioned so close that values of β ranged over 60°, the resulting interferogram due to cantilever deformation was of such low visibility that the fringes were hardly discernible. This was as expected since optical path differences varied with the changing direction of illumination. As the amount of displacement increased, moving up the cantilever,

this variation in path difference became greater and consequently the fringe visibility decreased. In order to analyse a simpler case, the illumination conditions were changed to just two simultaneous beams at widely different angles of β. The resulting interferogram was effectively a moire beat pattern between the two fringe patterns due to the separate illumination beams. Moving up the cantilever image from the base, the resultant fringe visibility varied periodically as a linear function of the beat frequency of the constituent patterns. This beat frequency could be predicted from the difference of the $(\cos\alpha + \cos\beta)$ terms for the two constituent patterns. The most conspicuous beats were those due to coinciding dark fringes, and their positions were found to be as predicted. The appearance of this form of beats is shown in Fig. 4.2 which is explained below.

This method using two simultaneous, but different, illumination directions could perhaps be useful for measuring relatively large deformations. By counting the beats, instead of individual fringes due to a single illumination beam, HI would effectively be desensitized. For example by arranging the two illumination beams such that the difference in the two $(\cos\alpha + \cos\beta)$ terms is 0.1, beats would occur at displacement increments of 10λ, or ¼ thou ($6\mu m$) for He-Ne laser light. It is foreseen that the beats (of fringe visibility) would become less perceptible as the fringe density in the constituent patterns increased, since the intensity averaged over several fringes is constant across the image. The result of a preliminary trial to confirm the principle is shown in Fig. 4.2. Two beams were arranged to illuminate a cantilever object, such that the difference

in the respective ($\cos\alpha + \cos\beta$) terms was 0.09. The displacement of 38μm at the top of the cantilever is represented by 5½ beats, whereas the number of fringes in each of the single beam interferograms would have been over one hundred.

From the form of equation (4.1) and the early experiments summarized above arise several implications concerning the interpretation and application of interferograms;-

(i) By suitably arranging the illumination and viewing directions, particular directions of displacement can be detected with high or low sensitivity. For example, by both illuminating and viewing a surface normally, the interferogram will represent directly the out-of-plane component of displacement, while the sensitivity to the in-plane component will be zero. There is no such equivalent for detecting in-plane displacement while eliminating sensitivity to the out-of-plane component, as that would imply a grazing angle to the surface for illumination and viewing.

(ii)(ii) The viewing direction may be varied, after taking a hologram, within the limits set by the boundaries of the hologram. The consequent changes to the interferogram can reveal information regarding the magnitudes of displacement in particular directions. In particular, if the viewing direction can be continuously changed such as to maintain a constant fringe number for a selected object point, then the locus of the line of the changing viewing direction describes the surface of a cone, with the displacement direction as its axis. Also, the zero order fringe

can be identified (if present), by the fact that where there is zero surface displacement there can be no fringe movement when altering the viewing direction. (Unfortunately no fringe movement is also observed under a special condition of surface displacement. That is when the displacement lies on an elliptical path with the points of illumination and observation as foci, as diagrammatically explained by ABRAMSON (1968). This ambiguity must be distinguished by an independent test.)

(iii) When using a divergent beam to illuminate an object, sensitivity to any one particular displacement direction will vary across the object. This effect complicates quantitative analysis, but can be avoided by use of collimated illumination. A corresponding situation exists for the viewing directions, when viewing with an unaided eye. The viewing direction may effectively be collimated by a telecentric viewing system, though this becomes impracticable for large objects.

(iv) For cases in which the displacement direction is known, if the zero order fringe is present absolute displacements at points of interest over the object can be calculated straightforwardly. If it is absent, relative displacements can be found, providing the sense of the fringe order count is unambiguous. Also, the possibility of some form of bodily movement should not be overlooked, as this could modify the interferogram.

(v) A single interferogram does not reveal whether an optical path has been shortened or lengthened due to surface displacement. Thus from the interferogram

of a deformed surface, 'hills' cannot be distinguished from 'hollows'. A real time investigation may be necessary to determine this feature.

(vi) Again for those cases in which the displacement direction is known, the accuracy of measuring a displacement depends to some extent on the values of α and β used. Some error arises in measuring the angles α and β, and since the cosines of these angles are taken, accuracy improves as α and β are arranged to be smaller, to the limit of 0°.

The analysis and description so far has been limited to the case of a single displacement with static end states (the situation implied by double exposure HI). Meaningful interferograms are also obtained for certain other forms of surface displacement, the most common of which is the case of a single exposure recording of steady state sinusoidal vibration. STETSON and POWELL (1966) have shown for this case that the intensity of the image is proportional to:-

$$\left[J_0^2 \left\{ \frac{2\pi a}{\lambda} (\cos\alpha + \cos\beta) \right\} \right] \qquad \ldots(4\cdot2)$$

in which J_0 is a zero-order Bessel function, and a is the amplitude of vibration at any particular point of the interferogram. Interpreting this expression, dark fringes occur at the zeros of the function. Unlike double exposure HI the fringe order number is not a linear function of displacement (in this case amplitude of vibration). However, to a good approximation, beyond the first fringe cycle, one fringe period represents an increment of vibration amplitude of $\lambda/2(\cos\alpha + \cos\beta)$

With increasing amplitude the maxima of the J_0^2 function

decrease in value and accordingly the bright fringes become less intense and the fringe visibility decreases. The form of vibration fringes, as given by equation (4.2), has been verified experimentally by LURIE et al (1968).

4.2 PRACTICAL ACCURACY OF HOLOGRAPHIC INTERFEROMETRY

Interferometry is established as a primary standard for the measurement of length, but, at the present stage of development of holography, HI falls far short of this status. It is known that in the method of holography as described here, certain imperfections can apply, including:- emulsion movement; temperature change in the time interval between comparing the two common paths; wavefronts that are not smooth to wavelength tolerances due to the use of less than top quality optical elements; uncertainty in the (laser) source wavelength. These features, which collectively may be termed practical imperfections, are particularly significant in real time HI. The literature up to 1968 showed that whilst the theoretical accuracy of HI had been discussed or implied, little had been reported on practical accuracy. Therefore this topic was investigated, mainly experimentally, as a continuation of the early experiments reported in the previous section. The aim was to establish the accuracy of applying equation (4.1) for measuring displacements, and to assess the effect of the above practical imperfections on the accuracy.

The change in a given optical path length due to temperature change can be predicted. Using the equation derived by BARRELL and SEARS (1939) for the refractive index of air,

as a function of temperature, pressure, and partial pressure of water vapour, it is calculated that the change in refractive index is one part in 10^6 per centigrade degree change. (For a change in pressure of one millibar, the refractive index change is one part in 4×10^6 .) Thus over a metre path a temperature change by 1° C would cause a shift to an interferogram by 1½ fringes. When calculating a surface displacement by HI, the error in assuming that the refractive index of air is unity is only three parts in 10^4. The size of displacements encountered is so small that for engineering purposes this error is negligible. Therefore the factor μ in equation (4.1) is disregarded throughout this thesis. With regard to uncertainty in laser wavelength, the gain curve width for the He-Ne lasers used in this work is of the order of 1700 MHz. Thus the uncertainty in the wavelength, even accounting for mode drift, is less than one part in 10^5 , and again can be neglected in engineering work.

Initial experiments to investigate the accuracy of applying equation (4.1) for displacement measurement were done using an improved version of the cantilever object shown in Fig. 3.2. This new cantilever object was machined from a single piece of steel to ensure built-in rigidity at the cantilever base, and is shown in Fig. 4.3. Displacement of the cantilever was by means of a 40 threads per inch screw hollowed out at its end to take a ball bearing which pressed against the cantilever. Fringes were counted, relative to the base, at the level of the displacement screw. The cantilever was vertical, so its displacement was assumed to be horizontal, and illumination and viewing paths were

arranged to be in this horizontal plane. Fig. 4.4 shows the results of fringe numbers observed, in real time, plotted against the angle at which the screw was set. By reading the protractor against a knife edge the accuracy of setting was ± ⅛ degree. This corresponded to displacement resolution of 10 microinches (0·25μm) though the quality of the thread would not justify any analysis based on this figure. Fringe numbers were estimated by eye to the nearest ¼. It is seen that all plotted points fell within these error boundaries. This result indicates the degree of accuracy obtainable in real time work using basic technique. However the poor resolution of the screw displacement, together with the limited range over which the live fringes could be counted directly, did not afford an assessment of practical imperfections.

The limitation of a mechanical screw for independently measuring displacement showed that an instrument of at least equal resolution and precision to that of HI was required. Accordingly a new experiment termed a "Michelson assessment" was devised, using a Michelson interferometer as the independent means of measurement. The holographic object was a vertical plate mounted on a translating horizontal slide running on three ball bearings in two machined, straight vee grooves. This slide was driven by a micrometer spindle acting through a lever with a reduction of about 12:1 enabling fringes to be counted in real time as the object was translated. Mounted on the far side of the object was a plane mirror, to form the adjustable arm of the Michelson interferometer. Both interferometers used light from the same He-Ne laser. The selected point on the object was

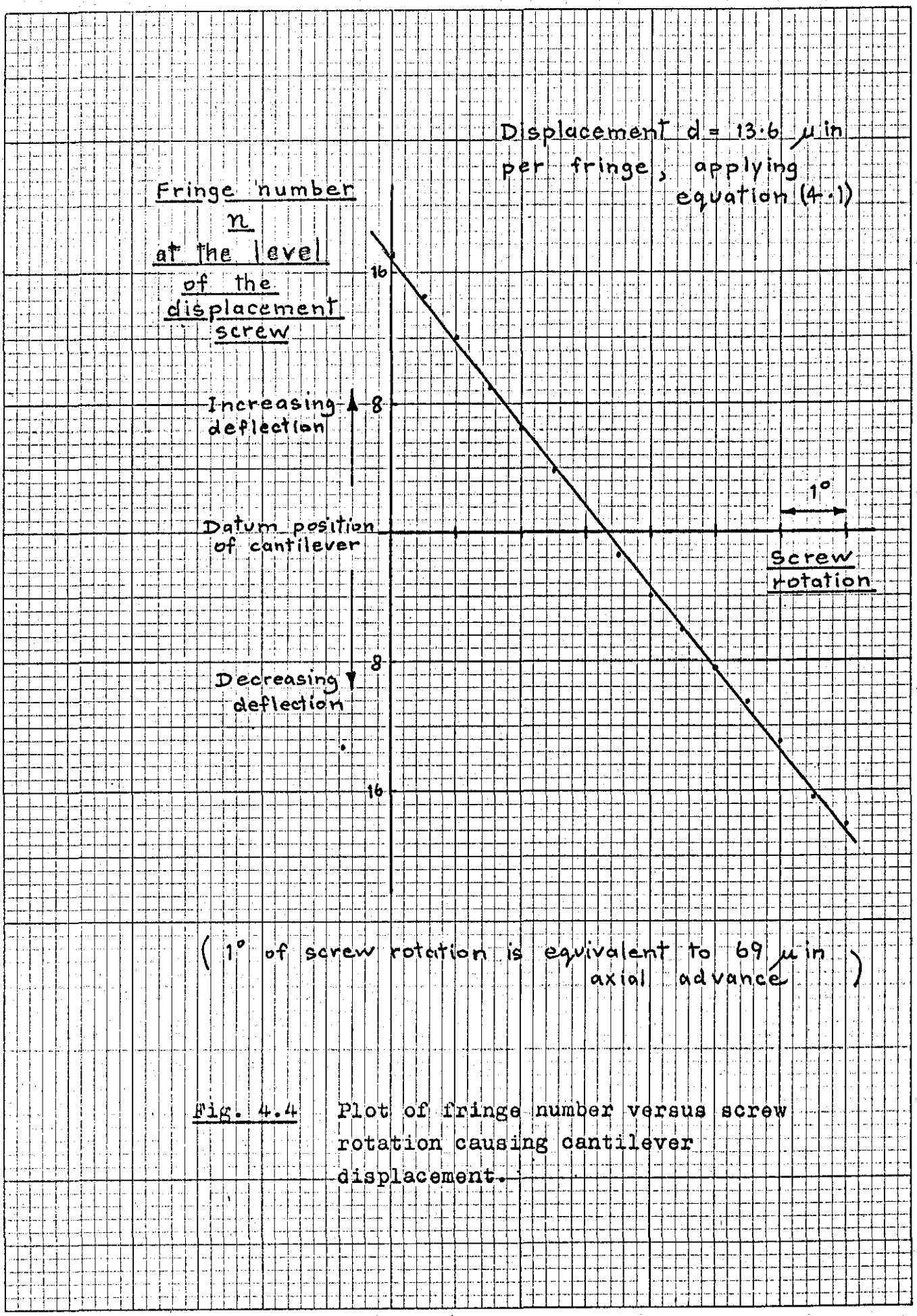

Fig. 4.4 Plot of fringe number versus screw rotation causing cantilever displacement.

illuminated at an angle of 31.5° ($\pm 1^{\circ}$) and viewed at an angle of 1° ($\pm 1^{\circ}$), both angles being with respect to the displacement direction. Having set up the interferometers, with suitable apertures to define the viewing directions, the procedure was to count fringes in both simultaneously, in real time. Since no electronic fringe counter, or other means for recording, was available, the counting had to be done by eye. Two observers were therefore necessary, one to each interferometer. It was found that 50 to 60 fringes was the maximum that could be counted before eye fatigue set in. Even so it was apparent that an error of one fringe was quite probable. Therefore a series of counts was taken, all in one session. The results of a series of nineteen counts is shown graphically in Fig. 4.5, plotting the number of fringes in the respective interferometers along the two axes. The scatter about the best line, determined by Least Squares, suggested a few miscounts of one fringe. Also, estiminating the final number to the nearest half fringe contributed to the error.

In comparing the measurements of the object displacement by the two interferometers, the error in fringe counting was treated statistically. Combining this with the possible error in the measurement of angles α and β gave a probability of 99.9% that the overall experimental error did not exceed $\pm$ 1.5% . During the period of the fringe counts the laboratory temperature changed by 1°F . It was considered that the likely change during a single count would cause negligible error in the differential fringe count for the two interferometers. It was found that the holographic analysis of the object displacement, applying equation (4.1), agreed with the

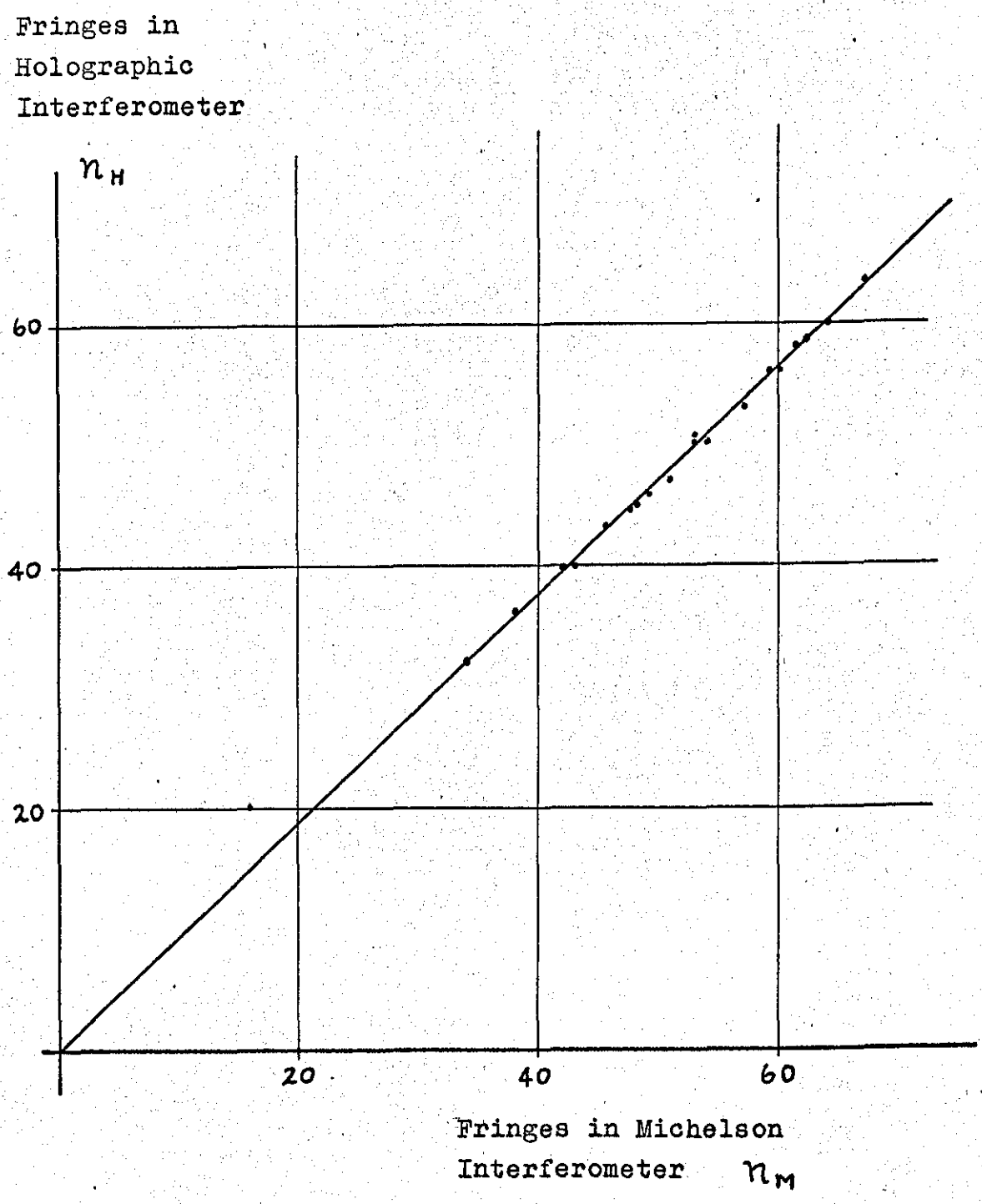

Fig. 4.5 Results of the "Michelson assessment" :- a plot of simultaneous fringe counts in the two interferometers.

Michelson interferometer measurement only just within the limits of the error. Thus practical imperfections did not have so large an effect as to cause the discrepancy to be greater than the limit of accountable error, but it remained inconclusive whether some small effect within the bounds of the estimated error was present.

As a consequence of this result a final experiment was devised to drastically reduce the accountable experimental error. The largest source of error had been fringe miscounts, and therefore a holographic interferometer was arranged in which object displacement caused no path change. Ideally the fringe order number would remain constant regardless of the amount of object displacement, and so the experiment was termed a "null path change test". In addition, error in measuring the angles α and β was greatly reduced by making both angles zero. These conditions were satisfied using a ground glass screen as an object, mounted on the same translation slide used in the Michelson assessment. It was illuminated by a collimated beam from behind, and viewed by transmission such that the displacement, illumination and viewing directions were all co-linear, as shown diagramatically in Fig. 4.6. Great care was taken to align these paths, and the estimated error in the angles was such that a displacement along AB of at least 0.160 in (4.05 mm) would have been necessary to cause ¼ fringe shift in the observed interferogram.

Again the experiment had to be carried out in real time, but the fringe observation in this case was far less prone to error than in the "Michelson assessment". The experiment was carried out in the quietest conditions possible in the

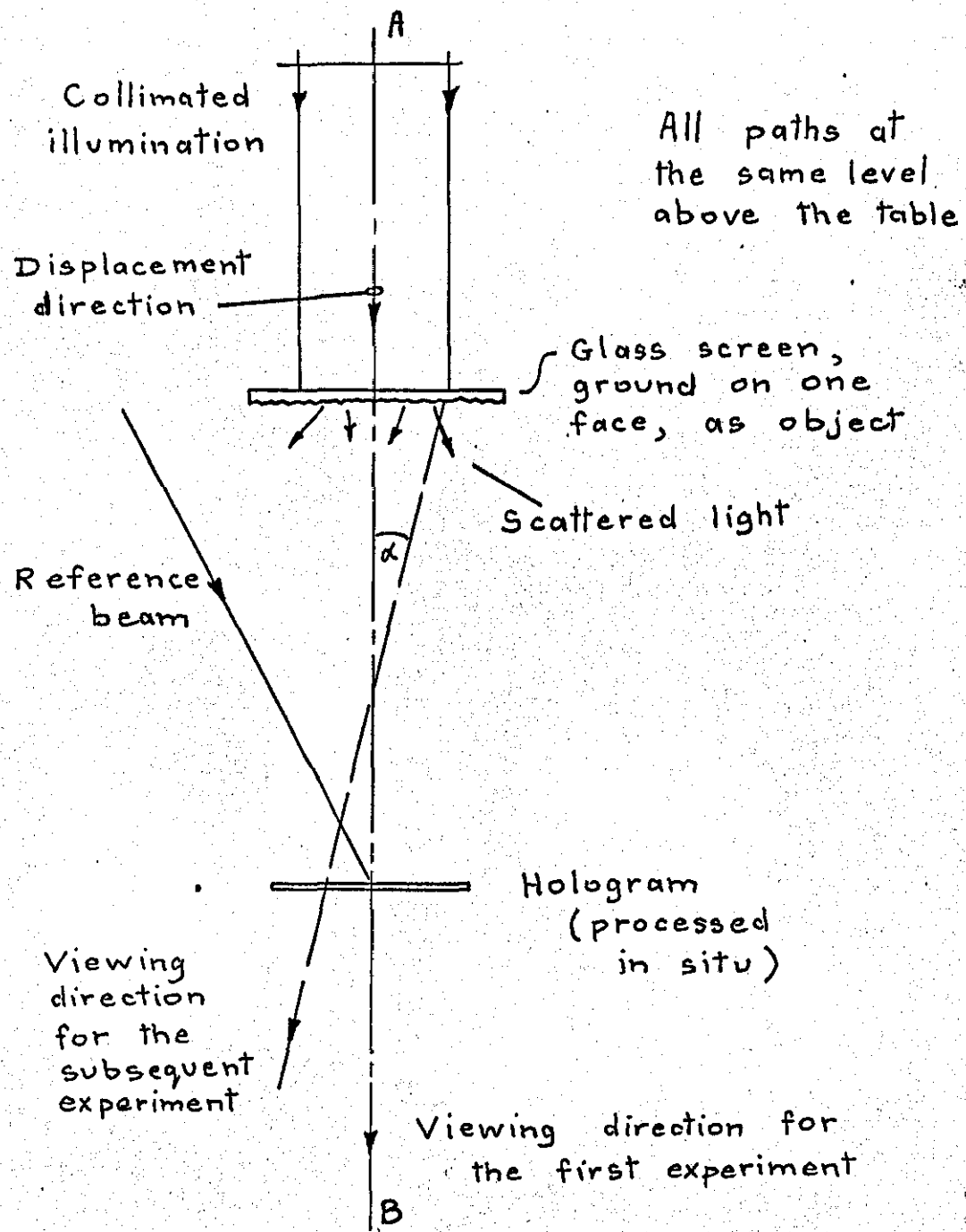

Fig. 4.6 The arrangement of the interferometer for the "null path change test".

laboratory. Displacement of the object was remotely controlled and the temperature varied by less than ½° F during a test consisting of several displacements. Despite the precautions taken, random shifts of the fringe pattern by ¼ fringe were experienced, usually followed by a return to the original condition within a few seconds. It was considered that a shift by ¼ fringe could reliably be judged by eye. Therefore the procedure was to translate the object until a fringe shift by one quarter had developed. In one test this was done six times, using different parts of the slide's range of movement. The (mechanically) measured displacements for the six observations ranged from 0.005 in (0.13 mm) to 0.016 in (0.41 mm) and averaged 0.009 in (0.23 mm). Thus, the observed fringe shift was far greater than that allowed by the calculated experimental error. However a significant feature was that slight fringe shifts of less than ¼ fringe occured suddenly, rather than continuously and gradually, suggesting unevenness in the slide. It was calculated that ⅛ fringe shift could be caused by unevenness such as to produce 250 μin (6 μm) lateral movement of the ground screen. This was a likely explanation; other possible causes were small air disturbances due to temperature gradients within the room and due to human presence. It was considered that emulsion instability would have only relatively long term effects, and could not have caused these sudden fringe shifts.

In order to obtain a positive measurement using the same real time hologram, a viewing direction at the largest possible angle (α) was subsequently selected, shown in Fig. 4.6. Due to limited apertures, this value of α was only 4° ($\pm$0.4°).

The value of the factor ($\cos\alpha + \cos\beta$) was thus 0.0028, with a possible error of ± 0.0006. Consequently the sensitity of this arrangement was one fringe shift per 0.009 in (0.23mm) of displacement (± 0.002 in, ≅ 0.05 mm). Two observations were made, each time translating the object so as to cause a fringe shift of one fringe. The mechanically measured displacements were 0.011 in (0.28 mm) and 0.007 in (0.18 mm) respectively. These results were both satisfactorily within the limits of experimental error, considering the additional possible error of ± ¼ fringe in judging the fringe number.

This experiment successfully demonstrated the practicability of measuring displacements (in a known direction) of up to several thousandths of an inch, working to a fraction of a fringe. The effects of practical imperfections were limited to the bounds of experimental error, which in this case was ± ¼ in the fringe order number. (A quarter of a fringe in this experiment represented 90 wavelengths of displacement, but equally well it could represent ⅛ wavelength of displacement, at maximum sensitivity.) The last of the results in this null path change test were obtained 24 hours after making the hologram (processed in situ), and during this interval a couple of fringes had developed over the 1 in (25 mm) DIA circle of illumination at the ground screen object. These fringes were attributed to either emulsion creep or temperature change, or a combination of both. Such spurious fringe formation is concluded to be a long-term effect, insignificant (beyond the possible error already noted) during relatively short observations lasting some minutes. (However these spurious fringes

would be troublesome in a situation requiring comparison of fringe order numbers at different points of the object.)

These experiments narrowed down the effects of practical imperfections to the limits of experimental accuracy obtainable by basic technique. To have investigated deeper would have required considerable sophistication, including laboratory temperature control, fringe counting instrumentation, and mechanical devices and optical elements to finer tolerances. Therefore the topic was not pursued further.

To summarize, these experiments have shown that when working in real time accuracy is limited to ± ¼ fringe due to human presence and random disturbances such as air temperature gradients. Practical imperfections, which would require sophisticated equipment and procedure to evaluate, have been shown to be limited in effect to ± ¼ fringe, over a short term of some minutes. Besides these sources of error, the accuracy of applying equation (4.1) to measure surface displacement (in a known direction) is concluded to be limited to the error in measuring angles α and β, and in determining fringe order numbers. As noted the effective error from measuring angles α and β becomes smaller as these angles approach zero. In judging fringe order number the unaided eye can achieve little better than ± ¼ fringe when observing a virtual interferogram over an image. The "Michelson assessment" demonstrated the need for automatic fringe counting apparatus for dynamic work. (It also inspired great admiration for the manual fringe counting feats performed by Michelson!)

4.3 INTERFEROGRAM ANALYSIS IN THE GENERAL CASE.

This chapter has so far considered only cases of surface displacement measurment in which the direction of displacement is independently known. When both the magnitude and direction have to be found by analysis, this being referred to as the general case, three separate data are required from the observed interferogram(s). This is apparent from equation (4.1), in which d, α and β are now unknown quantities. The problem of analysing an interferogram in the general case received the attention of a few researchers, and two basic approaches became established.

The first of these (HAINES and HILDEBRAND, 1966A, 1966B) was an analysis based on the form of the interferogram due to the displacement of a region of the object surface. The displacement of this region was considered as the combination of a rigid body translation and rotation. It was proposed that co-ordinate components of the translation and rotation could be determined by first measuring the fringe spacings in the two co-ordinate directions lateral to the line of sight. In addition it was necessary to measure the distance along the line of sight of the fringe localization from the object (image) surface, and then to repeat the measurments of fringe spacings in the two lateral directions using a different line of sight.

The other approach, proposed by ALEKSANDROV and BONCH-BRUEVICH (1967), was a development of a basic equation (in principle, the same as equation (4.1)) relating the displacement of a point in the object surface to the phase

change in the optical path via that point. The principle of their analysis was to determine the change to the interferogram caused by altering the viewing direction. This was done by counting the number of fringes which passed the line of sight to one chosen point in the image, while changing the viewing direction(within the aperture of the hologram). Repeating this procedure twice, using such parts of the hologram so as to obtain independent data, yielded three simultaneous equations, with the three components of displacement referred to a selected co-ordinate system as the unknowns.

Thus, whereas the first analysis required the measurement of fringe spacings and the position of localization, the second required fringe counts related to measured directions within a co-ordinate system. Neither required knowledge of the absolute fringe order number. Thus it is apparent that not all the information available about an interferogram is needed to solve point displacements.

In assessing these two approaches to the problem it as seen that the former makes the basic assumption that the region of the surface around the point of interest behaves as a rigid body. In contrast, the latter analysis considers only a single point, independent of the rest of the object, and in this respect it can be regarded as a more general form of analysis. The reason (in part) for assuming rigid body movement, in Haines and Hildebrand's analysis, is effectively to enable the position of fringe localization to be predicted. The position of localization is taken to be that at which the fringes have maximum visibility, and it depends on the nature of the surface displacement and the conditions of illumination and viewing. VIENOT et al (1968)

and others have derived relationships for the distance of localization from the object surface for specific translations and rotations of the surface. However when the surface suffers flexural deformation, the prediction of fringe localization becomes extremely difficult, and the fringes are unlikely to localize in one single plane. It is common experience that in such cases the fringes appear at or very close to the surface. Moreover fringes caused by surface flexure have varying spacing. The majority of engineering investigations using HI involve flexural deformation, often with curvature in two directions in the surface. Therefore it was concluded that Haines and Hildebrand's analysis was inappropriate as a general method for measuring displacements in engineering components.

In comparison, Aleksandrov and Bonch-Bruevich's analysis appeared to be applicable whatever the form of displacement. However, they gave no experimental results, so in order to assess the practicability of the method, it was applied to a simple case of displacement measurement. For this, a plate mounted rigidly on a translation slide driven by a micrometer spindle was used as the object, to enable the displacement of a selected surface point to be conveniently measured with sufficient accuracy. The fact that this was a rigid body translation did not remove generality from the assessment of the method. Cartesian axes were selected with two in the plane of the table surface and the third perpendicular. The translation slide was arranged to give finite components of displacement on all three axes. In order to obtain appreciable changes of viewing direction through the hologram, a full size plate (9 x 12 cm) was used, arranged close to the object. Either the real time or the double exposure technique

could have been used, but the latter was chosen to simplify the procedure. A relatively large translation of 0.0086 in (0.22 mm) was applied to the object between exposures, to provide plenty of fringesshifts when altering the viewing direction.

For fringe observation, four small apertures, each defining a viewing direction, were set up on the observation side of the hologram, as shown in Fig. 4.7. The fringes were found to localize on the observation side of the hologram. This caused a little difficulty in observing fringes against the selected point in the image, but in fact it was possible by eye to assign a relative fringe order number to within half a fringe. Some initial counts were made to verify that in moving between two apertures the number of fringes observed was independent of the route taken. To account for fringe movements in opposite senses, positive and negative signs were arbitrarily assigned to the respective directions. Fringe counts were made starting at aperture No. 1 in each case, and were repeated to obtain agreement within one fringe. (As with the "Michelson assessment", an error of one fringe in a count of about 50 was found to be not uncommon.)

The analysis is outlined as follows, starting from equation (4.1):-

$$n_1\lambda = d(\cos\alpha_1 + \cos\beta)$$

where the subscript (1) refers to that viewing direction. Thus in altering the viewing direction the observed number of fringes crossing the line of sight is (n_2-n_1) given by:-

$$(n_2-n_1)\lambda = d(\cos\alpha_2 - \cos\alpha_1) \qquad \ldots(4.3)$$

The angle α is the angle between the displacement direction and the respective viewing direction. Both directions are

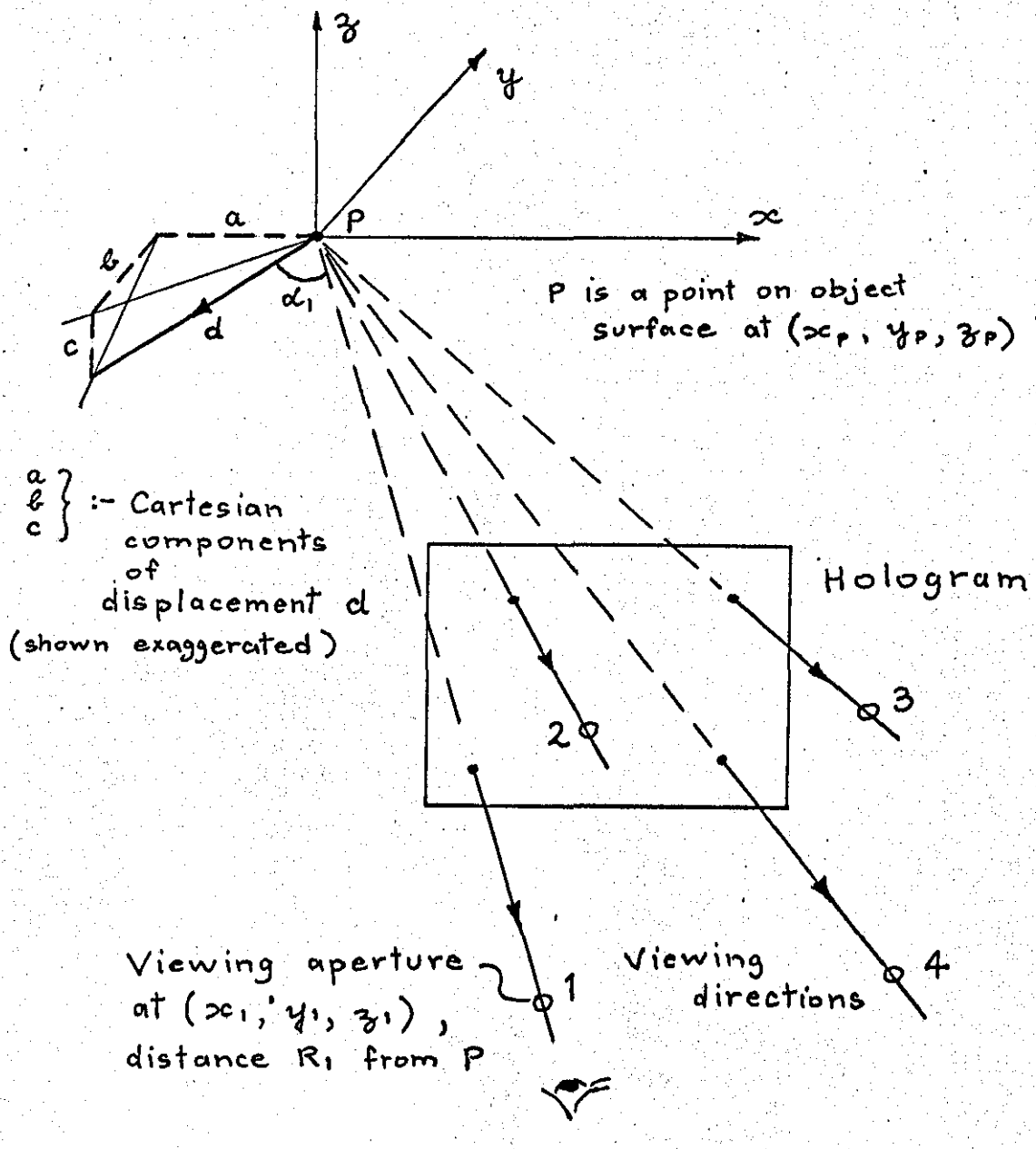

Direction cosines for viewing direction № 1 :-

$$\cos\alpha_1 = \left(\frac{x_P - x_1}{R_1}\right)\frac{a}{d} + \left(\frac{y_P - y_1}{R_1}\right)\frac{b}{d} + \left(\frac{z_P - z_1}{R_1}\right)\frac{c}{d}$$

Fig. 4.7 The four viewing directions used for displacement measurement by Aleksandrov and Bonch-Bruevich's analysis.

expressed as direction cosines, referred to the x, y, and z axes. Thus $\cos\alpha$ is expressed as

$$\cos\alpha_1 = K_1 K_p + \ell_1 \ell_p + m_1 m_p$$

in which $K_p = a/d$; $\ell_p = b/d$; $m_p = c/d$;

and $K_1 = (x_p - x_1)/R_1$
$\ell_1 = (y_p - y_1)/R_1$
$m_1 = (z_p - z_1)/R_1$

where a, b, c are the components of the overall displacement d shown in Fig. 4.7, x_1, y_1, z_1 are the co-ordinates of viewing aperture No.1, and R_1 is the distance of this aperture from the point P.

Thus equation (4.3) is rewritten as :-

$$(n_2 - n_1)\lambda = \left(\frac{\Delta x_2}{R_2} - \frac{\Delta x_1}{R_1}\right)a + \left(\frac{\Delta y_2}{R_2} - \frac{\Delta y_1}{R_1}\right)b + \left(\frac{\Delta z_2}{R_2} - \frac{\Delta z_1}{R_1}\right)c \quad \ldots(4.4)$$

in which Δx_1 stands for $(x_p - x_1)$, etc. The Δx, Δy, Δz and R_1, R_2 terms are calculated from the measured co-ordinate positions. Corresponding equations to (4.4) are obtained for the other two routes varying the viewing direction. Thus three simultaneous equations are obtained, which are then solved for a, b and c.

Having taken averaged fringe counts in the experiment described, the component displacements thus found are shown in Table 1, together with the component displacements calculated from the micrometer readings.

Direction	Displacements by fringe analysis (10^{-3}in)	Displacements as directly measured and calculated (10^{-3}in)
x axis	-6.7	-5.3
y axis	-11.7	-6.8
z axis	+1.02	+0.32

Table 1

Although the relative signs of the x, y and z components were given by the fringe analysis, there was no means of finding the direction of the displacement d. (In such cases

a repeated experiment in real time may be necessary to determine this, as previously noted.) The accountable error in the directly measured components was ± 5%. This indicated that the results by the fringe analysis were highly inaccurate. In fact, an examination of the errors involved revealed that large errors were probable in calculating direction cosines from the measured co-ordinates, due to small differences. This led to a possible error in the component displacements of greater than 100%. There was no reason to doubt the validity of the method, since it was an extension of the basic equation (4.1), which has been proven not only in this thesis but by other workers also.

No attempt was made to repeat the measurement for improved accuracy, since the general feasibility of the method had now been demonstrated. Its main weakness is clearly the tendency for high experimental error, due mainly to the limited angle subtended by a hologram at an object. It has subsequently been noted (SOLLID, 1969) that in the case where the zero order fringe exists and can be identified, the method can be modified to counting absolute fringe order numbers, in three widely spaced viewing directions by means of three separate holograms. This should improve accuracy considerably, but the complexity for recording three holograms simultaneously is objectionable. High error could be expected (in the original single hologram method) when the surface displacement is small (say, about fifteen wavelengths) because the number of fringe shifts would then be very few. This implies the need to determine accurately fractional fringe orders. In principle this could be accomplished with photo-detectors, though the instrument would need

to be sophisticated to provide the required scanning movement with the facility to focus over a very wide range. If such an instrument incorporated the means of accurately measuring co-ordinate positions, the method would of course become attractive for measuring the displacements of many surface points, solving the equations by computer. However, as yet no application to justify the development of such equipment is apparent.

It is concluded that the measurment of surface displacement in the general case, by the method of Aleksandrov and Bonch-Bruevich, or variations thereon, is a laborious procedure prone to appreciable experimental error. It is however generally applicable to any form of surface movement, whereas the analysis forwarded by Haines and Hildebrand depends on non-flexural movements and is therefore inapplicable for most engineering investigations. The position where fringes localize is of limited use as a source of data in analysing surface displacement, because it is predictable only for simple rigid body translations and rotations, and is a difficult quantity to measure.

4.4 A NEW METHOD FOR DETERMINING THE RELATIVE SENSE OF FRINGE ORDER NUMBERS.

It has been noted that fringes representing a shortening of an optical path due to surface movement cannot be distinguished from those representing an increase of path, by their intensity or static form. Likewise a single static interferogram, as produced by double exposure HI, does not reveal whether adjacent fringes have an increasing or a decreasing order number. When counting fringes between

separate image points, whether to find the absolute fringe order number or simply the relative number, it is essential to determine the relative sense of the fringes, i.e. whether the order number continues in the same direction so:-

.... n, n+1, n+2, n+3, n+4 ....

or alternatively reverses its direction so:-

.... n, n+1, n+1, n, n-1 ....

As noted earlier, this ambiguity can be solved by conducting the test in real time and observing the movement of the fringes whilst judiciously applying extra displacements to the object. However, this can be inconvenient, for it is time-consuming and does not give a permanent record. The following method to be described was devised in the work of this project, as an alternative, practically more convenient method for determining the relative sense of the fringe numbers. It involves the recording of a second double exposure hologram.

Consider the sketch of the imaginary fringe pattern shown in Fig. 4.8(a). The square frame shows part of an interferogram, representing normal displacement of a surface. When the whole frame is present it is obvious that the deformed shape is a hill (or a hollow), such that the cross-section at AG is as shown in (e). However, if only a thin band of the interferogram, shown dashed, was present - representing, for example, a bar in flexure - an alternative valid interpretation would be as shown in (f). This example demonstrates the ambiguity to be resolved.

The method depends on the principle of superposition. If an optical path in an interferometer suffers successive path length changes, the overall fringe order number produced is the sum of the effects of the individual changes.

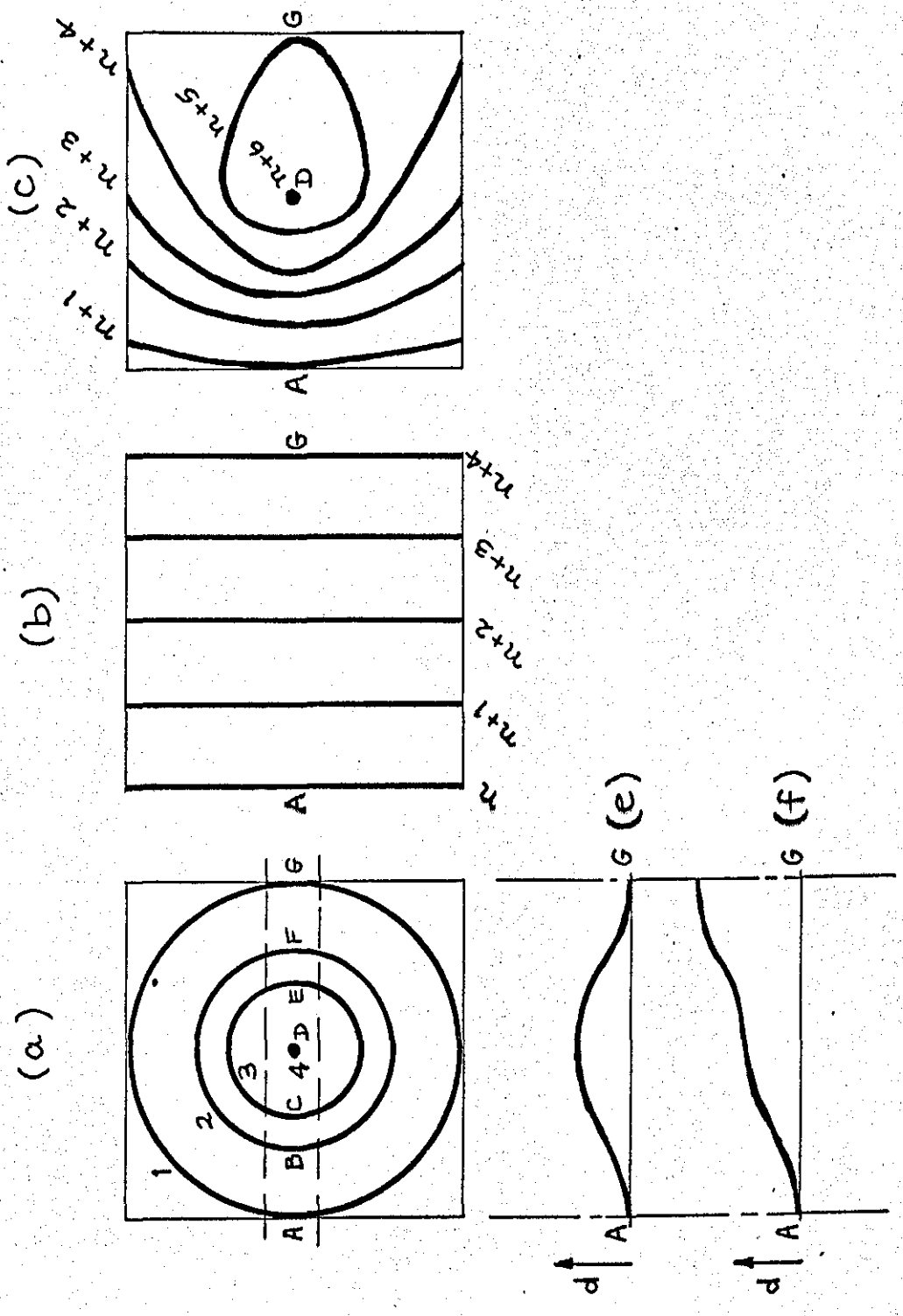

Fig. 4.8 Superposition of fringe patterns;- Superposition of (a) and (b) gives (c), Cross-sections (e) and (f) show possible interpretations of (a) when the fringe numbering is unknown.

Extending this to the case of a broad interfering beam, if two deformations across the beam aperture are introduced, then the resultant interferogram is the sum of the two interferograms which separately would be produced. This resultant can be determined by adding fringe order numbers at corresponding points of the two separate interferograms. Thus if the fringe numbering of one of these interferograms is known, the relative sense of the fringe numbering in the other can be determined by examining the form of the resultant.

This is explained by the sketches (a), (b), and (c) of Fig. 4.8. All three frames represent the same corresponding image space. The pattern in (a) represents surface deformation, while that in (b) represents a prescribed change in the object illumination beam, such as would be produced by a small rotation of a mirror directing this beam. Such a change causes a pattern of uniformly spaced fringes over the image, with a regularly advancing fringe order number across the field. Thus these fringes depicted in (b) may be numbered n, n+1, n+2, ..., and at this stage the choice of direction is arbitrary. The fringes in (a) are numbered to represent a hill (or a hollow), with increasing order number radially inwards. Having assigned fringe numbers for these two interferograms, the result of superimposing them is determined by adding fringe order numbers at corresponding points. The resultant is shown in (c). The significant feature of this pattern is its fringe spacings, compared with those of (a). Because the fringe order in (b) is constant along all vertical lines there is no difference in fringe spacings between (a) and (c) along corresponding vertical lines. It is along horizontal lines that the difference

occurs. Where the fringe orders in (a) and (b) are both increasing in the same direction, as between A and D, the fringe density in (c) is greater. Between D and G however, the fringe orders are increasing in opposing directions, causing the fringes in (c) to be more widely spaced. Thus the reversal in the fringe count along the line AG in (a) is established by the relative change in fringe spacings in (c). It is clear that had the fringe numbering in (b) increased instead from right to left, the pattern in (c) would simply have been reversed, likewise if the fringes in (a) had instead been numbered radially outwards. Also, considering the case of the narrow band from A to G, if the fringe numbering had progressed from 1 at A, to 7 at G, as depicted in (f), the resultant pattern would have been symmetrical about the central point D. In this case, the left hand side from A to D in (c) would have appeared the same, but the right hand side would have appeared as a mirror image of this.

Thus the relative sense of the fringes due to surface deformation can be determined. However, further deduction is possible if the absolute sense of the change causing the interferogram in (b) is known. Suppose that this is due to a mirror rotation such as to reduce the path lengths of all rays within the beam, with an increasing change from A to G. Then, examining the resultant interferogram in (c), wherever the fringes are more densely packed than in (a), the fringe numbering in (a) must be in the same sense as in (b). For the example given this is so between points A and D. Thus the surface deformation causing pattern (a) would have been such that relative to point A, point D had moved to become closer to the point of observation. That is, in the usual

convention of viewing the earth from the sky, the region would have deformed as a hill, not a hollow.

This method was verified by interpreting the deformation of the square plate object shown in Fig. 4.9. This object consisted of a 1/16 in (1.5 mm) thick flat steel plate, 3 in (75 mm) square, screwed to a rigid pillar and deformed by hanging small weights on a loading bar welded to the back of the plate at its free vertical edge. Double exposure HI was used, with one set of weights to apply a pre-load, and the second set added to apply an incremental load after the first exposure. The object was illuminated by a diverging beam, finally directed to the object by a large aperture mirror mounted with a facility to provide small controlled rotation. The interferogram caused by adding a set of weights is shown in Fig. 4.10. The pattern is seen to be virtually symmetrical about the horizontal line AB. Displacements at the corners D and F relative to the pillar were measured, from the interferogram, to be 9.7λ (assuming the deformation of the plate to be normal to its surface). From the manner of loading the plate, the directions of these displacements are obvious, but without this extra knowledge the interferogram can be interpreted ambiguously. It is convenient to call displacements away from the point of observation positive, and those towards, negative. Then the displacement at D could be positive, and that at F negative, or vice versa, or they both could be positive or negative.

In order to demonstrate that this uncertainty can be resolved, the double exposure hologram was repeated, but with a small rotation of the beam directing mirror in addition to the load increment. This interferogram is shown

in Fig.4.11. (For completeness of the explanation, the interferogram due to rotation of the mirror alone is shown in Fig. 4.12. In fact it was unnecessary to take this hologram in applying the method.) Fringes due to mirror rotation are evident along the object base, with a uniform spacing horizontally. Since, from Fig. 4.10, the plate distorted very little in the region of the screws, comparison between Figs. 4.10 and 4.11 is made over that part of the plate lying to the right of the vertical line 1 in from the left hand edge. Comparing fringes along the top edge CD, the interferogram of deformation alone shows 17 fringes between the 1 in and 3 in lines, whereas the composite interferogram shows 22 fringes. However, along the bottom edge EF, 17 fringes in Fig. 4.10 is reduced to 12 in the composite interferogram. Thus the displacements at D and F must have been of opposite sign, as predicted by the loading configuration. (It is to be noted that precise repetition of the loading of the object, when rotating the beam for the second hologram, is unnecessary. All that is required is a repeat pattern that is sufficiently like the first that significant changes in fringe density due to the beam rotation are clearly evident. From this aspect it is necessary to know roughly the fringe spacing due to the beam rotation.) Furthermore, the rotation of the mirror was such as to increase the optical path more so at the right hand edge of the plate, DF, than at the left hand edge, CE. Along the top edge CD in Fig. 4.11 an increased fringe density has resulted, indicating that the plate deformation must also have increased the optical path. Thus D's displacement was positive, i.e. away from the hologram, and by similar deduction F's displacement was negative. Again this

agrees with prediction.

This method of determining relative fringe sense was subsequently applied in an investigation of an engine casing model, in which certain displacements and surface strains were to be measured (see Chapter 5). The method was found to be convenient, requiring only the virtual duplication of double exposure holograms. This enabled many interferograms to be obtained in an experimental session, for later analysis, compared with taking real time holograms and doing part of the analysis at the same time.

4.5 QUALITATIVE FRINGE INTERPRETATION

In section 4.3 it was concluded that the measurement of displacement, in the general case, is a laborious procedure prone to error. By comparison, measurement in the case when the direction of displacement is known is simple, with faster and more accurate analysis. However, meaningful and useful deductions about surface deformation can be made without even the need to measure fringe positions, or to measure the geometry of the optical arrangement. When such precise measurements are not required the interpretation may be termed qualitative, depending on such features as the presence or lack of symmetry in the fringe pattern, and various irregularities like isolated rings of fringes, bunching, and discontinuities. This field of HI has become known as non-destructive testing, though in fact application of these principles extends considerably wider than the common meaning of inspecting materials for faults.

The common fringe features sought for in qualitative interpretation may be understood from the basic equation (4.1).

For example a set of fringes one inside the other almost always represents deformation as a hill or a hollow, analogous to contour lines on maps. This assumes that the direction of displacement is predominantly normal to the surface, which is in fact commonly the case for thin-walled structures. Also, making this same assumption, and making the small simplification that angles α and β do not vary over a small distance in the surface, then the spatial frequency of the fringes is given, from equation (4.1), by :

$$\frac{\Delta n}{\Delta s} = \{(\cos\alpha + \cos\beta)/\lambda\}\,\frac{\Delta d}{\Delta s}$$

where s is a direction in the surface crossing the fringes. In this, $\Delta d/\Delta s$ is recognised as the slope of the deformed surface. (Complications such as bodily translations and rotations are ignored here.) Writing this in the limit, and differentiating a second time gives:-

$$\frac{d^2n}{ds^2} = \{(\cos\alpha + \cos\beta)/\lambda\}\,\frac{d^2d}{ds^2} \qquad \ldots(4.5)$$

The quantity d^2d/ds^2 is the reciprocal of the radius of curvature of the deformed surface and, from beam theory, is therefore proportional to the surface stress. The left hand side of this equation is the rate of change of the fringe spatial frequency. The purpose of this approximate derivation is to show that a changing fringe spacing is representative of surface stress and strain due to flexure. Thus the feature of fringe bunching indicates a local stress concentration, though its detailed form can be difficult to infer. Fringe discontinuities over a surface can only be accounted for by discontinuities in the surface itself, such as cracks.

A few typical fringe features are shown in Fig. 4.13, a double exposure interferogram of the distorted end wall of an engine casing model (details in Chapter 5). Load was

applied to the centre shaft by a hydraulic cylinder in the right hand cylinder box (upper right), to represent a firing stroke. Since the casing was relatively thin-walled it was assumed that out-of-plane buckling displacements would be larger than in-plane displacements. Therefore it was both illuminated and viewed close to the normal to the surface, for maximum sensitivity to the former. This also enabled the object to be viewed squarely. In the large panel to the right of and above the centre shaft a typical contour system of fringes is present representing a hill (or hollow). Higher up, beneath the inclined web are a few instances of marked variation in fringe spacing, indicating relatively high stress. These positions would thus be favourable for strain gauging. In this way double exposure HI could be a valuable aid in experimental stress analysis. Finally, fringe discontinuities are observed over the horizontal join between the split casting that houses the shaft bearing. Thus the joining bolts could well have been insufficiently tightened, and consequently any strain gauge readings in this condition could have been unrepresentative.

Qualitative inperpretation of interferograms in this manner is finding application for detecting defects in materials and components of sandwich structure (WELLS, 1969) and laminated structure. Particular merits are that the procedure is usually quite uncritical. Tests can work over a considerable range of load causing deformation, and loading can take various forms such as force, pressure and heat. Due to the high sensitivity of interferometry, loading can be light, and sub-surface faults can be revealed. Information about the object is provided over the full field of view,

and significant features of its deformation are quickly deduced. Certain aspects of vibration analysis (HOCKLEY, 1969) involve qualitative interpretation, and the information gained can aid design, besides contributing to inspection.

4.6 CONCLUSIONS

The analysis of holographic interferograms can be undertaken using, as a basis, equation (4.1), which relates fringe order number to the change in the optical path caused by object surface displacement. When the direction of this displacement is independently known, interpretation is reasonably simple and quick. An extension of the use of this equation, in the form of a method proposed by Aleksandrov and Bonch-Bruevich, enables displacements to be measured in the general case, (for which their directions are unknown). However the experimental procedure and the analysis become laborious, and the displacements so determined are prone to high error. Consequently it is anticipated that a majority of HI applications will be directed to non-destructive testing and the simpler cases of quantitative analysis. This is proving to be so from known work, including investigations into the deformation of diaphragms and thin plates, vibration analysis of turbine engine components, and inspection of laminated and sandwich structure materials.

Accuracy of measurements of displacement by HI can be considered in two parts. Firstly practical imperfections, notably emulsion movement, and random air disturbances due to temperature gradients and human presence, have been found to limit accuracy to $\pm \frac{1}{4}$ fringe in a single 'reading'.

This was found to be so in real time work, when practical imperfections are especially prevalent. Secondly, there is accountable error due to error in measuring the angles α and β, and in assigning fringe order numbers. In principle, these sources of error can be reduced by attention to procedure, so as to achieve accuracies customarily associated with (classical) interferometry. In real time dynamic work observation by eye of virtual interferograms imposes a considerable strain. Photographic and video recording equipment form useful aids, but there is clearly potential for equipment that will scan and count fringes and fractional fringes, and process and store the data. Not only would this reduce certain errors, but would provide speedy and automatic analysis. In fact, an instrument recently developed by DAVIES et al (1973) is able to scan moire fringe patterns, compute fringe separations, and print out values of strain. Such an instrument would be valuable for HI analysis, though would require development to contend with the problems of fringe localization and poor visibility which can arise.

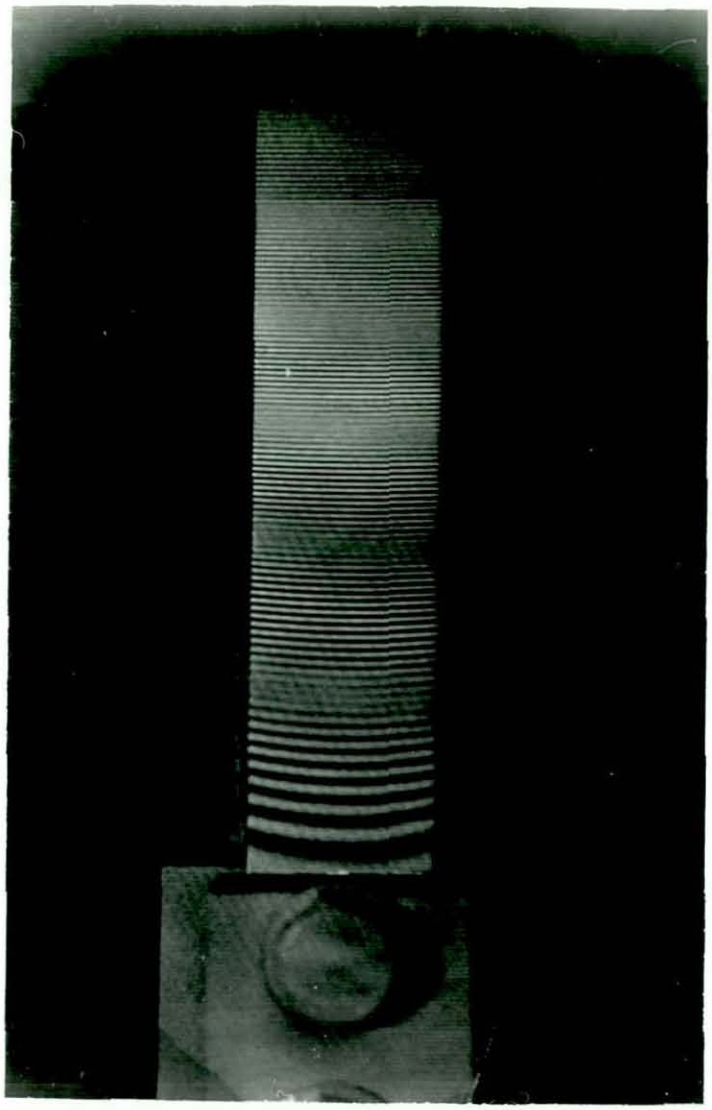

Fig.4.2 Cantilever deformation : beats of fringe visibility, obtained by two beam illumination

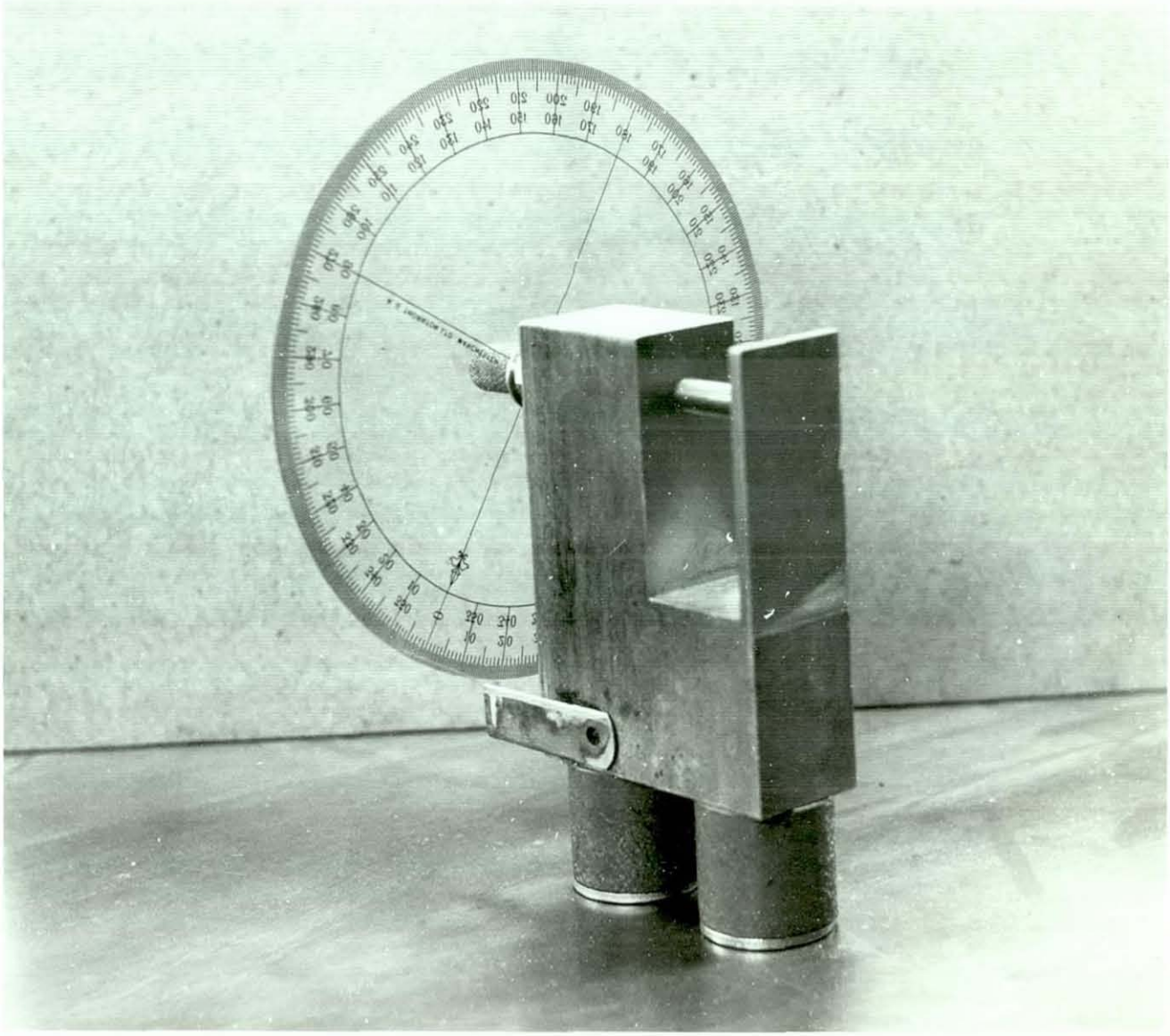

Fig. 4.3 The cantilever object of improved rigidity

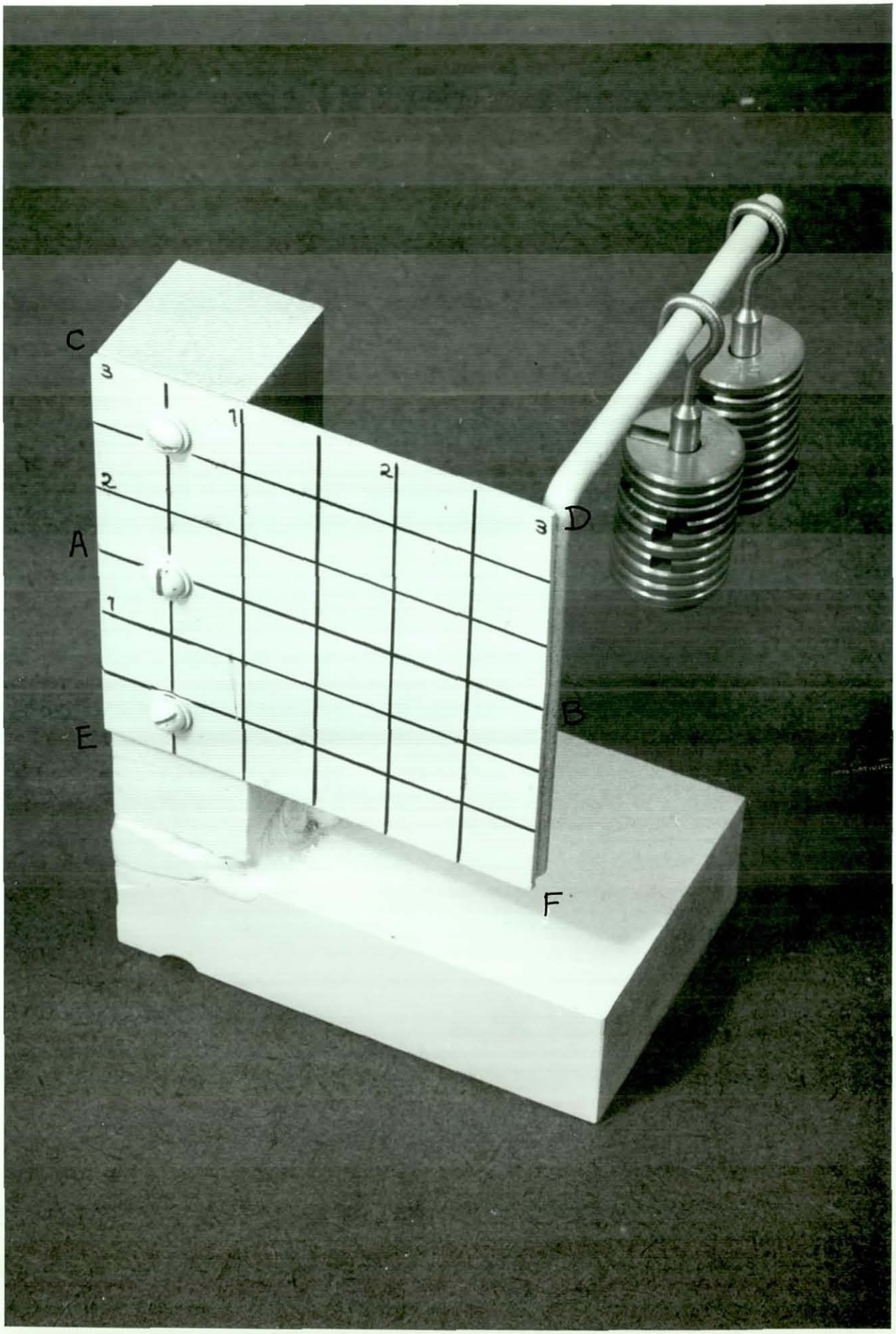

Fig. 4.9 The square plate object

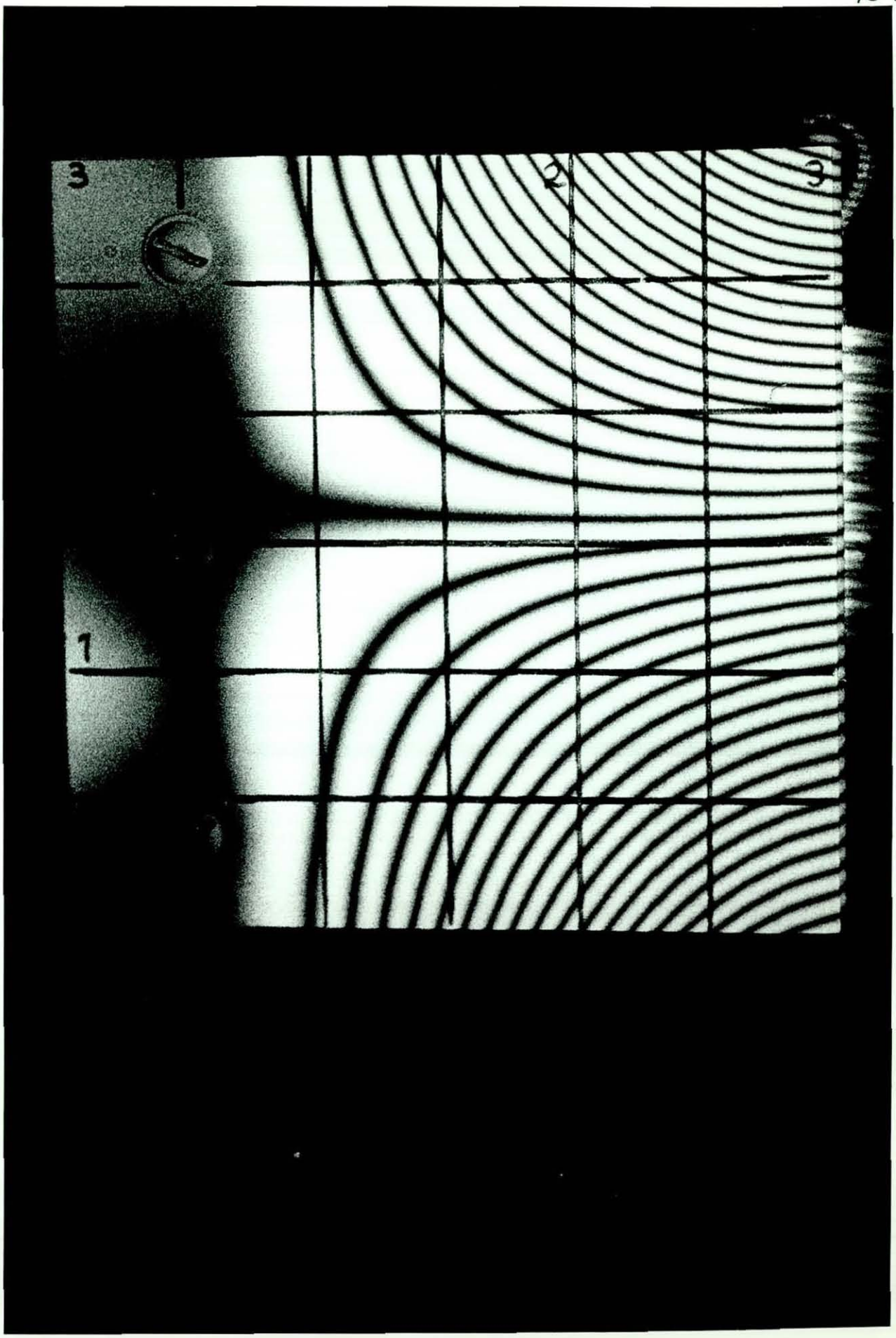

Fig. 4.10 Interferogram by double exposure HI of plate deformation due to an incremental load

Fig. 4.11 Interferogram due to the combined effects of an incremental load and a small rotation of the beam directing mirror

Fig. 4.12. Interferogram over the plate due to a small rotation of the mirror directing the object illumination beam

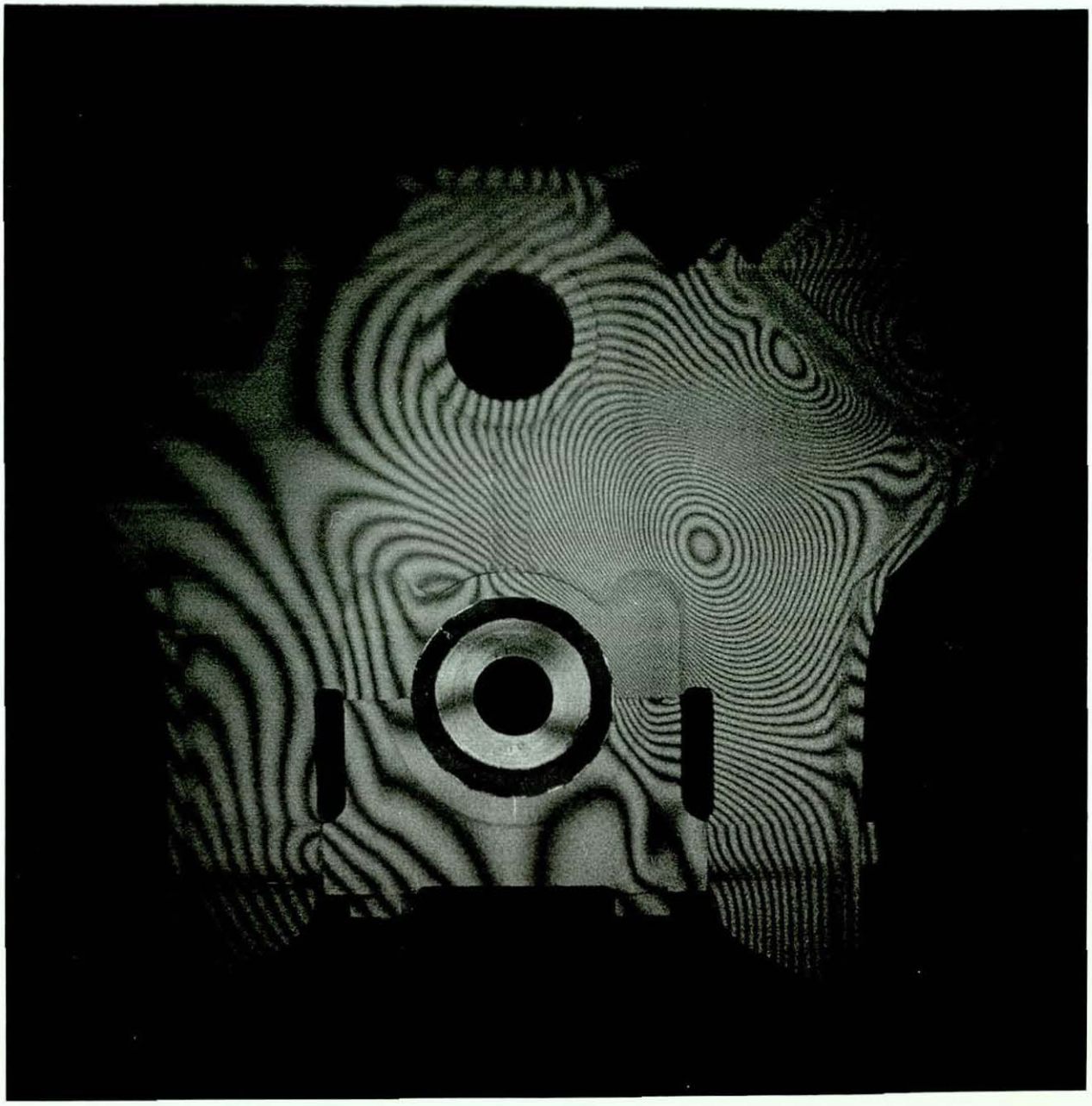

Fig. 4.13 Interferogram of the distorted end wall of the JV crankcase model

Chapter 5

ASSESSMENT OF AN ENGINEERING MEASUREMENT MADE BY HOLOGRAPHIC INTERFEROMETRY

5.1 INTRODUCTION

The last chapter examined the accuracy of HI for the measurement of surface displacement, in experiments specially devised for this purpose. Real life cases usually introduce experimental problems and restrictions, and consequently measurement performance falls short of that achieved under laboratory designed conditions. The present work to be described formed part of an industrial experimental stress analysis programme, and thus provided the opportunity to assess the use of HI applied to an engineering problem.

This work was done in collaboration with Ruston and Hornsby Ltd. As part of an engine development programme they had produced a perspex model of an engine crankcase in order to carry out some strain analysis. Load was applied to the casing by a hydraulic cylinder situated in one of the two cylinders, bearing on a shaft representing the crank shaft at the lower end and loading the cylinder head through six studs at the upper end. This represented a firing stroke in the cylinder. This loading arrangement is seen in the photograph of the model, Fig. 5.1. The base measured 15 in by 11½ in (38 cm by 29 cm) and the majority of the casing was made of 5/16 in (8 mm) thick clear perspex. For their own analysis 84 resistance strain gauges had been bonded to the

model. The object of the holographic analysis was to obtain maps of the surface in-plane strain distribution over selected flat areas of the model, for a known cylinder load. Ruston and Hornsby Ltd. supplied sample sets of strain gauge readings, to enable the accuracy and feasibity of the holographic method to be compared with strain gauging. This assessment was made using the results of the holographic analysis carried out on the side wall, cylinder A, shown in Fig. 5.2.

5.2 ADAPTATION OF A HOLOGRAPHIC METHOD OF STRAIN MEASUREMENT

As noted in Chapter 4 there is no direct in-plane equivalent of detecting the out-of-plane component of displacement. Since in-plane strain may be accompanied by out-of-plane displacement, its measurement falls in the category of the "general case", that is for which the resultant displacement direction is unknown. Thus a general method of analysis of the type by Aleksandrov and Bonch-Bruevich could be applied. However, by restricting interest to components of in-plane displacement in a single direction, the problem is reduced to two dimensions and is considerably simplified. Instead of obtaining three independent data, as in the general case, only two are required. A method using this principle was devised by ENNOS (1968), and was the basis of the method employed here. The following equations for the measurement of strain are derived from the basic equation (4.1) and the relevant geometry shown in Fig. 5.3.

Let the object surface lie in the xy plane, and let d be the displacement component of a point P in the xz plane. All ray paths lie in the xz plane, and consequently it is the component of in-plane displacement in the x direction that is detected. It is convenient to regard d as being composed of vector components u and v as shown. Then the interferogram from hologram (1) will be related to u and v by the equation:-

$$n_1\lambda = u(\cos\theta_3 + \cos\theta_1) + v(\sin\theta_3 + \sin\theta_1)$$

Similarly for hologram (2) :-

$$n_2\lambda = u(\cos\theta_3 - \cos\theta_2) + v(\sin\theta_3 + \sin\theta_2)$$

—— oo ——

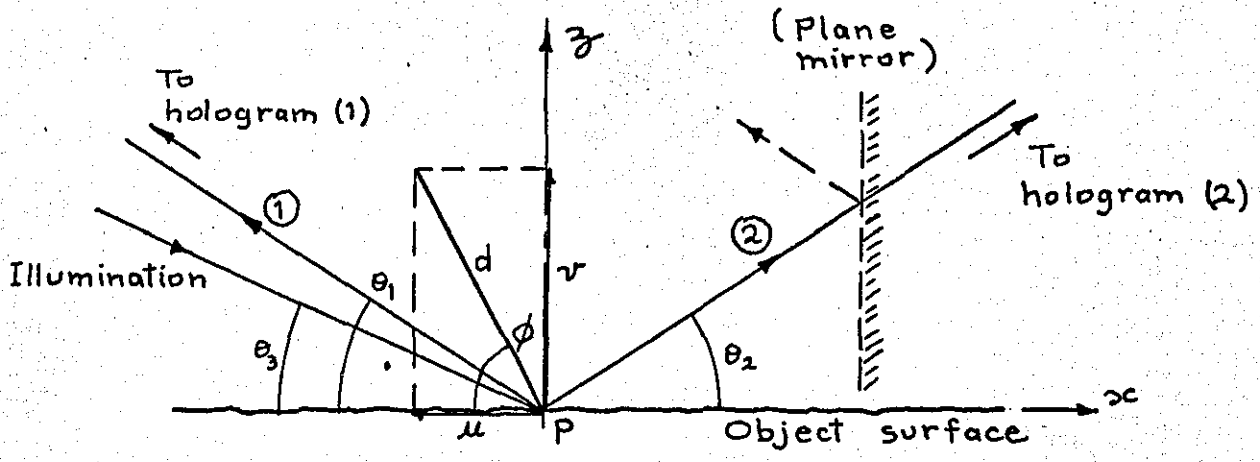

Fig.5.3 Relevant geometry for the method of in-plane strain measurement.

—— o o ——

If the two simplifying cases quoted by Ennos are simultaneously combined, that is, if $\theta_1 = \theta_2 = \theta_3$, the equations respectively become:-

$$n_1\lambda = 2u\cos\theta + 2v\sin\theta \quad \ldots\ 5.1$$

$$n_2\lambda = 2v\sin\theta \quad \ldots\ 5.2$$

Then by subtraction, the desired component u remains:-

$$n_1\lambda - n_2\lambda = 2u\cos\theta \quad \ldots\ 5.3$$

Suppose P and Q are two surface points, with displacement components as shown in Fig. 5.4. If θ in equation (5.3) has the same value at both points, this equation may be written for each using subscripts P and Q :-

$$(n_{P1} - n_{P2})\lambda = 2 u_P \cos\theta$$

$$(n_{Q1} - n_{Q2})\lambda = 2 u_Q \cos\theta$$

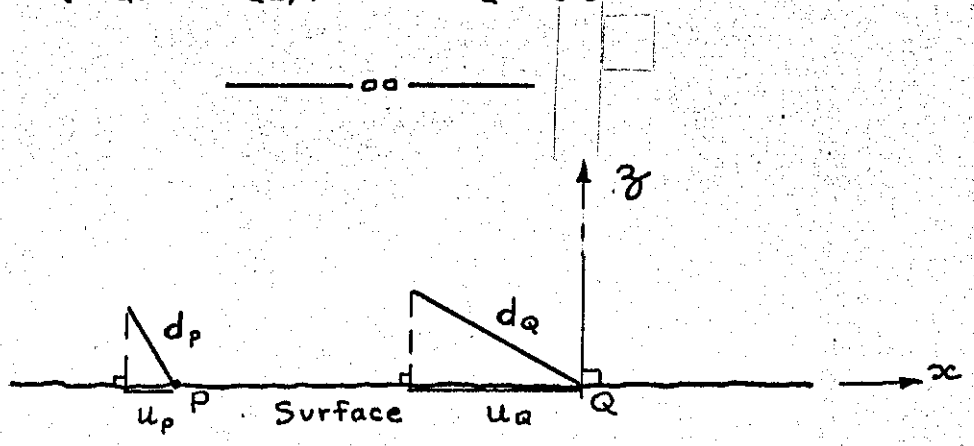

Fig. 5.4 Displacements at two surface points

The average strain, ϵ , in the surface along the line joining these two points is :-

$$\epsilon = (u_Q - u_P)/PQ$$

$$= (n_{Q1} - n_{Q2} - n_{P1} + n_{P2})\lambda / 2\cos\theta . PQ$$

$$= \{(n_{Q1} - n_{P1}) - (n_{Q2} - n_{P2})\}\lambda / 2\cos\theta . PQ$$

.... 5.4

Thus, strain in the x direction can be measured. It is seen that knowledge of the absolute fringe order numbers is unnecessary: relative fringe numbers are sufficient, providing the relative sense of the fringe order progression can be determined. Using the method explained in Section 4.4 to determine the fringe sense, the entire analysis can be done from frozen-fringe holograms, which has practical advantage over the alternative method of

determining fringe sense during a real time test.

5.3 HOLOGRAPHIC ANALYSIS OF THE CRANKCASE STRAIN

Procedure

Strain distribution over the side wall shown in Fig. 5.2 was required. It was considered that the highest strains would lie mainly in the vertical direction, nominated as the x direction, and therefore the model was lain over on its end face with the x direction horizontal, and an optical arrangement set up to detect displacement in this direction. It was desired to examine the complete wall, over its flat expanse up to the $x=7$ in line, in one go, this being a length of 6 in (15 cm) and a width of 11½ in (29 cm). In order to simplify the work of analysis as much as possible, equation (5.4) was to be used, though in practice, approximations had to be made as a consequence of this large surface area to be examined. There were no available optical elements to provide collimated illumination and telecentric viewing of such a large area. Therefore divergent illumination and direct viewing had to be used, causing the true angles $\theta_1, \theta_2, \theta_3$ to vary for different regions of the surface. To minimise this effect, both the point source of illumination and the hologram were positioned as far as possible from the model, 1½ metres away. The optical arrangement was such that angles $\theta_1, \theta_2, \theta_3$ were all equal to 32° for a region of the object near the middle of the wall. At the $x=1$ in line, θ varied by a maximum of 2° from this value. Thus in this case equations (5.1) and (5.2) were not strictly valid, with

consequent effects of varying sensitivity to in-plane displacement in the x direction, and a slight net sensitivity to normal displacement. Also there was slight sensitivity to displacement in the y direction.

Preparation of the model consisted of spraying the perspex surface matt white, and then drawing on an x-y grid of black lines, spaced by ½ in, so as to be able to identify surface points. Shadows were cast by two protruding bolt heads, and by a rib along the $x=0$ line, causing areas where analysis could not be done. To simplify the optical arrangement, a large plane mirror was positioned as indicated in Fig. 5.3, enabling both holograms to be recorded on one plate. There was found to be little difference between the intensities of light scattered in the two viewing directions. The illumination beam had to be blocked so as not to shine directly on to the mirror, otherwise there would have been two illumination directions. (In fact, this is the basis of another method of strain measurement, referred to in Section 5.5.)

A known load increment was applied to the model using the hydraulic cylinder actuated by a dead weight pressure gauge tester. One or two trials were necessary to find what load provided a workable number of fringes. After recording a double exposure hologram, another was recorded with an additional small rotation to the illumination beam, to enable the fringe sense to be determined as described in Section 4.4 Preferably the model would also have been examined to find strain distribution in the y direction, but circumstances did not permit this.

Analysis and Results.

Fig. 5.5 shows the two interferograms representing deformation of the side wall: that from viewing direction (1) on the left, and from viewing direction (2) (via the mirrors) on the right. (In fact the images are inverted top to bottom.) Examination directly from the hologram showed that the zero order fringe was not present. Comparison with the interferograms formed by the additional beam rotation enabled the directions of positive going fringe counts to be established as shown in Fig. 5.6. The (dark) fringes were numbered from zero upwards in the two cases, (these being relative fringe numbers). At this stage the positive going count was neither assumed to be a displacement towards the observer, nor away; its significance was in determining the relative sense of the two patterns. It was then apparent that one interferogram was virtually a mirror image of the other, indicating that out-of-plane buckling had dominated in-plane movement. At each grid point where fringes existed, the fringe order number was estimated, to the nearest ½ where possible. Fringe numbers at corresponding points in the two patterns were then subtracted, and, working along lines of constant y value, each new number was subtracted from that at the adjacent grid point. This was done in a consistent manner, taking account of sign. The numbers obtained represented the strain averaged over the ½ in 'gauge' lengths between grid points, and multiplication by the appropriate factor according to equation (5.3) gave the value of strain. The sign of the numbers

View 1
(direct)

View 2
(via mirror)

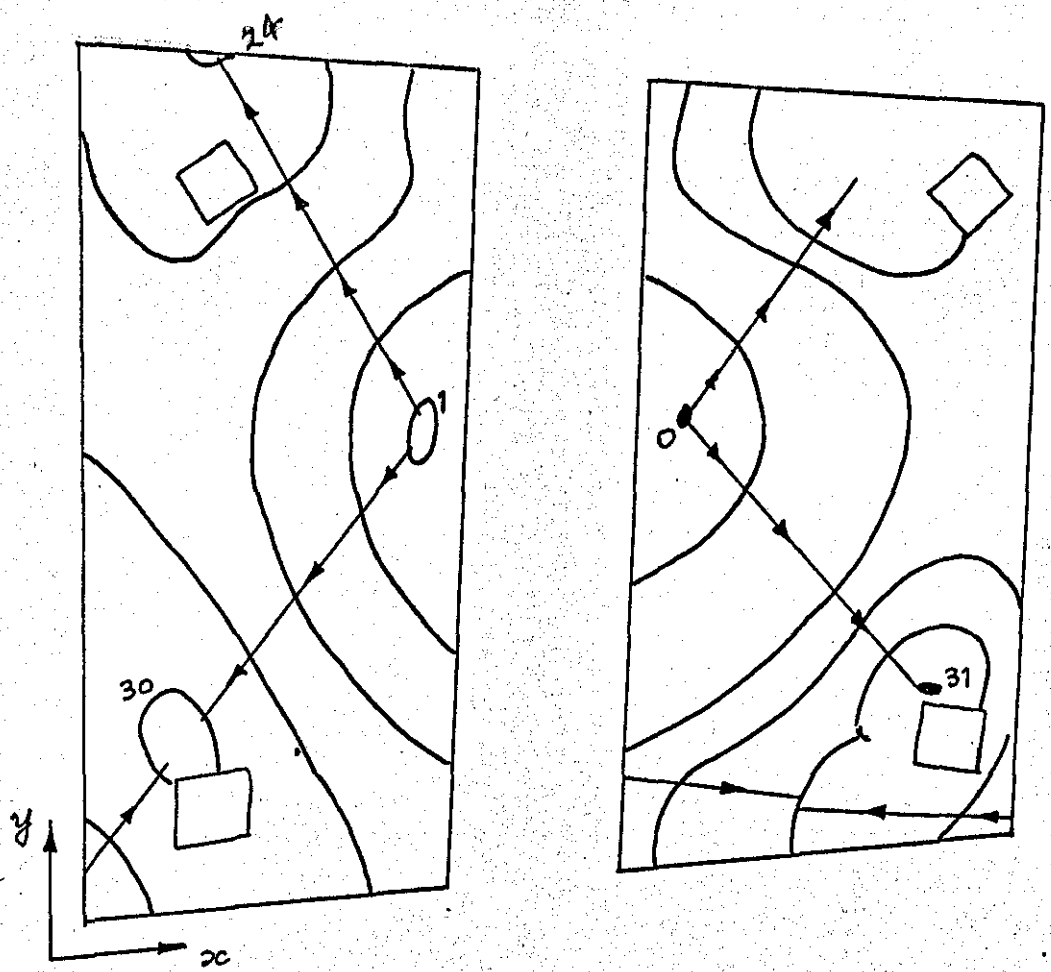

: +ve going fringe count

Fig. 5.6 Sketch from interferogram of Fig. 5.5, showing the fringe sense as determined.

did not reveal whether the strain was tensile or compressive, though a change of sign did mean a change from one to the other.

Selected direct strain results thus obtained are shown in Fig. 5.7, the values, in microstrain, appearing between their respective grid points (shown as dots). These values were scaled up by a factor of 1.4, to correspond to an applied load increment of 200 lbf (890 N), for direct comparison with the strain gauge results. Also shown on Fig. 5.7 are the positions of the three strain gauges used by Ruston and Hornsby Ltd., on this part of the model.

There is some indication of strain concentration around the bolts, though the extent of this is unknown due to the considerable scatter in the strain values. Even when the values along a y ordinate are plotted, the true strain variation remains questionable. This scatter is seen to be a consequence of experimental error and approximation. Near the centre of the wall, where $\theta_1 \approx \theta_2 \approx \theta_3$, equation (5.4) was accurately applied, and error was confined to the individual terms: fringe number n; λ ; $\cos\theta$; and gauge length. Of these, the most significant was error in estimating the fringe number, due to the subsequent subtractions. At best the fringe numbers were accurate to within a tenth, and the likely error in the final subtraction was estimated to be equivalent to ± 10 microstrain (scaled up by 1.4). For other regions where θ_1 differed from θ_2 error was additionally introduced, due to approximation in the value of θ, and due to a net sensitivity to out-of-plane displacement. The former caused up to $\pm 3\%$ error, but no generalisation about the latter

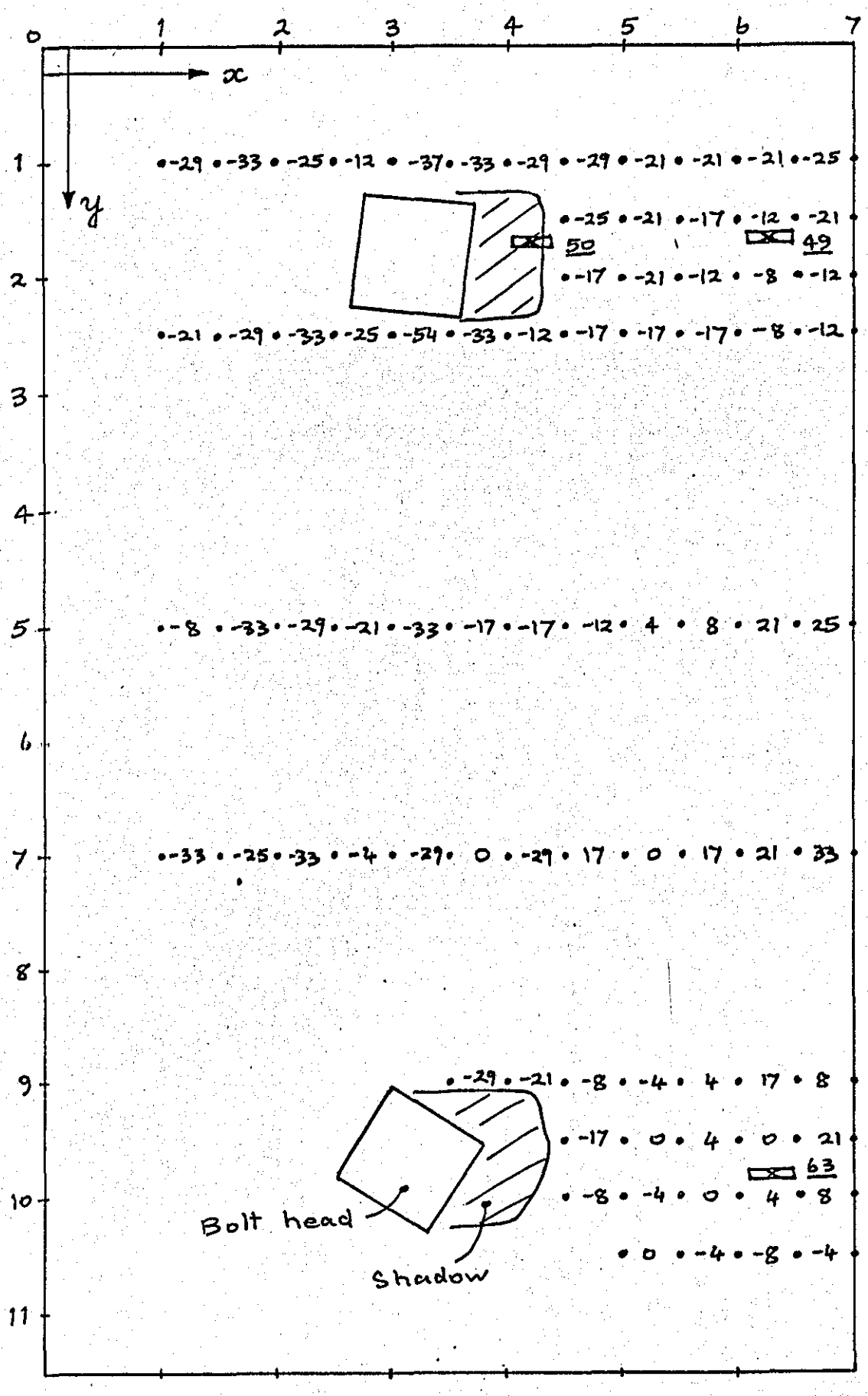

▭ : Strain gauge position

Fig. 5.7 Strain results in microstrain by HI on the side wall, scaled for 200 lbf load increment.

could be made; at many gauge length positions it caused error of a few percent. There was also the possibility of error in the event of a bodily translation of the surface, but this could not be established from the interferograms obtained. (This source of error would be avoided by maintaining constant values of θ across the surface.)

A significant feature apparent from this examination of error is the effect of the out-of-plane displacement. Over much of the wall, the out-of-plane component was several times greater than the in-plane component. Thus, despite a reasonable number of fringes in the original patterns, the subtracted numbers representing in-plane displacement were small, and consequently error in the original fringe numbers was very significant. If the deformation had been predominantly in-plane, the strain distribution could have been examined at a much higher magnitude, above a hundred microstrain, with the same number of fringes. Then, the same error of ± 10 microstrain would have been acceptable, giving a reasonable percentage accuracy, and the distribution of strain would have been clear. One way of circumventing the problem would have been to examine smaller areas of the wall at a time, to obtain a proportional increase in the number of fringes per unit length of the surface. However, the time schedule for the investigation prevented this being done.

5.4 ASSESSMENT OF HOLOGRAPHIC STRAIN MEASUREMENT AGAINST STRAIN GAUGING.

Strain gauge results by Ruston and Hornsby Ltd., for the three gauges of interest (identified in Fig. 5.7) are reproduced in table II. (The conditions under which tests (i) and (ii) were conducted are not known.)

Gauge No.	Test No.	Applied load (lb_f)				
		200	400	600	800	1000
49	i	9	21	37	79	107
	ii	1	17	27	54	83
50	i	-4	-8	-23	-24	-39
	ii	-4	-9	-19	-17	-34
63	i	12	22	32	37	81
	ii	2	12	34	39	87

Table II Strain gauge results, in microstrain, on the side wall.

The holographic values of strain at locations closest to gauges 49 and 63 are -12 and +4 microstrain respectively (for 200 lb_f incremental load). These two values bear little relation to the strain gauge results. However, high experimental error ($\pm$ 10 microstrain) has been estimated for the holographic results, and a similar magnitude of error appears to exist for the strain gauge results. (This is seen by scaling these values to correspond to a 200 lb_f load, and by comparing tests (i) and (ii).)

Thus, no detailed comparison of strain values obtained by the two methods is justified. It is clear that the range of strain that could be measured holographically was very limited compared with the large range possible by strain gauging.

Although the fringe analysis resulted in low strain values, which were consequently unreliable, relative merits of the holographic method became apparent. The method is of value in providing the distribution of strain over the entire surface. In this investigation no holographic results were obtainable alongside gauge 50, but surrounding results suggest higher values of strain than that registered by this gauge. In this case the gauge was not in the best position. Thus, by doing a preliminary holographic analysis of strain distribution to determine the significant positions where strain gauges should be attached, holography would be an aid to strain gauging. Probably, less strain gauges would be used consequently. The use of a simpler holographic arrangement, detecting out-of-plane displacement, to provide this information was described in Chapter 4. It is not as accurate, but has the advantages of providing some information on all in-plane directions, and of permitting assessment without any time-consuming numerical fringe analysis.

Holography also enabled a deficiency in the loading of the model to be evaluated. It had been suspected that there was difficulty in repeatedly loading the model to achieve precise deformation, possibly due to the perspex construction of bonded and bolted joints. Tests were done using a simple holographic arrangement (to detect out-of-plane deformation),

which was quick to set up and analyse, and yet accurate (to within 1½%). Using a dead weight pressure gauge tester, but following an imprecise loading cycle, variations in deformation by 20% were obtained, for the same nominal load. When a precise loading cycle was followed, this variation was reduced to 3 %. This result indicates that imprecise loading procedure was partially responsible for discrepancies in the strain gauge results.

To conclude, maps of strain distribution are obtainable by HI, though in this particular investigation the strain values were low and consequently unreliable. Nevertheless, the provision of strain information over the entire field is seen both as a complement, and as an aid, to strain gauging. In general, for isolated spot measurements of strain, the following advantages of strain gauging cannot be disputed :-

(i) rapid readings, conveniently taken ;
(ii) large range (up to thousands of microstrain) ;
(iii) measurement under dynamic conditions ;
(iv) measurement in awkward locations ;
(v) direct determination of tensile and compressive strain ;
(vi) acceptable accuracy in most situations.

However, holography would be favourable when no contact with the surface is critical. Also, by means of optical magnification it could work with smaller gauge lengths, for situations requiring very detailed examination. The main limitations of the method as used in this investigation, namely laborious procedure and poor accuracy, have subsequently been reduced, as described in the next section.

5.5 CURRENT AND FUTURE DEVELOPMENTS

Only part of the available information from the subtraction of the two interferograms was used to obtain the (direct) strain values presented above. Just as the subsequent subtraction of fringe numbers at adjacent grid points along a y ordinate represents direct strain, so the difference between fringe numbers along an x ordinate represents the relative shearing of these adjacent grid points. The additional measurement of shear strain could be the means of deriving the principal strains at a point in the surface by this method. The general state of surface strain may be solved from three strain components; ϵ_x, ϵ_y, and ϕ_{xy}, where ϵ denotes direct strain and ϕ denotes the total shear strain. When the optical paths are arranged in a plane parallel to the x direction, the relative shearing of grid points detected is only a component of the total shear strain. This component can be denoted by $\frac{\delta x}{\Delta y}$, and likewise there is another component $\frac{\delta y}{\Delta x}$ which is detected by an optical illumination arrangement parallel to the y direction. In practice two such optical arrangements would be used in sequence. The first would enable ϵ_x and $\frac{\delta x}{\Delta y}$ to be measured, and the second would give ϵ_y and $\frac{\delta y}{\Delta x}$. Using a sign convention of clockwise shear being positive and anticlockwise shear being negative, the total shear strain would be given by subtraction of the two components:-

$$\phi_{xy} = \frac{\delta x}{\Delta y} - \frac{\delta y}{\Delta x} \quad \ldots\ 5.5$$

(In fact, the apparent shear components can be due, in whole or in part, to a bodily in-plane rotation of the surface, which is not easily distinguished from the true shear. However, since any such bodily rotation would appear equally in both shear components, it would be eliminated by subtraction, in equation (5.5).) The sense of all strain components would need to be unambiguously determined, which should be possible in a real time test by relating fringe movement to known displacement.

It would of course be laborious to undertake such measurements by means of the analysis procedure used on the engine model. The amount of laboratory time and manual analysis would be prohibitive compared with strain gauging. However the state of the art has advanced in the period between the work done on the engine model and the present time of writing. A more direct method of obtaining the in-plane displacement was described by BQONE (1970). Two illumination directions, at equal but opposite angles of incidence to the surface were used, with a single (normal) viewing direction. This produced two superimposed interferograms with a moire beat representing loci of in-plane displacement resolved in one direction. Thus, to analyse strain, only one set of fringe numbers needed to be assigned and only one subtraction process was involved; the work of analysis was halved. Unfortunately the perceptibility of the moire beat fringes could be very poor, depending on the nature of the two constituent patterns, and especially in cases of complex strain. However, the same basic optical principle was already being applied in speckle pattern interferometry (LEENDERTZ, 1970). This method had the clear advantage of providing a single

interferogram directly representing in-plane displacement, with no sensitivity to out-of-plane displacement. Interpretation was as for the holographic beat fringes. In addition it was quite easy to visualise the strain distribution directly from the interferogram. Currently, method and technique are being improved by the use of a TV camera and monitor with a video recorder and an electronic subtraction unit in place of photographic recording and processing. (TV camera tubes cannot record holograms, because their resolution capability is insufficient.) This is much faster and more convenient than photographic processing, making real time tests a practical proposition. (DENBY and LEENDERTZ, to be published).

Thus the specific advances that have been made are: improved quality interferograms enabling strain distribution to be directly visualised; a halving of the fringe analysis in strain measurement with consequent improved accuracy; (typically, to within 5 %, as confirmed by strain gauged tensile specimens) and the development of practical, real time procedures. There is still a manual processing stage in the calculation of strain, which limits the potential application of the method. In principle it should be possible to scan the fringe field to determine fringe numbers and positions, and these data could be automatically processed to compute strains. It is conceivable that such a complete optical strain meter and recorder could be developed, and would rival strain gauging for speed of operation and accuracy in special applications.

5.6 SUMMARY

In this investigation of holographic strain measurement applied to an engineering problem, surface strain distribution in one direction was obtained. However, strain values were low (up to only 40 microstrain) because out-of-plane deformation was relatively greater, contributing most of the fringes in the overall interferogram. Consequently, accuracy was poor, and strain analysis of the engine model was accomplished better by the strain gauges, able to work at much higher strain increments. Nevertheless, in general, the holographic method has the distinct merits of avoiding surface contact, and of providing strain distribution over the entire surface. The latter should enable holography to aid strain gauging. The laborious holographic procedure described has subsequently been greatly reduced by developments in electronic speckle pattern interferometry. As a result strain analysis is now a practical, real time method, with improved accuracy. It should be noted, however, that image resolution is far superior by holography than by speckle pattern using TV equipment, and consequently HI remains valuable, especially in its more suited role of measuring deformation normal to a surface.

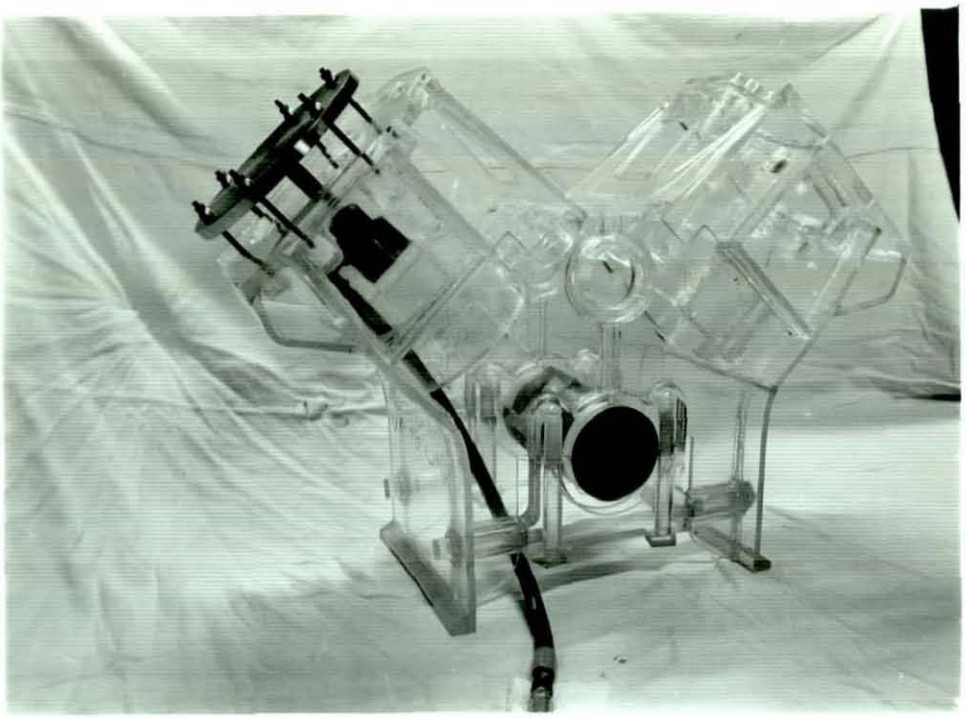

Fig. 5.1 The perspex JV engine crankcase model

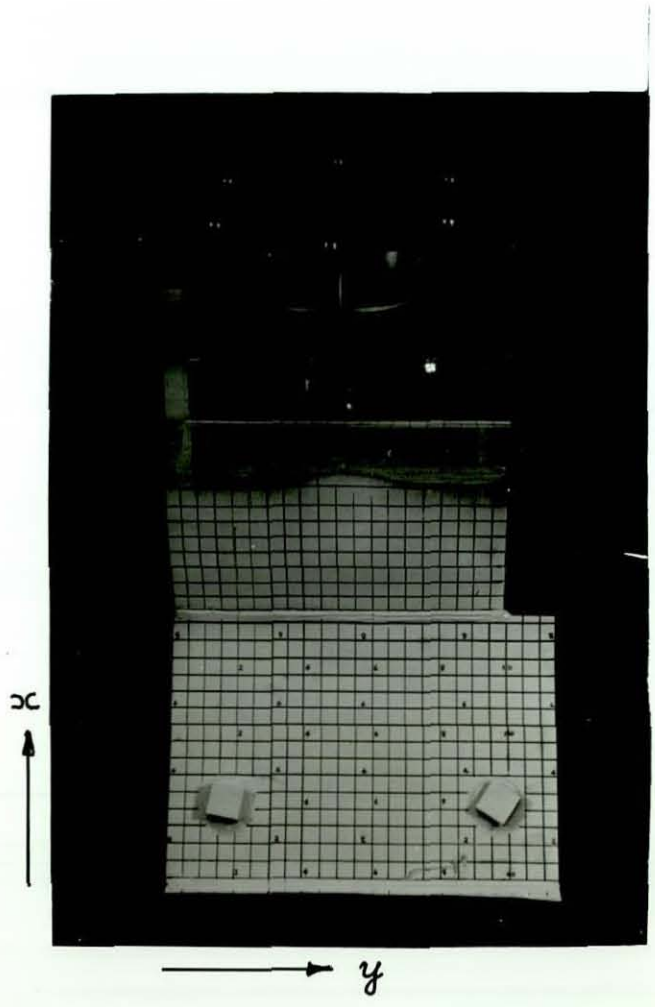

Fig. 5.2 The side wall on which measurements of strain were made

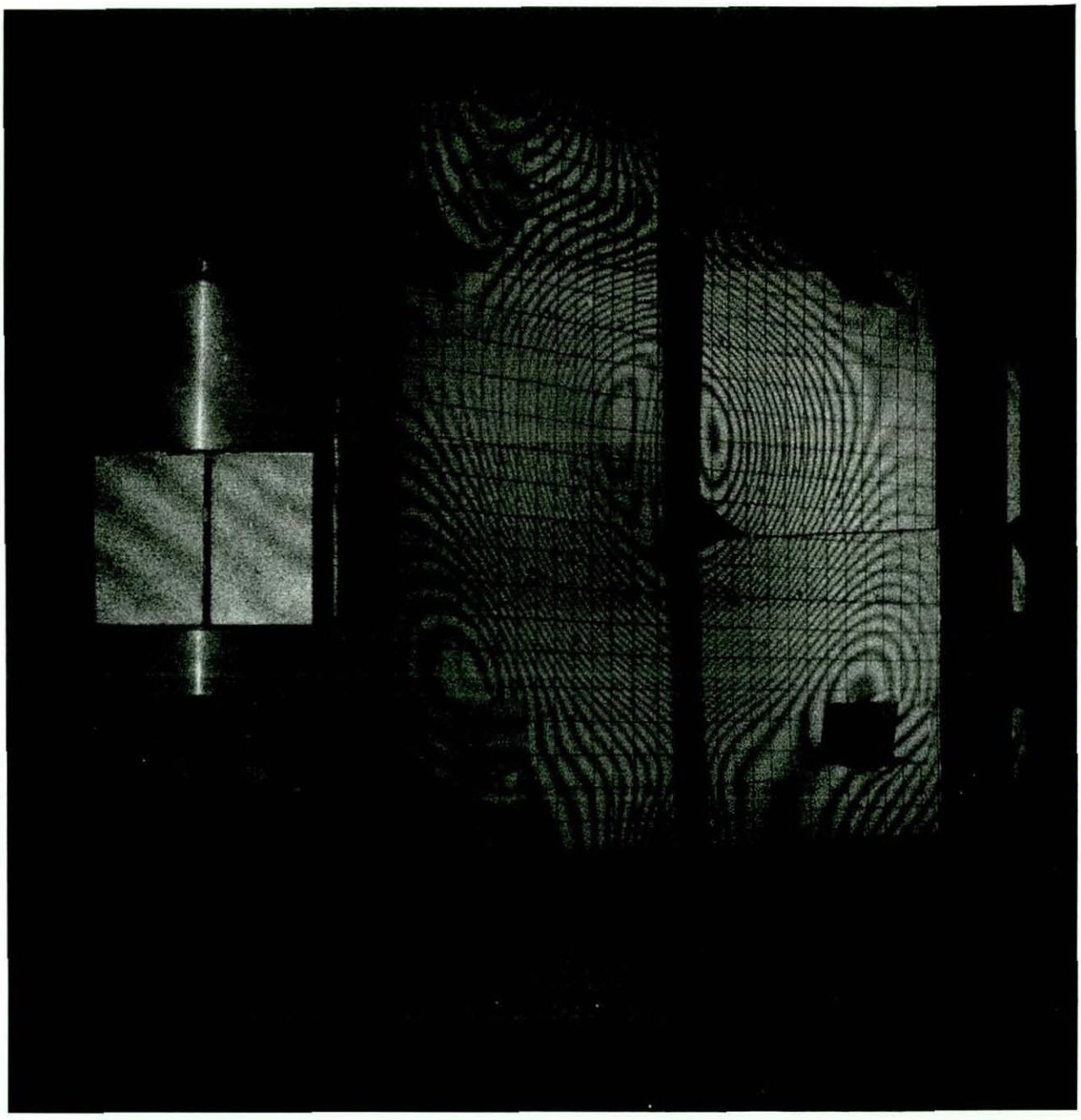

Fig. 5.5 The pair of interferograms (mirror view on right) analysed to determine strain in the side wall

Chapter 6

FOCUSED IMAGE HOLOGRAPHY AND ITS PRACTICAL BENEFITS IN HI.

6.1 INTRODUCTION

By the term "focused image hologram" (FI hologram) is meant the holographic recording of an aerial image of an object, achieved by focusing the image upon the recording material. In contrast, the usual recording of scattered wavefronts may be termed a conventional hologram. A FI hologram has the merit of permitting a sharp image to be formed by reconstruction using white light, and this can be achieved simply with a table lamp. Even an extended source does not degrade the image sharpness, though to contribute to reconstruction, the light must be incident at the appropriate angle for diffraction. A FI hologram forms the frontispiece to this thesis and may be viewed by reconstruction using a table lamp or direct sunlight.

In Chapter 2 it was concluded that the application of HI was partly limited by laboratory procedures, both for recording and reconstruction, and that developments were most needed in lasers and recording materials. The published literature during the first year's work of this project indicated a fair degree of effort in these

directions:- the performance and range of He-Ne and argon lasers were being improved; pulsed lasers had successfully produced interferograms of rotations, impacts and stress waves (WUERKER et al, 1968; GOTTENBERG, 1968); and research was being done into photo-chromic and other photo-sensitive films as recording materials (CHEN et al, 1968; LIN, 1969; TUBBS et al, 1969; MEZRICH, 1969). However, none of these materials was yet developed to be as practical as silver halide emulsions, and pulsed lasers were not generally available. Thus in these respects the position of HI as a method in engineering measurement had not significantly changed. At the same time, however, techniques of HI were continually being developed, opening up further areas of potential application. The following are examples:-

(i) New techniques of vibration analysis provided further information beyond that of straightforward time average holograms (ALEKSOFF, 1969; SHAJENKO et al, 1968);

(ii) HI was found to be a neat method for measuring Poisson's ratio (YAMAGUCHI et el, 1969);

(iii) Improvements were being made in contouring methods (ZELENKA et al, 1968).

Thus the previous conclusions, concerning the need for more practical procedures, still applied. It was thought that the technique of FI holography had potential benefits for HI, by simplifying the procedures of reconstruction and analysis in the following ways. White light reconstruction using image projection would enable two or more people together to view results, outside the laboratory. Photographic prints of interferograms for analysis purposes

could be avoided. By eliminating lasers from the reconstruction process, economy and general convenience would be gained, while eye fatigue and risk of eye damage would be avoided. FI holography would then be advantageous in industrial applications such as routine testing of vibration modes and non-destructive testing, based on a standardized recording rig.

At the time of pursuing this idea (early 1969), the recording of FI holograms was established (for example, STROKE, 1966), though little had been done to develop the technique for HI. The occurrence of white light fringes using a "direct image" hologram had been noted by BURCH et al, (1966), but without published elaboration. KLIMENKO et al, (1967), had obtained double exposure FI holograms of transmission objects and had likened the effect to the superposition of two diffraction gratings of slightly different periods, causing a moire pattern of fringes. Subsequently, during the work of this project, they published an extension of the technique for diffusely reflecting objects (1970).

FI holograms and subsequent white light reconstruction exhibit certain effects not (usually) encountered in conventional holography. These include :-

(i) Characteristics of reconstruction concerning image colour, image geometry, and viewing position.

(ii) Effects of the aperture of the imaging lens (in recording):

(a) image brightness as recorded, and in reconstruction;

(b) speckle pattern, affecting final image resolution.

(iii) Recorded image depth, affecting image clarity in reconstruction.

These effects are explained in the next section. Again, when FI holography is used for double exposure HI, distinctive effects occur :-

(iv) Reduced fringe visibility, as a result of object displacement lateral to the imaging axis;

(v) Colouring around the fringes and apparent fringe movement, associated with the use of a large lens aperture in recording.

In order to justify the use of FI holography in HI, and to enable interferograms so formed to be understood, these effects are analysed in Section 6.3. Results of supporting experiments are presented. A white light FI hologram projector is then described. This was designed and constructed to aid research in this topic, and to realize fully the benefits of the FI method in HI.

6.2 GENERAL PRINCIPLES

Reconstruction characteristics

Focused image holograms of diffusely reflecting objects are recorded using normal recording procedures but with the addition of a lens positioned so as to focus some of the scattered light as a real image in the recording plane. When the FI hologram has been processed a negative silhouette of the image may be recognised in diffused lighting, but the original detail in the image is only obtained by wavefront reconstruction. This is achieved with a reconstructing reference beam, producing two first orders of diffraction in the normal way. It is because the recorded image is in the plane in which the light is diffracted, that a white light reconstructing reference beam will produce a clear image.

Although the white light is dispersed spectrally, the different colours emanate from points in the image. Thus the image is seen coloured, and the colour may be varied by altering the viewing angle. Since the image appears in the plane of the hologram, any marks or density changes in the emulsion tend to degrade the clarity of the image. Thus careful handling and processing of FI holograms, together with 'clean' reference beams, are important (whereas this is of less concern in conventional holography).

An important feature is that the geometry of the image in the hologram plane is fixed. It cannot be altered in reconstruction, whatever the angle, wavelength and radius of curvature of the reconstructing reference beam. Thus, all that is required for accurate reconstruction is any light source incident at the appropriate angle for diffraction. There is typically a tolerance of several degrees on the reconstructing angle of incidence. This is because holograms made with design angles of less than 45° record relatively little fringe modulation through the thickness of the emulsion, and are therefore predominantly two-dimensional diffracting media.

Of the two first orders of diffraction in reconstruction, the image in the primary direction is normally viewed, because this produces the same viewing direction of the object as was selected by the imaging lens when recording. Although the image in the conjugate direction is initially the same, it would be seen obliquely (depending on the design angle used) and accordingly one direction in the image would be foreshortened. When viewing the image in the primary direction it is seen 'lit up' by a virtual

image of the recording lens. Thus the extent of the image in the hologram plane that may be viewed from one position is restricted, depending on the angle subtended at the eye by the virtual image of the lens. This is illustrated in Fig. 6.1 (a), for a case in which the image size at the hologram is greater than the lens aperture. For simplicity, monochromatic light reconstruction is initially considered. One way of seeing the entire image from one viewing position is to view it through a converging lens positioned near the hologram. A simpler way, however, is to reverse the direction of the reference beam. This causes a real image of the recording lens to be formed in place of the previous virtual image. This determines a certain volume of space inside which the entire image may be viewed from any one point, as represented in Fig. 6.1 (b). When the reconstructing reference beam is of white light, the focal length of the hologram takes on a range of values (equation (3.4)), and in addition spectral dispersion takes place. As a result the image space of the recording lens becomes extended in both the x and z directions (Fig. 6.1). Therefore the volume of space for viewing the entire image is correspondingly enlarged, and the positioning of one's eye, for direct viewing, is not so critical.

In practice it is satisfactory to simply reverse the hologram and leave the reconstructing reference beam as a divergent beam. This avoids the complication of arranging a convergent beam of sufficient aperture at the hologram to illuminate the image. The effect of the changed reference beam is to alter the position of the real image of the recording lens, as can be approximately calculated using

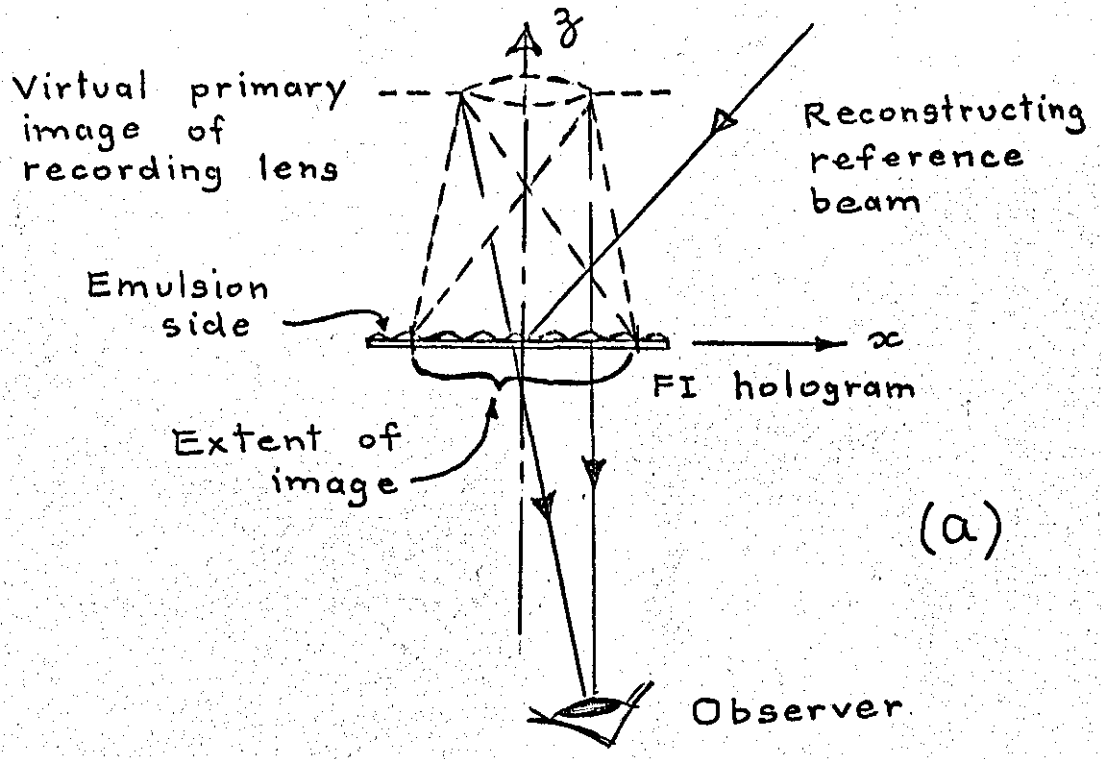

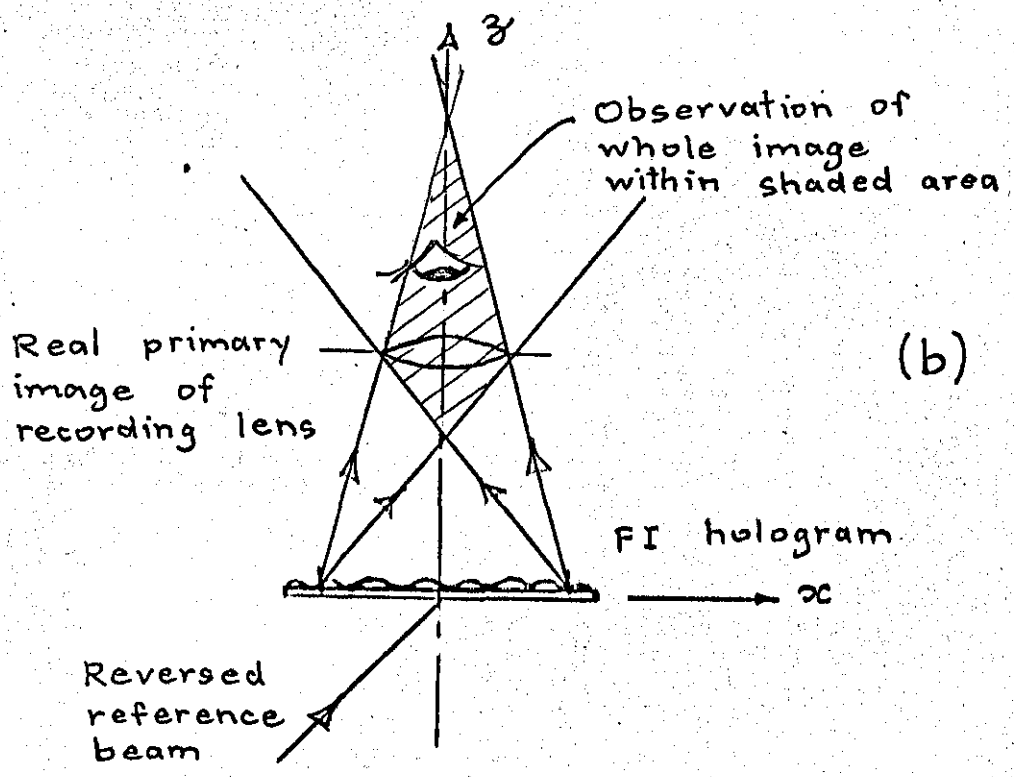

Fig. 6.1 Reconstruction from a FI hologram (monochromatic light)

(a) image partially observed;

(b) complete image observed.

the hologram focal length formula (equation (3.1)). For example, suppose a FI hologram is recorded with the reference point source 50 cm from the hologram, and the recording lens 10 cm away. Then, in reconstruction, using a small white light source 30 cm from the hologram, the position of the image of the recording lens is given approximately by (equation (3.2)):

$$1/s_p = 1/10 - 1/50 - 1/30$$

This image is formed approximately 21 cm from the hologram, and placing one's eye slightly further away, as sketched in Fig. 6.1 (b), would be a convenient viewing distance. (This has assumed the selection of the same colour in reconstruction as the laser output used for recording.)

When viewing a FI hologram by the procedure just described, the image may be viewed with correct vertical attitude, but it will then be reversed left to right. Also it will be inverted back to front. The left to right reversal can be easily corrected, either in advance by using a plane mirror in the imaging path of the recording arrangement, or by viewing via a plane mirror in reconstruction. The inversion can be eliminated using another imaging lens in reconstruction, though in fact the inversion effect is usually insignificant due to limited depth in the image (to be discussed below). However, the use of a projection lens in reconstruction has a more significant benefit. It has already been explained that direct viewing of the image by eye requires rather critical positioning of one's eye, which is an inconvenience. It is far more convenient to project an image on to a diffusing screen, using a projection lens positioned in the real image space of the recording lens.

The final image on the diffusing screen is then viewed by transmission, with the advantages of desired magnification and the facility of two or more observers viewing it together. There are no further difficulties concerning the attitude of the final image, because the hologram can be simply rotated 180° in its own plane, and the reference beam directed from the other side, in order to compensate for the extra reversals introduced by the projection lens.

Imaging aperture effects : image brightness and beam ratio

An important parameter in recording FI holograms is the aperture of the imaging lens, since this directly affects image brightness and resolution. In the case of double exposure HI it also influences the differences in phase for imaging paths through different parts of the lens. This aspect is particular to HI and is discussed in Section 6.3.

Since image brightness to be recorded is directly related to the lens aperture, this is a convenient means of adjusting the beam ratio, which, in FI holography, requires different considerations. The brightness of reconstruction from a holographic recording is proportional to the square of the visibility of the fringes formed by interference between the reference and signal beams (NISHIDA., 1968). Therefore maximum brightness can be obtained using a beam ratio of unity. In conventional holography a beam ratio of about 4:1 instead of unity is used to avoid noise in the form of higher orders of diffraction in reconstruction. However, in FI holography one avoids viewing this source of noise because the

diffracted light permitting image observation is restricted in a narrow angular range. Thus a beam ratio of unity may be used without disadvantage.

A feature unique to FI holography occurs when the object has regions of varying brightness. Whereas in conventional holography the scattered light intensity at the hologram is nearly uniform, it varies in a focused image according to the object brightness. Consequently, not only does the beam ratio vary over the image, but also the exposure. In such cases the reconstruction brightness cannot be at a maximum for all parts of the image, and a compromise must be sought to make that part which appears dimmest in reconstruction as bright as possible. This requires consideration of two characteristic curves. One is the diffraction efficiency as a function of fringe visibility (fringes formed by interference between the reference and signal beams). The other is the diffraction efficiency as a function of exposure.

In order to demonstrate that satisfactory results can be obtained for an object with regions of differing brightness, an object was illuminated such that three distinct rectangular regions had brightnesses in the ratio 1:4:16. A uniformly bright reference beam was arranged, making the same design angle with each of the three focused areas. The beam ratios for the regions 1, 2 and 3 were respectively 0.5:1, 2:1, and 8:1. All regions were exposed for the same time (to correspond to a practical case), with the optimum exposure for region 2. In reconstruction region 2 was brightest, region 1 slightly less so, and region 3 considerably dimmer. An inaccurate reproduction of this result is shown in Fig. 6.2; the brightnesses are inaccurate

due to non-uniform white light illumination of the FI hologram in reconstruction, and possibly also due to non-linear processing of the negative and print. Nevertheless it is seen that the fringe information in each region is clear, with good visibility. (The fringes are due to a small rotation of the object surface about a vertical axis, made after half the exposure.) Thus a brightness ratio of up to 16:1 in the image has been shown to present no problem. In fact satisfactory reconstruction of brightness ratios considerably higher can be expected, since a much higher dynamic range is obtained holographically from an emulsion than by normal photography. It is interesting to note the negative effect in reconstruction for image regions where the beam ratio is less than unity, such as for region 1, and as demonstrated by NISHIDA (1968).

Imaging aperture effects : speckle pattern

In all cases of image formation using laser light, resolution must be considered in terms of the characteristic speckle pattern. This phenomenon is due to random interference from scattering points within the resolution limit of the imaging system. The speckles forming the pattern are distributed in both size and intensity over ranges governed by statistical properties. A minimum speckle size may be calculated based on Rayleigh's criterion for resolution. For circular apertures this gives a minimum speckle size s of :-

$$s = 1{\cdot}2\lambda v/D \qquad ----(6.1)$$

in which v is the image distance of the image plane from

the lens, and D is the lens aperture. An alternative concept is of speckles forming spatial frequencies in the image plane. These frequencies exist over a range from zero to some maximum value which corresponds to the minimum speckle size.

In the holographic recording of a speckled image, the speckles are modulated by fringes caused by interference with the reference beam. Consider a practical case in which a 75 mm imaging lens is opened up to f/3.5, giving D=21 mm, forming an image at a distance v=110 mm, with a design angle of 32°. Using equation (6.1), the minimum speckle size is 6λ, which is equivalent to the maximum spatial frequency of speckles in the image plane. The separation of the interference fringes forming the hologram, in the same plane, is $1{\cdot}9\lambda$, (chapter 3). Thus modulation can occur even within the smallest speckles. Of course, the speckle intensities vary over a wide range, and those which are either very dark or bright form low contrast fringes. Consequently, in reconstruction, these speckles diffract little light and appear dark, accounting for the grainy appearance of the image, whether reconstruction is by white light or laser light. If a smaller lens aperture is used in recording, the average speckle size is larger, and so the grainy appearance is more pronounced. This becomes especially significant in the case of holographic interferograms having densely spaced fringes, when it can be difficult or, in extreme cases impossible, to resolve the fringes. The effect of the recording lens aperture on the speckled appearance of the final image is shown in Fig. 6.3, this being a case of cantilever deformation. For the image (a), the lens was stopped open at

f/3.5, while for (b) it was stopped down to f/11. Otherwise the recording arrangement was the same for both, and was as cited for the example above concerning speckle size. Clearly (b) is the more speckled, though in this case even the closest spaced fringes are easily resolved. The image (a) also serves to show the effect of inattention to washing and drying procedure for a FI hologram.

It is to be noted that the scattered light from an object in conventional holography also forms a speckle pattern at the hologram plane, as has been shown by photomicrographs (SMITH, 1969). In this case the minimum speckle size and spacing depend on the maximum angular extent of the object from the hologram.

In reconstruction, using white light, the degree of speckle in the image is little affected by the aperture of the lens used to view it. As explained, the speckled appearance is established during the recording stage, and depends for its degree of coarseness on the aperture of the recording lens. If the same quality lens at the same aperture is subsequently used for imaging in reconstruction, the same speckles in the hologram plane will be resolved. If the lens is stopped down, resolution will suffer to the extent that the finest speckles will not be resolved. In practical cases however, the effect is hardly significant, as shown by Fig. 6.4. Cantilever deformation was again used for this demonstration. Both photographs were taken from the same FI hologram, under similar conditions of white light reconstruction, except that (a) was taken with the imaging lens stopped at f/3·5 (as was the lens which recorded the hologram), and (b) with the lens at f/16. As seen, there is no difference

in the definition of the fringe information.

Aperture in reconstruction : image colour

Another effect of the imaging lens aperture, this time in reconstruction, concerns the image colour as explained with the aid of the sketches in Fig. 6.5. Suppose a FI hologram is recorded with red light using a relatively small aperture. Let this same arrangement be used in reconstruction, but substituting a white light reference beam in the reverse direction. The lens will just be filled with red light of the same wavelength. By diffraction other colours will be radiated in defined directions, for example, as shown for blue light from one image point. The directions of particular colours may be found using the simple diffraction grating relationship. In case (a) predominantly red light is received by the lens and the image formed will be of this colour. If the angle of incidence θ of the reference beam is continuously decreased, the image will change colour through the spectrum towards the blue end. If instead a large aperture is used, as in (b) different colours are received by the lens and the colour of the image is mixed, becoming white in the limit. A white image is also produced by an extended white light reference source, even with a small lens aperture. Such a source may be considered as a multitude of reference beams covering a range of directions, and thereby causes all colours to be dispersed over a large range of overlapping directions.

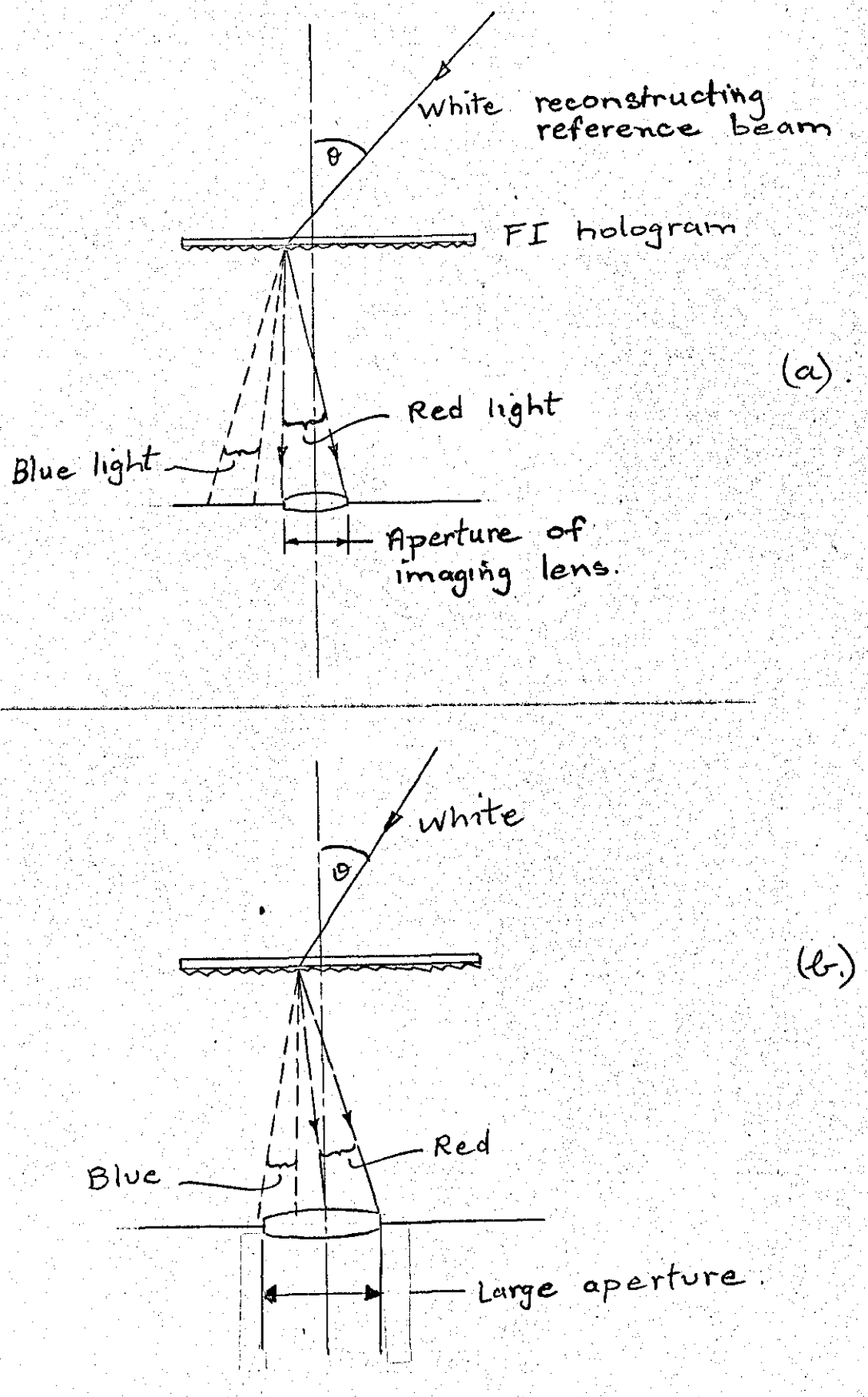

Fig. 6.5 Effect of imaging lens aperture in white light reconstruction on image colour :
(a) small aperture, same as for recording;
(b) large aperture.

Image depth and blur.

In the discussion so far it has been assumed that all image points are perfectly focused in the hologram plane. This of course cannot be achieved with a deep object. Consider such a case in which an image point P focuses at a distance Z from the recording plane (either side), on the imaging axis which is normal to the recording plane, Fig. 6.6. For white light reconstruction, this image point will appear at P in the same colour (λ_1) as was used to record the hologram. For a different wavelength λ_2, the same image point will appear at Q, in the direction OQ given by:

$$\sin \gamma = \frac{(\lambda_1 - \lambda_2)}{\lambda_1} \cdot \sin \theta$$

treating the hologram as a simple diffraction grating.

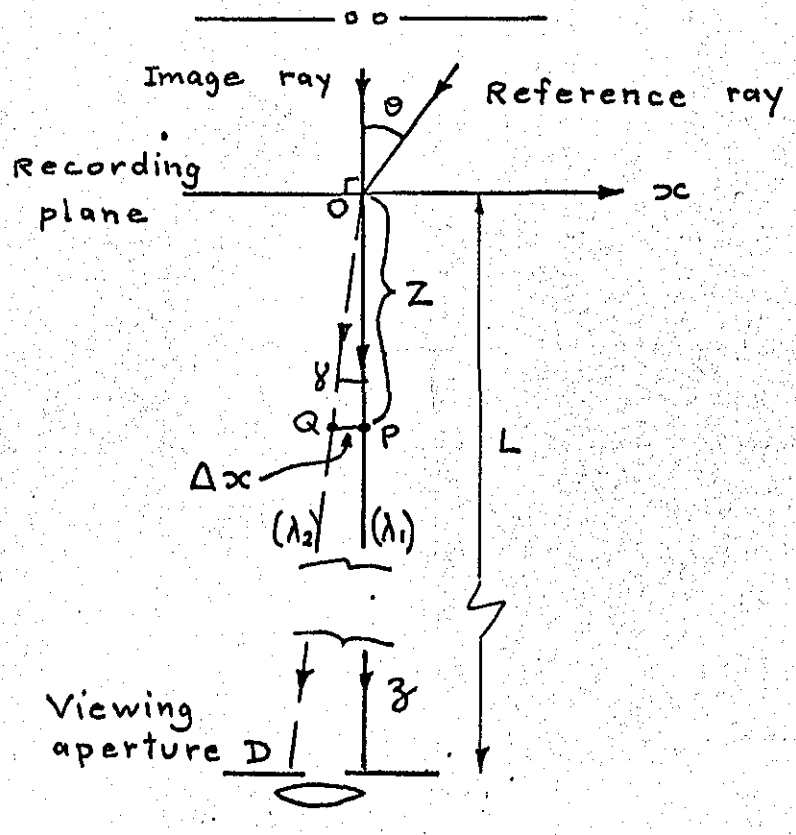

Fig. 6.6 Blur for an image point not in the recording plane.

Thus the lateral blur Δx of this point will be:

$$\Delta x = Z \sin\theta \frac{(\lambda_1 - \lambda_2)}{\lambda_1} \quad ---- (6.2)$$

(ignoring the change in Z for a different wavelength). Thus the angular dispersion and the amount of blur is proportional to $\sin\theta$, and can be reduced by decreasing the design angle θ . However, as noted by BRANDT (1969), if the angular spread γ of the dispersion is larger than the angle subtended by the viewing aperture at the hologram, the amount of apparent blur Δx_{app} is then independent of θ and λ , and is given by:

$$\Delta x_{app} = ZD/L \quad ---- (6.3)$$

in which L is the distance of the viewing aperture D from the hologram. This case is significant for visual observation. If the angular limit of resolution of the eye is taken as 0.0003 rad, the maximum value of Δx_{app} for no resolved blur is then 0.0003 L, and the condition correspondingly set for Z, from equation (6.3) is:

$$Z \leq 0.0003\, L^2/D \quad --- (6.4)$$

For example, if viewing a hologram at the near distance of distinct vision, 250 mm, and taking the eye pupil diameter to be 4 mm, no blur will be observed for an image depth up to 5 mm either side of the hologram. The corresponding limit on the depth of the original object depends on the magnification employed at the recording stage. Differentiation of the simple lens focal length formula gives the axial magnification as M^2, M being the lateral magnification. Therefore, in this respect, objects of appreciable depth should be recorded employing a magnification M of less than unity.

When a lens is used in reconstruction, to form a real image on a diffusing screen, it is more likely that equation (6.2) will apply for predicting image blur Δx. This is because the lens aperture D is likely to be greater than the eye pupil, and the distance L considerably shorter, allowing the full angular dispersion to be received by the lens. In order to demonstrate that image blur Δx could be reduced by decreasing θ, a FI hologram was recorded in which the reference beam was in line with the imaging axis. This was done using a beam splitter positioned between the imaging lens and the hologram, so as to transmit the image rays and reflect the (divergent) reference beam, causing θ to be nominally zero. A cantilever object was used, deformed between exposures to produce frozen fringes. The total image depth was about 30 mm, with the furthest point lying 18 mm from the hologram plane. When viewed by eye using white light reconstruction, the entire image appeared sharp, and colour dispersion was negligible so that the image appeared grey. A photograph of this image by reconstruction is shown in Fig. 6.7. This does not adequately demonstrate the freedom from blur Δx, because the image exceeded the depth of field of the photographic arrangement! (Likewise, it would not be possible to project such an image on to a diffusing screen for observation with all parts simultaneously in focus, though different planes in turn could be brought into focus.) Of course, the reconstructing beam for such a hologram forms a bright in-line background. The eye has the ability to largely disregard this annoyance, but, for the photograph shown, the direct light was eliminated

by a small stop at the focused image of the reconstructing source. It is seen that the fringe contrast is good high up the cantilever, but decreases towards the base. This is attributed to the position of the reconstructing source which was in line with the second fringe up from the base and caused more scattered light to be seen in this region of the image. Further points of interest, including comparisons with speckle pattern interferometry, have already been published (DENBY, 1971).

6.3 APPLICATION TO HOLOGRAPHIC INTERFEROMETRY

In conventional double exposure HI it is common practice to photograph the image formed by reconstruction, for convenient examination of, and subsequent reference to, the interferogram. This involves two recording stages. The use of FI holography effectively combines these two stages into one, for the purpose of obtaining an interferogram that may be conveniently examined using white light. By either method an imaging lens must be used, and essentially the same interferogram will be formed whether the lens is used before or after recording the hologram. Since the interfering beams lie along a common path, there is no need for a first quality lens. Examples of double exposure interferograms by FI holography have already been referred to, and the mechanism of fringe formation is now examined to justify the method.

As noted, the image formed at the recording plane is composed of speckle pattern, the individual speckles having varied size and intensity. In the previous section a practical case was considered, which showed that even the

smallest speckles would be modulated by fringes, due to interference with the inclined reference beam. The modulated intensity across a single speckle may be expressed as:

$$I_1 = I_r + I_s + 2(I_r I_s)^{1/2} \cos\omega \quad ---- (6.5)$$

in which I_r, I_s are respectively the intensities of the reference beam and the isolated speckle, and ω is the relative phase, which is a function of distance x across the speckle. For simplicity, I_r and $d\omega/dx$ may be regarded as constant over the entire image. Where I_s is much brighter or dimmer than I_r, the modulation of I_1, is weak causing weak diffraction in subsequent reconstruction, and accounting for the darkly speckled appearance of the observed image.

Considering the case of double exposure HI, suppose the object is deformed such that the positions of the speckles are unchanged. For the single speckle considered, its intensity will be the same, but its amplitude vector will be altered in phase by δ, directly related to the change in optical path via the corresponding object point. (The path through the imaging lens is taken to be well defined.) Thus the new modulated intensity across the speckle is:

$$I_2 = I_r + I_s + 2(I_r I_s)^{1/2} \cos(\omega - \delta) \quad --- (6.6)$$

For two equal exposures, the total exposure of the emulsion across the speckle will be proportional to :

$$I_1 + I_2 = 2(I_r + I_s) + 2(I_r I_s)^{1/2} \{\cos\omega + \cos(\omega - \delta)\}$$

$$= 2(I_r + I_s) + 4(I_r I_s)^{1/2} \cos(\delta/2) \cdot \cos(\omega - \delta/2) \quad -- (6.7)$$

Ignoring nonlinearities in the photographic process, the intensity across the processed speckle will remain proportional to $-(I_1 + I_2)$. It must be noted that δ is constant for any one speckle, and changes across the image relatively

slowly compared with ω. Thus equation (6.7) has the same form as equation (6.5), but the modulation term is modified by the factor cos $(\delta/2)$, which will vary periodically across the image. Therefore the visibility V of the modulation fringes forming the FI hologram likewise varies across the image, given by:

$$V = \frac{2(I_r I_s)^{1/2}}{I_r + I_s} \cdot |\cos(\delta/2)| \quad ---- \quad (6.8)$$

If one ignores the fine scale effect of the randomly varying I_s values, the brightness of reconstruction (being proportional to V^2) is seen to be proportional to $\{\cos(\delta/2)\}^2$. Thus the spatial and intensity distribution of the fringes over the image is the same as in conventional double exposure HI (described in Section 4.1).

In the case of steady state sinusoidal vibration of the object surface, equation (6.5) would be modified to include a periodic time-dependent term in the cosine factor. This would then be integrated over the exposure time, following the derivation given by STETSON and POWELL (1966) for the conventional time-averaged case. The resulting visibility of the modulation fringes would be:

$$V = \frac{2(I_r I_s)^{1/2}}{I_r + I_s} \cdot |J_0(\delta)| \quad ---- \quad (6.9)$$

and, again, the fringe system would be the same as that obtained using the convential method.

In order to verify that the form of the interferogram would be the same by either convential Fresnel or FI holography, both types of hologram were recorded simultaneously alongside one another on the same photographic plate. A 75 mm long turbine blade (shown in Fig. 3.5) was selected as the object, and set vibrating at a resonant frequency of 1647 Hz,

excited by a small piezoelectric crystal stuck on the rear face. The recording arrangement was as shown in Fig. 6.8. The interferograms from the two holograms are shown in Fig. 6.9, and are seen to be identical in form. Although the viewing directions for the two holograms differed slightly, this caused a theoretical difference in sensitivity of only 1 part in 400, which cannot be detected with this small number of fringes. Also, there was no difference between white light and laser light reconstruction on the form of the interferogram from the FI hologram.

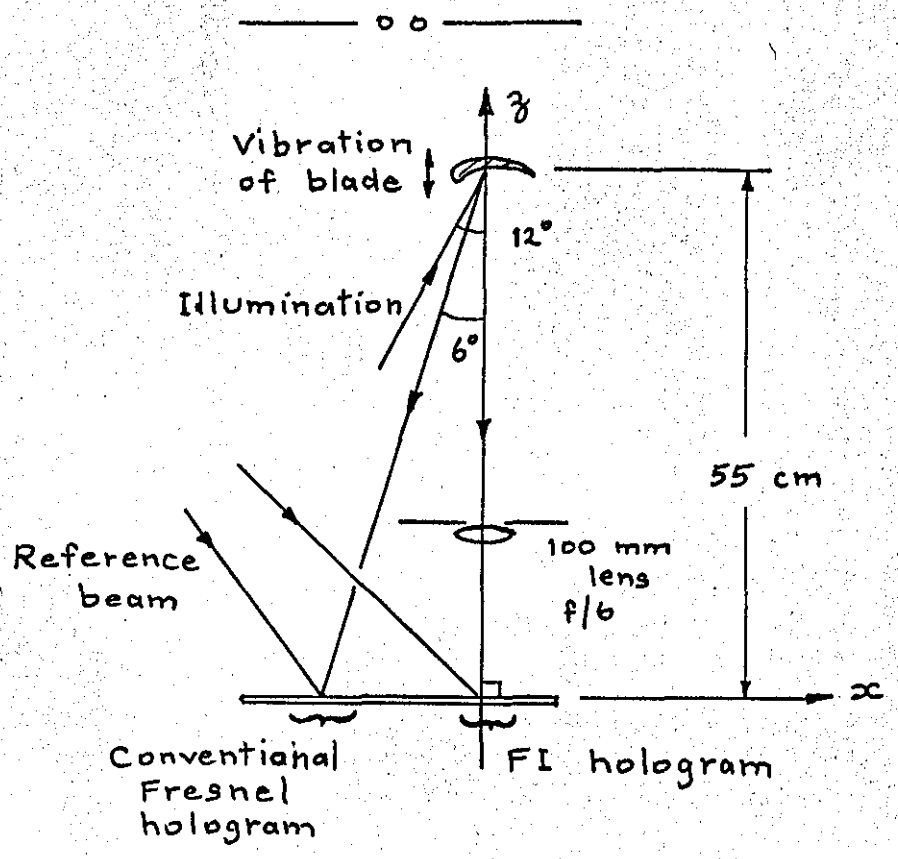

Fig. 6.8 Recording arrangement for simultaneous conventional and FI holograms.

Lateral object displacement

So far considered has been the case of object deformation such that the speckles in the image do not change position. This is seen to occur when the direction of deformation lies along the imaging axis, as was the case for the turbine blade vibration. When the direction of deformation has a lateral component, the speckles in the image are also shifted in the emulsion plane, by an amount depending on the magnification M. For any one speckle in the image, only in the region of overlap of its two positions does the change in phase δ, due to surface displacement, influence the modulation of the recorded intensity, as in equation (6.7). For those parts which do not overlap, the modulation of intensity will be as given by equations (6.5) and (6.6) separately, and these regions will simply diffract light as though only one of the two exposures had been made. Consequently the overall brightness in reconstruction of this image point will be modified :- had it been part of a dark fringe it would be somewhat brighter, and had it been a bright fringe it would be dimmer. Thus the effect of speckle shift in the recording plane due to a component of object displacement lateral to the imaging axis, is to reduce the visibility of the fringes observed in the image plane representing object deformation. As the degree of correlation of the two speckle patterns decreases, so the visibility of these fringes is further reduced. In this respect the effect is a loss of information as opposed to a source of error.

In fact, this explanation is complicated by the presence of adjacent speckles. When a shift in the speckle pattern occurs there will be a partial overlap of adjacent speckles, with a consequent modification of the modulated intensity in each individual case. However, the intensity and phase from speckle to speckle vary randomly. Although the value of $d\omega/dx$ is approximately constant across the image, the period of this fringe spacing is therefore disrupted at each speckle boundary. Thus when adjacent speckles partially overlap there is no regular effect across the image to modify the brightness of reconstruction.

Unfortunately there is no simple relationship between the loss of fringe visibility observed and the amount of speckle shift, because the speckle sizes vary, in a random distribution. (Experimental work subsequently done in speckle pattern interferometry has shown that a relative shift of the speckle patterns by an amount equal to the minimum speckle size still produces an acceptable fringe visibility (DENBY and LEENDERTZ, to be published). This implies that sufficient fringe information is provided by partial overlap of speckles of average size and larger.)

Lateral object displacement, as considered here, is one situation in conventional HI causing fringes not to be localized at the object surface. Concepts of fringe localization may also be applied to FI holography. For these cases, it is apparent that the phase change due to displacement of a single object point is detected over a finite area of the image. Consequently, at any one point

in the image, there is a confusion of phase change, causing reduced fringe visibility in the image plane. Thus, by white light reconstruction poor fringe visibility is inevitable. However, by reverting to laser light reconstruction it is possible to obtain high fringe visibility, if the fringe plane is located and focused upon.

In contrast, cases of object deformation giving fringes localized at the image surface can be viewed in that plane with almost maximum visibility either by white light or laser reconstruction. This has been confirmed by KLIMENKO et al (1970) who made densitometer plots of the fringes by white light and laser reconstruction from frozen-fringe FI holograms.

Effects of large recording apertures

With certain frozen-fringe FI holograms made during experimental work, it had been noticed that, in white light reconstruction, a periodic change of colour around the fringes occurred, whatever the basic colour of reconstruction selected. Furthermore, as the basic colour was changed, by altering the angle of incidence of the illuminating beam, there was an apparent shift of the fringes relative to the image. These effects, illustrated in Fig. 6.10, presented a problem of uncertainty in defining fringe positions, and therefore required investigation.

These effects are recognized to be associated with the use of a large aperture when recording the FI hologram, combined with an object displacement direction such as to make a large angle with the imaging axis. Consider a situation for recording a double exposure FI hologram

shown in Fig. 6.11. For the two extreme 'viewing' directions shown, the fringe order numbers n_1, and n_2 will be given (from equation (4.1)) by :-

$$n_1\lambda = d(\cos\alpha_1 + \cos\beta)$$
$$n_2\lambda = d(\cos\alpha_2 + \cos\beta)$$

The difference is:

$$(n_1 - n_2)\lambda = d(\cos\alpha_1 - \cos\alpha_2) \quad - - - \quad (6.10)$$

Thus there is a confusion of phase change at Q, due to P's displacement. However, the different phase changes within this range are individually preserved, since each associated viewing direction forms a periodic modulation at a different spatial frequency, by interference with the reference beam. In subsequent reconstruction the different phase changes are preserved in the corresponding viewing directions, just as in Fresnel holography different wavefronts are formed in different directions from a small region of the hologram.

The effects of this may be understood referring to the diagrams in Fig. 6.12. Subscripts $_r$ and $_b$ are used to denote red and blue light respectively, while the subscripts $_1$ and $_2$ correspond to the directions ① and ② in Fig. 6.11. For simplicity, only these two directions for red and blue light are shown. The magnitudes of γ_r, γ_b depend on the value of γ in recording, and the wavelengths in each case, while the angular separation of the directions n_{1r} and n_{1b} depends on θ and the wavelengths (equation (6.2)). Under conditions when γ is large, the sectors of red and blue light diffracted from the FI hologram may overlap, as shown here. In case (a) the angle θ_1 of the reconstructing beam is such that

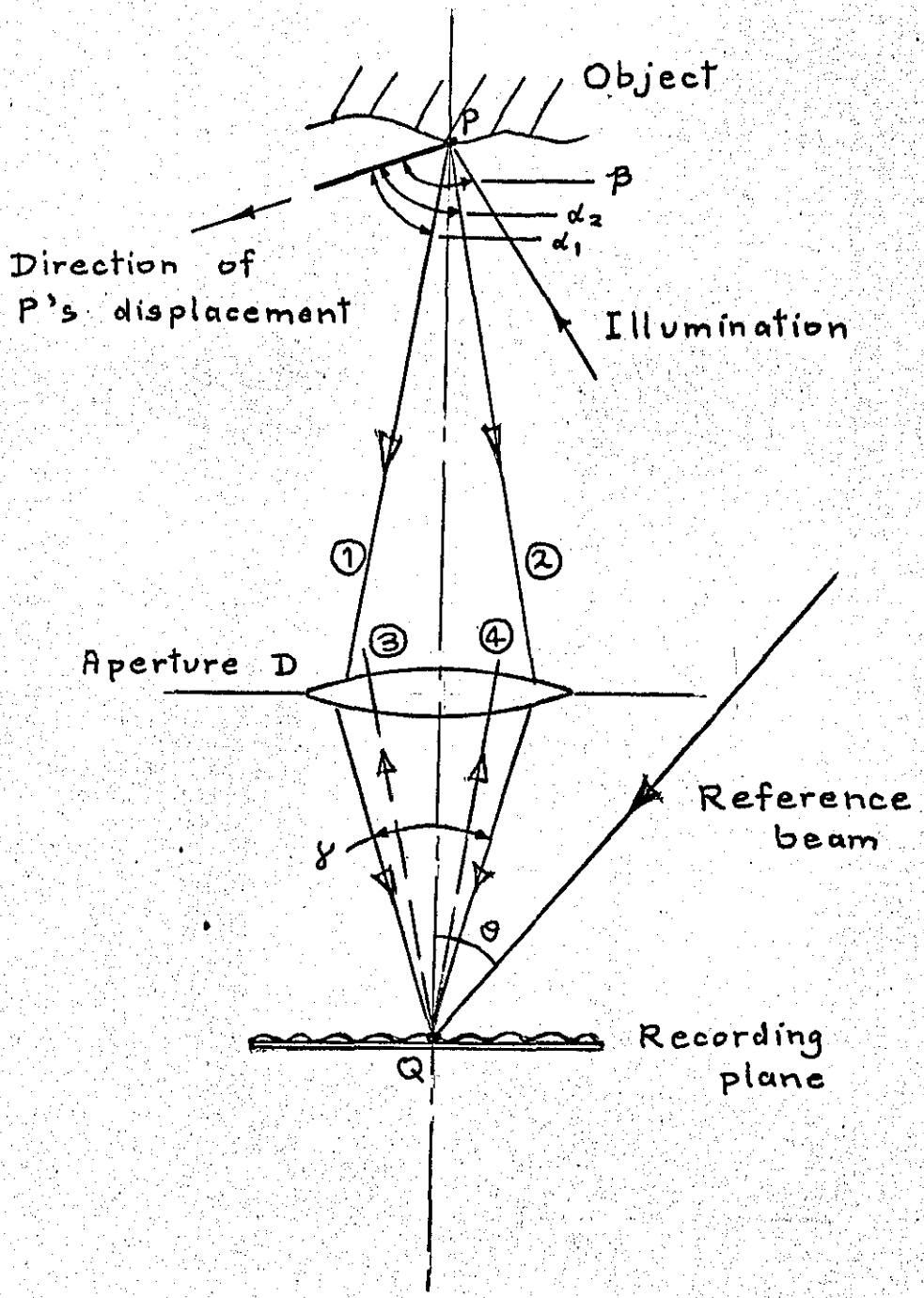

Fig. 6.11

Recording of a double exposure FI hologram in a situation causing a range of phase changes at Q.

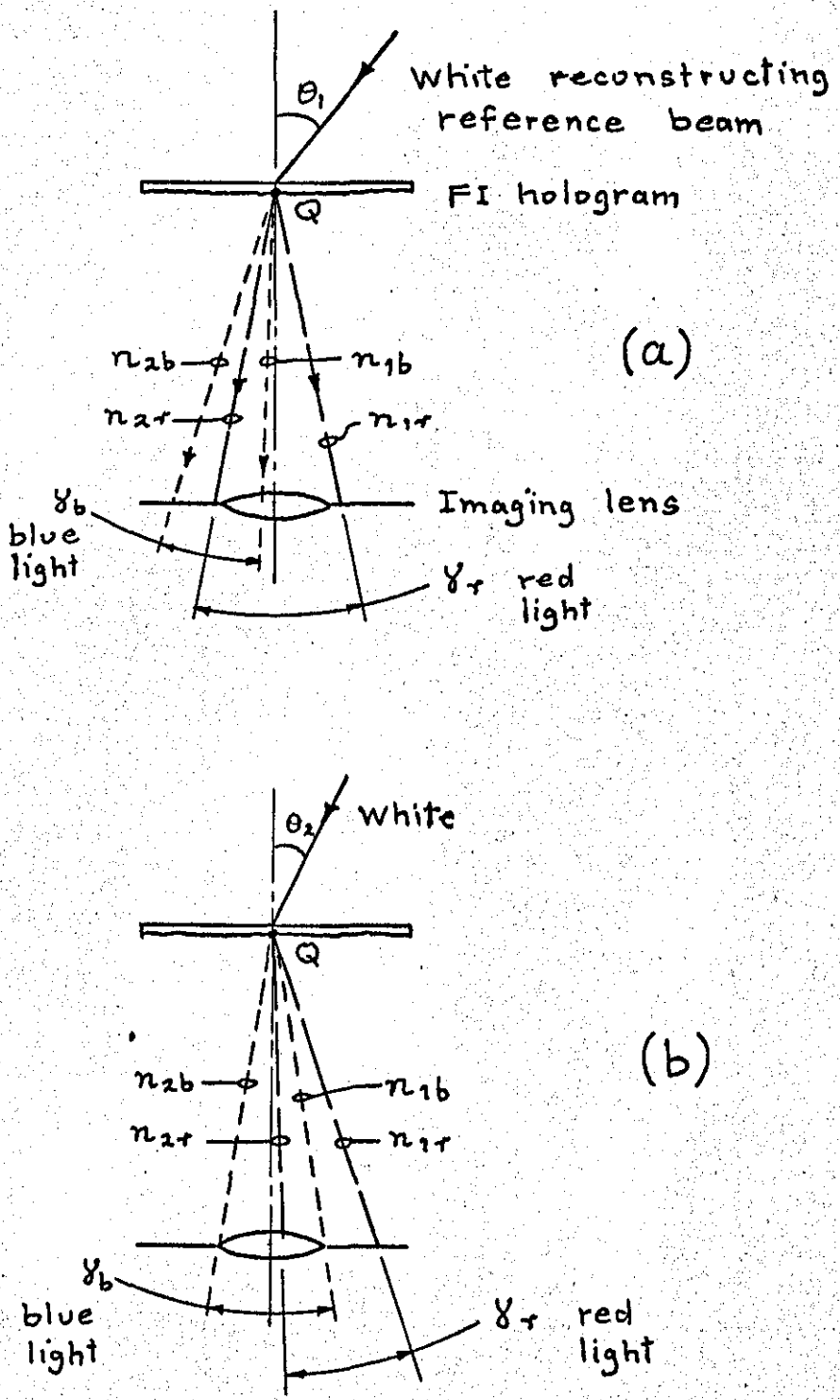

Fig. 6.12 White light reconstruction from point Q, from the situation in Fig.6.11
(a) viewing predominantly red light
(b) viewing predominantly blue light.

the imaging lens receives red light over the whole aperture and blue light over part. In forming the final image the lens integrates the light received within the aperture. Considering the red light alone, the intensity varies with the direction from Q, according to the value of n_r. Thus, for one colour alone, the visibility of the fringes seen over the image will be less than unity, and the visibility will decrease as the difference $(n_1 - n_2)$ becomes greater. Considering the spectrum of colours, for any one direction through the lens it is clear that the order numbers for the red and blue light diffracted along this line will be different. Thus, moving across the image so as to change the fringe order number, there will be a periodic fluctuation in the intensities of the two colours, with a certain lag between them depending on the difference $(n_r - n_b)$. Consequently the resultant colour observed across the image will change periodically with the 'average' fringe number. This is clearly seen on the colour prints of Fig. 6.10, showing an interferogram from a FI hologram of cantilever deformation. The effect is most pronounced around the fringes near the root, and also over the (supposedly) rigid pillar behind.

Suppose the reconstructing beam angle is reduced to θ_2, shown in Fig. 6.12 (b), such that predominantly blue light is received by the lens. While the colour mixing operates as described above, it is seen that the average fringe number is mainly influenced by the ② direction, whereas in (a) it is dominated by the ① direction. Thus in altering θ, the intensity at any one point in the image will change. This will occur in a regular manner over the

image, causing the interferogram to sweep across. This effect is also illustrated in Fig. 6.10, comparing (a) and (b), which show the minima of the dark fringes near the root in different positions relative to the short horizontal lines drawn on the object surface.

In order to support these predictions the following experiment was carried out. The cantilever object was used, with the direction of displacement arranged to be at 60° to the imaging axis. A double exposure FI hologram was recorded with a large lens aperture (f/3·5) such that for the two extreme directions ① and ② , the difference $(n_1 - n_2)\lambda$ was 0.11 d (equation 6.10). A second hologram was recorded with the same lens stopped down to f/8, giving a maximum value of the difference $(n_1 - n_2)\lambda$ of 0.05 d.

Photographs of the two interferograms were obtained in order to demonstrate some of the features of this type of FI hologram. Those of Fig. 6.13 were all obtained by laser reconstruction from the first hologram, using a 35 mm camera focused on the image in the hologram plane. In (a) a large aperture (f/2) was used, allowing the entire sector (γ_r) to be received. Thus fringe order numbers varied between n_1 and n_2 , and, as expected, the fringe visibility decreases with increasing order number. To confirm that different directions carried different order numbers, the lens was stopped down to f/16 and the image recorded in the directions ③ and ④ (shown in Fig. 6.11). These directions were as widely separated as was practicable; the interferograms appear in Fig. 6.13, (b) and (c) respectively. The fringes are seen to be of good visibility

right up the cantilever, and at the top there is a difference in n of ½, as predicted using equation (6.10).

White light reconstruction was used for the interferograms shown in Fig. 6.14, which in (a) and (b) are again from the first hologram. In (a) a large aperture (f/4) was used. Thus, not only did this receive different order numbers of the same colour, but also a large range of colours. Consequently the fringe visibility becomes very poor. Even when the aperture was reduced (to f/16) in (b), there was no improvement in fringe visibility, due to the integration of colours of varying order number. Comparison with Fig. 13 (b) and (c) shows the advantage of laser light in this situation. Finally, (c) shows the interferogram from the second hologram, photographed under the same conditions as in (a), that is, by white light reconstruction using a large aperture (f/4). This time good fringe visibility persists right up the cantilever, because the range of phase changes along different paths through the recording lens aperture was adequately restricted.

It is instructive to return briefly to the case of the colour prints of Fig. 6.10. Again, this hologram was of a cantilever type deformation, but the direction of deformation was almost parallel to the imaging axis. It is therefore surprising that the fringe colouring and shift effects have occurred. It is concluded that in manually applying the deformation, the object was inadvertently shifted laterally. From the observed apparent shift of nearly ¼ fringe, between red and blue reconstruction, it is calculated (equation (6.10)) that a lateral displacement

of only 2 wavelengths would be required to produce this effect. It is to be noted that the fringe colouring and shift effects become progressively less moving up the cantilever. This also is accounted for by the same explanation. Where the cantilever deformation was greater, the resultant direction of displacement would have been more closely aligned with the imaging axis, in comparison with the base which would have moved purely laterally. Thus the effects would decrease with increasing fringe number due to the cantilever deformation.

Conclusions

These results demonstrate that in the situation under discussion poor fringe visibility (beyond the first few fringes) by white light reconstruction is unavoidable. Reduction of the viewing lens aperture does not necessarily improve the visibility, because differing colours having differing fringe numbers are diffracted along any single direction (unless operating at one end or the other of the spectrum). In addition there is uncertainty in fringe position, as a consequence of fringe shift due to a change in the angle of the reconstructing reference beam. Thus, for accurate analysis of such interferograms it is necessary to revert to laser light reconstruction (or an alternative laboratory light source, such as a filtered mercury arc lamp).

For these reasons, and also the separate effect of reduced fringe visibility due to lateral object displacement discussed previously, FI holography is seen to be less appropriate in cases of object displacement lateral

to the imaging axis. Taking account also of image depth and blur, the method gives best results for relatively shallow objects which deform roughly in the direction of the imaging axis, implying buckling deformations of a surface. Fortunately many applications of HI include this category of object, particularly vibration analysis and non-destructive testing.

Of course, the method serves no purpose for real time experimentation with respect to white light reconstruction. (However, real time FI holography was used in one instance requiring magnification. The object was a cooler having individual parts measuring less than a millimetre. Satisfactory vibration investigations were carried out in real time by recording a FI hologram at about 6x magnification, using in situ processing.)

6.4 A PROJECTOR FOR DISPLAYING FI HOLOGRAM IMAGES.

It has already been noted that the image from a FI hologram may be conveniently viewed by projection on to a scattering screen. This is generally superior to direct viewing by eye largely because the viewing aperture has to be critically positioned. It was therefore a natural development to design and construct a white light projector for viewing FI hologram images, to apply fully the benefits of the method, and also to serve as a research tool.

Design Considerations

Since the projector was to be used for further study and development of FI holography, the main theme in its design was versatility. Where possible standard components

and materials were used, notably for the light source, to facilitate obtaining replacements, and in case further projectors would be required. The design was in British units throughout because at that time the Departmental workshop was still working to British units.

Basically the projector required an intense beam of white light to illuminate a FI hologram for reconstruction, a means of holding the hologram appropriately orientated to the beam, an imaging lens positioned so as to collect the diffracted light, and a scattering screen in the image plane. In order to accommodate holograms made with variations in: design angle, reference beam curvature, image distance, image size, and plate size, certain adjustments were required in the projector to obtain a bright, suitably sized image in all cases.

Firstly, images recorded in the hologram plane would vary in size, would be recorded on different sizes of plate (or film), and would occupy different regions within the plates. Therefore adjustment of the hologram position in the x and y directions (lateral to the imaging axis) was necessary. Consequently a multi-hologram mount (for comparing different holograms quickly in succession) was considered to be too complex, and so one hologram at a time was to be inserted. In view of the adjustments already needed, it was practical, to avoid undue complication, to have a fixed plane for all holograms. It was fairly obvious to choose the xy plane, so that in all cases the hologram plane would be perpendicular to the imaging axis. Furthermore no rotational adjustment of the hologram within this plane was to be provided; they would all locate on

their lower, straight edges.

With regard to the illumination beam, an intense light source was necessary because simply processed holograms have diffraction efficiencies of only a few percent. Also, a small source size was required in order to obtain a reasonably well-defined beam direction from the available light. Taking account also of portability of the projector and general ease of operation, a 250 W tungsten halogen standard projector lamp was selected. In preliminary trials this was found to produce a final image of sufficient brightness to be viewed in a normally lighted room, providing that direct light was shielded from the screen. Together with the lamp other standard projector parts were used: cooling fan, reflector, and heat filters. To complete the illumination beam, a converging lens was required that would form a beam of desired curvature at the hologram and of sufficient diameter to illuminate it uniformly. The desired curvature is that which enables the imaging lens to collect the light diffracted from the hologram so as to produce a complete image, uniformly bright. Thus the desired curvature of wavefront was related to the conditions under which the hologram would be recorded, and also would depend on the distance of the projector imaging lens from the hologram. In turn, this distance would depend on the desired final image size, and the focal length of the imaging lens. A few typical situations concerning objects of different sizes were considered, using the focal length of a hologram relationship, equations (3.2), (3.3), (3.4), to calculate the required illuminating beam curvature and imaging lens position in reconstruction. These showed that,

commonly, an approximate duplication of the optical geometry used in recording the hologram was required. Since the recording reference beam was usually simply divergent, this required a convergent beam (incident on the rear face of the hologram) in reconstruction. In other forseeable cases the reconstructing beam would need to be approximately collimated or divergent. Thus continuous adjustment of the beam wavefront shape was needed, and this was achieved by varying the distance of the beam forming lens from the lamp.

Having decided to keep the hologram plane and imaging axis fixed, the variable angle of incidence of the illumination beam was provided by arranging the complete light source as a unit mounted on a pivoted arm. Its axis of rotation was vertical, in the hologram plane, and intersecting the imaging axis. This is shown by the optical arrangement of the projector drawn to scale, in Fig. 6.15.

The main considerations for the imaging lens concerned the quality of image formation, the desired magnification, and the optimum position of the lens to collect the light diffracted from the hologram. It was apparent that a single lens could not produce the best image in a variety of circumstances, and therefore inter-changeable enlarging lenses of differing focal length were selected. An accompanying factor in lens selection was of course the imaging distance and size of viewing screen. This was a compromise between providing a useful range of magnification, and keeping the projector reasonably compact. Magnification curves for the two most commonly used lenses, viz 50 and 75 mm focal length, obtained from the projector, are plotted in Fig. 6.16.

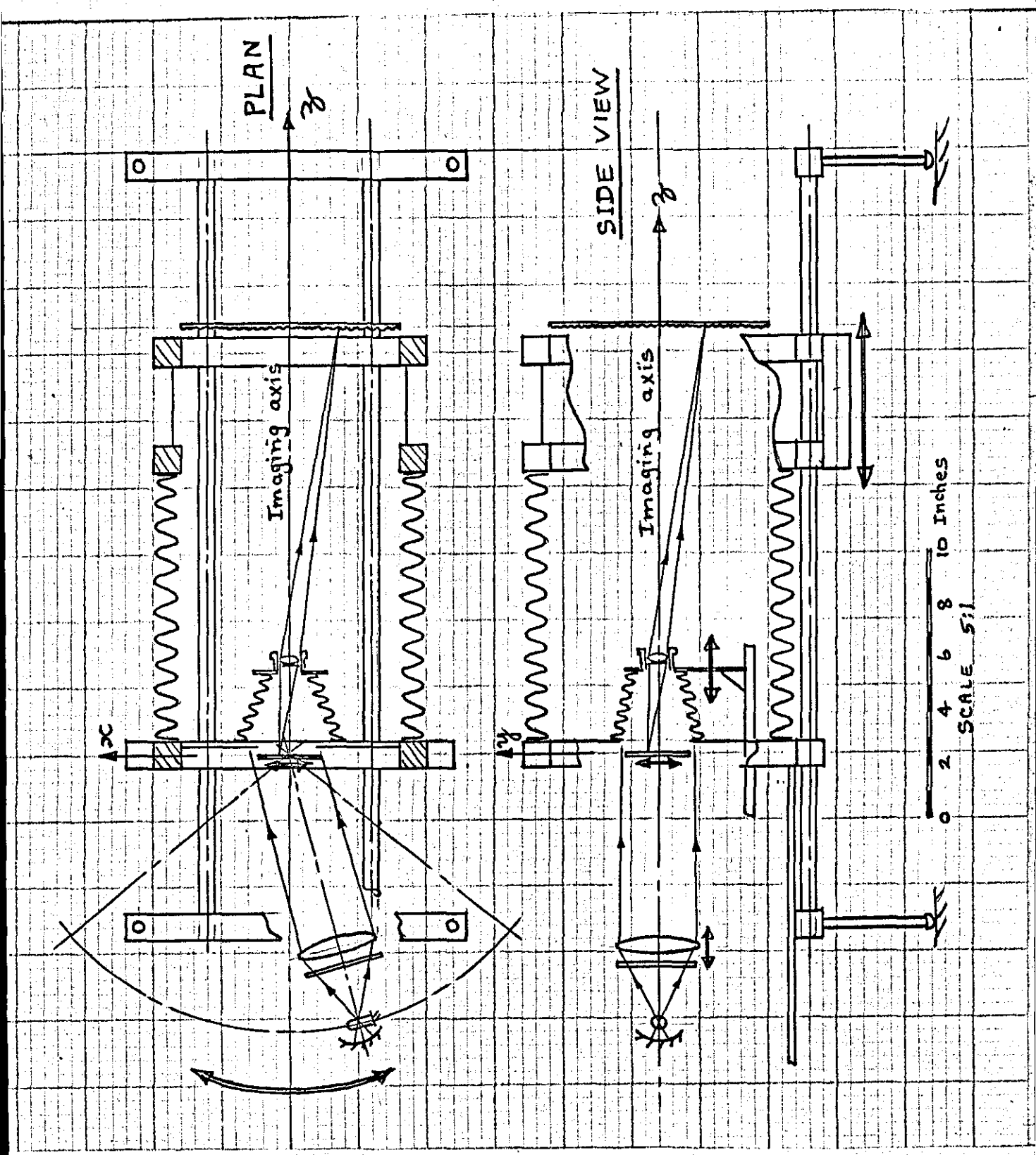

Fig. 6.15 The projector for viewing FI holograms : Principal layout to scale, showing ray paths, and defining axes.

⟷ : Adjustments.

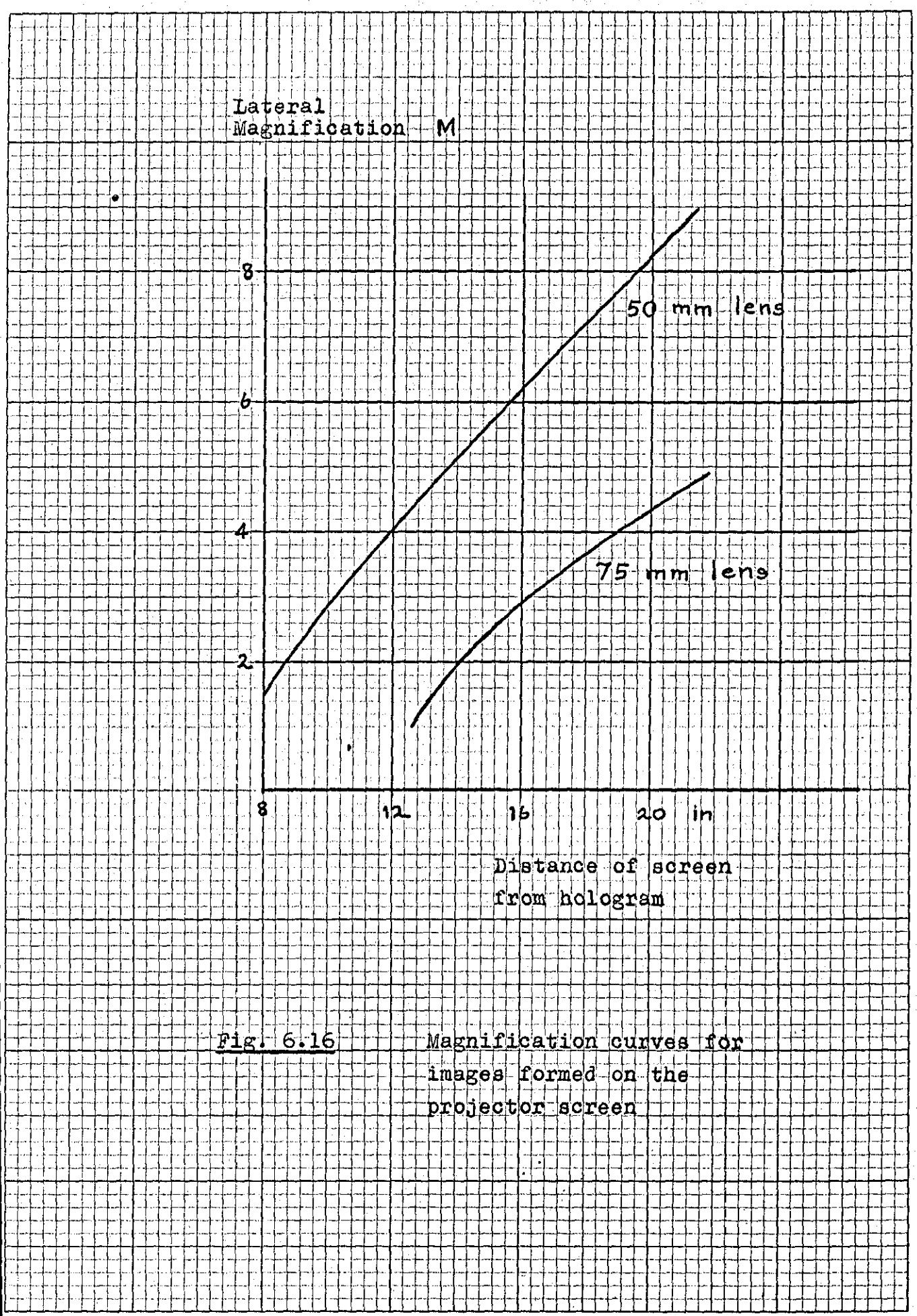

Fig. 6.16 Magnification curves for images formed on the projector screen

Especially in its role as a research tool, it was essential to be able to obtain photographic records of image presentation in the projector. Accordingly a facility for this was incorporated in the projector. The simple principle of replacing the viewing screen by the photographic material, as in plate cameras, was adopted. A double dark slide for 5 in by 4 in sheet film was used, this being simpler to incorporate than a mechanism for winding on a roll of film, and satisfactory for recording just a few images at one time. A sighting frame, 5 in by 4 in, was scribed on the viewing screen, in the position to be occupied by the film. The screen was mounted in a door, so that having focused the image within the scribed rectangle, the screen would be swung clear, allowing a second door containing the film slide to be closed. The exposure would be timed by a shutter mounted behind the imaging lens, and operated from outside by a bulb release. Lightproofing of the space between the imaging lens and the film slide was provided so that photographic records could be made in a lighted room, such as a design office or laboratory. Large, square section bellows were made to order for lightproofing the extendable space between the respective frames supporting the hologram and the viewing screen.

The design of the projector which resulted did place a few restrictions on how FI holograms should be recorded:-

(i) The plate (or film) should be perpendicular to the imaging axis.

(ii) The edge of the plate adjacent to the top of the image should be parallel to the plane containing

the reference beam and imaging axes (so that the hologram is correctly orientated for reconstruction in the projector).

(iii) The design angle should not exceed 45° (either side of the imaging axis).

(iv) The hologram plate and image should be within a range of sizes, as given in Projector Specification.

A Projector Specification sheet is given to summarize the main features. The photographs of Figs. 6.17 to 6.25 show details of interest, some of these photographs having been taken during construction. The completed projector, Fig. 6.17, shows the two knurled wheels for adjusting the angle of incidence of the illumination beam and the position of the viewing screen. The latter's position is indicated by a scale, to be used for reading off the magnification from the curves of Fig. 6.16. These two adjustment controls, together with those for focusing (imaging lens position) and varying the hologram's vertical position, are all within reach for adjustment while viewing the image on the screen. Two views of the pivoted arm unit for the illumination beam are shown in Figs. 6.18 and 6.19. The arm runs freely on bearings, but can be held in any set position by a simple friction screw. These views show the means of adjustment for initially setting the position of the reflector and lens relative to the lamp, and the fan and air duct for cooling the lamp base. In Fig. 6.20 a FI hologram is shown inserted in its mount, located in a shallow groove in a supporting bar, with a similarly grooved bar locating its top edge. This second bar is under the action of gravity, and the whole arrangement may be raised or lowered by the screw threaded through the top member of the frame. This photograph and that in Fig. 6.21 jointly show the sliding mount,

Projector Specification.

POWER SUPPLY : 240 V a.c.

HOLOGRAM SIZE : Height between 1 and 3½ in (25 and 90 mm)
Width up to 4 in (100 mm)
Thickness up to ¼ in (7 mm)

IMAGE SIZE : Maximum of 2 in (50 mm) square, or 2½ in (63 mm) diameter.

HOLOGRAM MATERIAL : Plate, or film mounted as a transparancy.

LIGHT SOURCE : 250 W, 24 V tungsten halogen projector lamp, type A1/223, with spherical concave reflector. Heat absorbing filters in beam.

BEAM FORMATION : F=3¼ in (82 mm) lens at f/1.1 forms beam; beam shape is continuously variable between divergency of F = -42 in (1.05 m) and convergency of f = +42 in (1.05 m), by axial adjustment of lens position.

BEAM ANGLE OF INCIDENCE AT HOLOGRAM : can be varied ± 50° in horizontal plane about imaging axis, remotely controlled by observer, at viewing screen.

HOLOGRAM MOUNT : Hologram plane perpendicular to imaging axis; screw adjustment of vertical position over 1½ in (38 mm) range; manual positioning sideways.

IMAGING LENS : Interchangeable standard thread enlarging lenses, of 75 mm and 50 mm focal length, built in iris.

VIEWING SCREEN : Ground glass, 7½ in (190 mm) square. Rack and pinion adjustment of position along imaging axis.

MAGNIFICATION ; Range x1 to x5 with 75 mm lens; range x1.5 to x9 with 50 mm lens.

FOCUSING : Rack and pinion adjustment of imaging lens position, with friction lock acting on slider.

PHOTOGRAPHIC RECORDING : uses 5 x 4 in double dark slide for film; projector light-proofing permits use in daylight.

SHUTTER : Compur, 1-1/400 s,B, and T, iris opening to 1 in (25 mm), remote release, detachable from projector.

FRAMEWORK : Stainless steel tubing, and aluminium alloy square section bar and sheet.

OVERALL DIMENSIONS : 38½ in (1 m) long x 26 in (0.66 m) wide x 18¼ in (0.45 m) high.

driven by rack and pinion, for the imaging lens. Stray light is prevented from by-passing the lens by bellows, not shown here. The free end of the slider allows the shutter to be fitted, as shown in Fig. 6.22, when photographic records are required. Access for inserting the shutter is through the opened viewing screen door, shown in Fig. 6.23. The other door holds the double dark slide for film, and shuts in position for recording images, as seen in Fig. 6.24. Finally the projector in use is shown, Fig. 6.25, with an interferogram of turbine blade vibration projected on to the screen. By turning the illumination beam arm, the colour of the projected image changes through the spectrum.

Benefits of the Projector

The examination of interferograms from FI holograms is far more convenient using the projector than by direct observation. Its use enables two or more people together to view and discuss the fringe information, at a suitable magnification. Fringe positions can be better judged from the screen than by observing directly a virtual image; if necessary they can be measured directly from the screen. Consequently the need for photographic prints of interferograms is often avoided, thereby reducing the time and effort of HI analysis. When photographic records are necessary, as for reports, the projector is quickly converted to a camera, using standard size (5 in by 4 in) film. Several photographs in this chapter (Figs. 6.2, 6.3, and 6.4) were obtained in negative form using the projector. (Exposure times ranged between $\frac{1}{25}$ s and 1 s, depending on the f number setting of the imaging lens. None of these holograms was bleached.)

In addition the projector has subsequently been useful for observing fringe patterns formed by a method of double exposure speckle pattern photography. In this particular method (ARCHBOLD et al, 1970; BUTTERS and LEENDERTZ, 1971), applied especially to in-plane displacement, better visibility fringes representing the surface deformation are obtained by introducing a relative shift of the two images, and subsequently viewing in the direction of the first order minimum. (Diffraction arises from a Young's two slit effect produced by the displaced speckle patterns.) The desired fringe system over the image can be produced either by laser or white light. The projector is suitable since continuous adjustment of the illumination beam angle is available. The advantage is then one of convenience, as in viewing FI holograms. The colour of the image is grey since the angle of diffraction is small, with a correspondingly small angle of colour dispersion. If an alternative laser light system is used, a means of restricting viewing directions within small angular ranges is required, such as a telescope, or a filter in the Fourier plane.

6.5 FUTURE DEVELOPMENTS AND CONCLUSIONS

It has been shown in this chapter that the method of FI holography may be used to advantage in HI. Principally, the benefit derived is in viewing an interferogram using a simple white light source for reconstruction. Thus a laser, normally used for reconstruction, is relieved for other work, eye fatigue and hazards of eye damage are avoided, and the hologram may be viewed outside the laboratory.

There are other purely technical advantages:-

(i) Greater dynamic range of intensity from an emulsion is obtained by reconstruction than by a conventional photographic image. This then is an advantage over the common procedure of photographing the image formed by reconstruction in order to study a positive print of the interferogram.

(ii) Once a FI hologram has been formed, no further distortion to the image can occur as a consequence of the reconstructing beam having differing wavelength and wavefront curvature from that of the reference beam used in recording.

Full benefits are realized by projecting the image on to a screen, as already described in the previous section. Apart from the addition of an imaging lens, procedure at the recording stage is essentially the same as in conventional Fresnel holography.

The interpretation of fringes has been shown to be the same as in conventional HI, namely, fringe order number being dependent on the angles α and β, of equation (4.1). Object displacement lateral to the imaging axis tends to cause poor fringe visibility, (as also occurs in Fresnel HI). There is the further restriction that deep objects tend to cause image blur in white light reconstruction. Although this effect can be reduced by decreasing the design angle at the recording stage, this remedy is not wholly satisfactory because the reconstructing beam then causes background glare in line with the viewing direction. Thus FI holography is best applied to relatively shallow objects which deform roughly in the direction of the imaging axis. In many cases

this implies predominantly out-of-plane deformation, of which a good example is resonant vibration of turbine blades and discs.

For the future development of FI holography, a natural course would be the design of a standardized rig to be applied in routine inspection and testing of components of similar form. Using a standardized rig and procedure, the operator would need only a moderate amount of experience, and a considerably simplified form of white light projector would be used to examine the results. Routine inspection rigs using conventional HI are in existence, such as that designed by HOCKLEY (1969) for the inspection of the resonance characteristics of turbine components. Such a rig could be adapted to gain the advantages of FI holography. Taking this example for an envisaged application, the following proposal indicates the form of standardization which could be implemented.

The optical recording arrangement (for centre-height rays) would be as shown in Fig. 6.26, all mounted on a single isolated table,or rigid frame. FI holograms, H, would be recorded on 35 mm film in a body such as the Ilford "Monobar", each within a 25 mm square frame. After processing, each frame would be mounted in a conventional transparency mount, for viewing in a projector. A 50 mm focal length, f/3·5 lens, L, with axial adjustment over 17 mm range for focusing would have an object field range of between 20 and 150 cm. This would accommodate objects of up to 75 cm diameter, the smallest object to fill the image frame being 7·5 cm diameter. The object would be illuminated by a diverging beam, directed by the adjustable mirror, M. According to

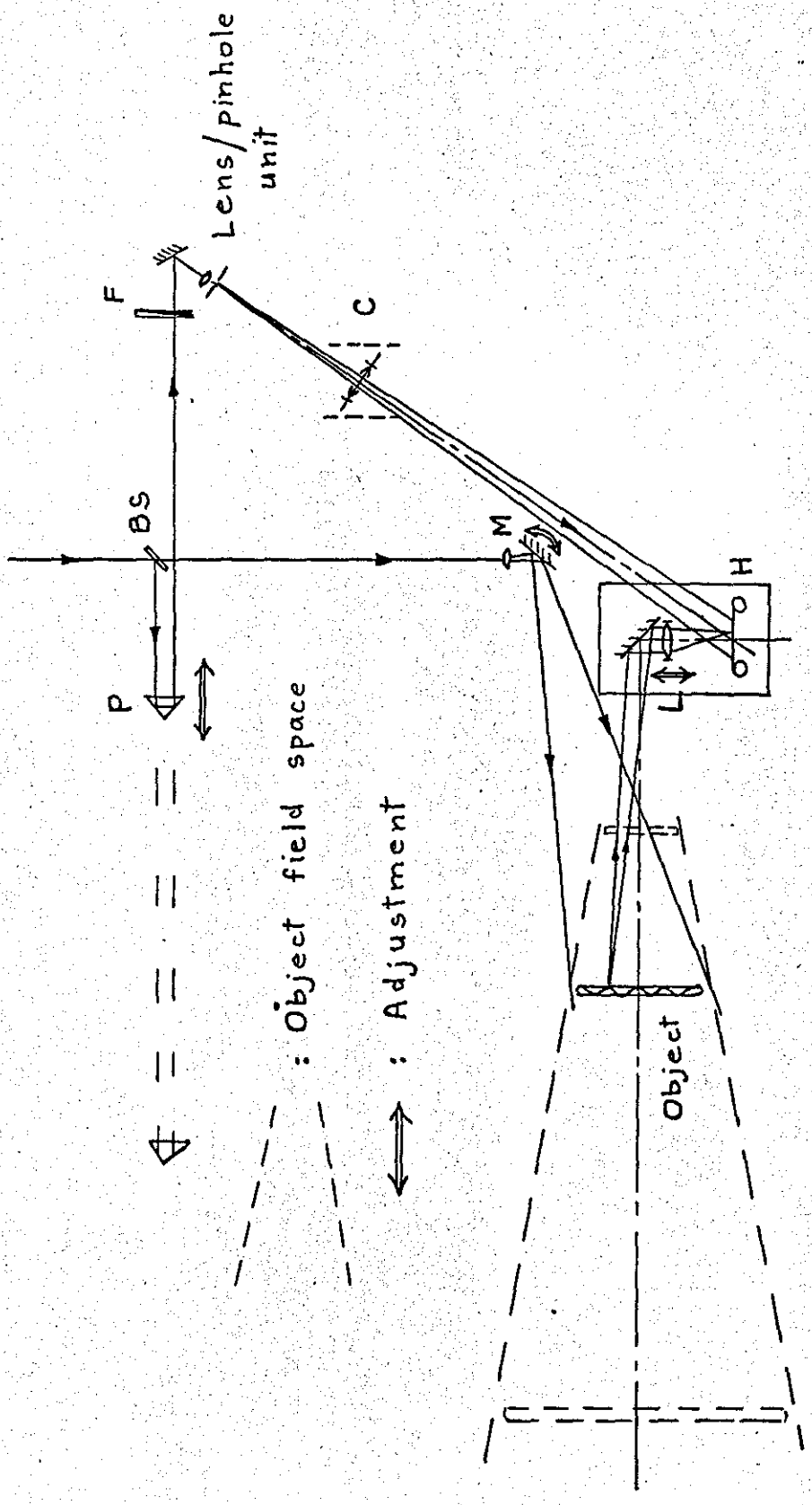

Fig. 6.26 Proposed standardized FI hologram recording rig for routine testing and inspection.

the position of the object, the path length of the reference beam would be matched by the adjustable prism P. The reference beam would be provided by a beam splitter, BS, coated to provide a 10:90 ratio of reflectance to transmittance, with a graded density filter, F, for adjusting the beam ratio. Since the object illumination beam would closely match the cone of the object field space, this lens alone would suffice for all objects in the range 7·5 to 75 cm diameter. For special cases, such as very small objects, a lens of different power could be interchanged. The following parameters would not be variable:-

(i) Design angle (35°) ;

(ii) Reference beam curvature (radius of wavefront is 61 cm).

An optional alternative would be a collimated beam, provided by changing the converging lens for a more powerful one, and inserting a collimating lens, C;

(iii) Recording plane attitude (perpendicular to the imaging axis);

(iv) Image frame size (25 mm square).

The imaging distance would vary between 52 and 67 mm. In considering the position of the imaging lens in the projector to collect the diffracted light, the mean distance (59 mm) would be regarded as the value in all cases. Thus, provided objects were recorded so as to fill the image frame, only one imaging lens, in a fixed position (apart from slight focusing adjustment) would be needed in the projector.

Considerable simplification of the projector constructed for this project work would then be possible. Whereas in the existing projector the following features are all

adjustable, for the standardized rig they would not be variable:-

(i) angle of incidence of illumination beam;

(ii) radius of curvature of illumination beam, incident at the hologram;

(iii) hologram position, vertically and horizontally lateral to the imaging axis;

(iv) screen position, and hence magnification.

The overall size would depend largely on the desired image size at the viewing screen. Such a projector could be simply and cheaply constructed, to be duplicated wherever required. Probably one projector, in a design engineer's office for example, would incorporate a camera for reproducing results.

This proposed development was envisaged for examining vibration modes and static deformation. However, recent developments in speckle pattern interferometry, using closed circuit television equipment to detect, process and display the optical information, have provided much faster and more convenient procedures than are possible by photographic procedures used in holography, (BUTTERS and LEENDERTZ, 1972). By this new technique, interferograms of component vibration are viewed virtually instantaneously, and step-function deformations may be examined in real time with only a short delay, depending on the type of video store used to record the initial state. The form of the interferogram, in either case, corresponds exactly to that obtained by the equivalent HI method. However there is a notable difference in terms of the image resolution. The resolution capability of a television (vidicon) tube is between one and two orders of

magnitude less than that of holographic emulsions. Consequently markedly superior image quality is obtained holographically, with many more fringes resolvable. In the case of vibration, only a few fringes beyond the zero order are visible by the speckle pattern method, because the visibility by speckle interference is inherently relatively poor. Thus for examination of vibration modes and static deformation, electronic speckle pattern interferometry is certainly more practical and versatile; when image quality is critical, HI is superior, and in these cases the FI method is favourable. Cost and laser power requirements also count in favour of (FI) holography. Good quality FI holograms can be made using He-Ne lasers of only a few milliwatts output (though of course high power is generally advantageous, to decrease exposure times). Electronic speckle pattern interferometry is relatively expensive, using (standard) closed circuit television equipment, and in general requires greater laser power than for holography, implying a more expensive laser.

Finally, the feature of white light reconstruction offers a potential application of FI holography as a means of display. For example, FI holograms recorded on film could be bound in book form, for specialized publications, as demonstrated by the FI hologram which appears in the frontispiece of this thesis.

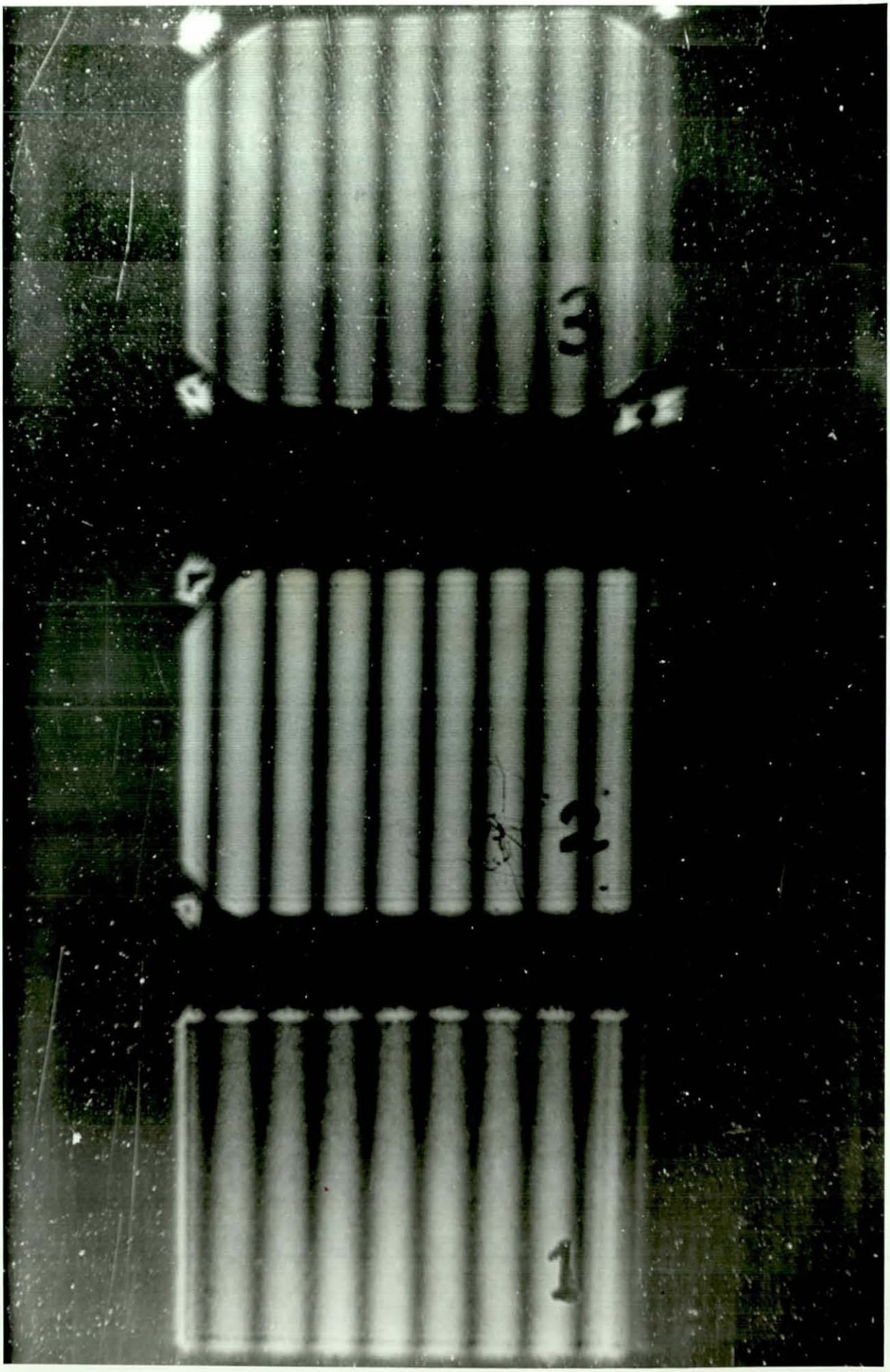

Fig. 6.2 White light reconstruction FI holography : object brightness ratio of 16:4:1 in areas 1, 2, 3

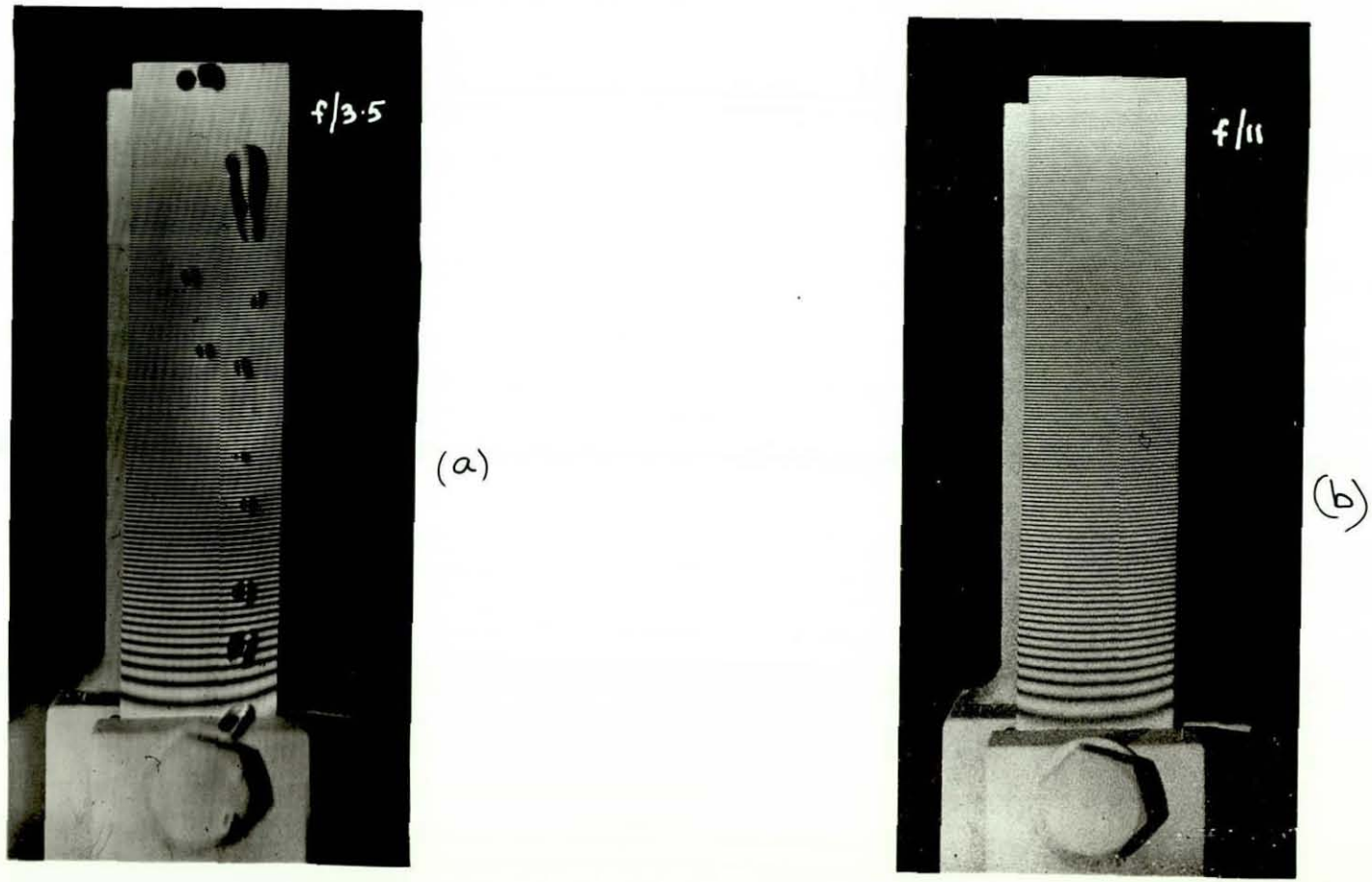

Fig. 6.3 Effect of recording aperture on speckled appearance of FI hologram images:-

(a) recorded at f/3·5

(b) recorded at f/11

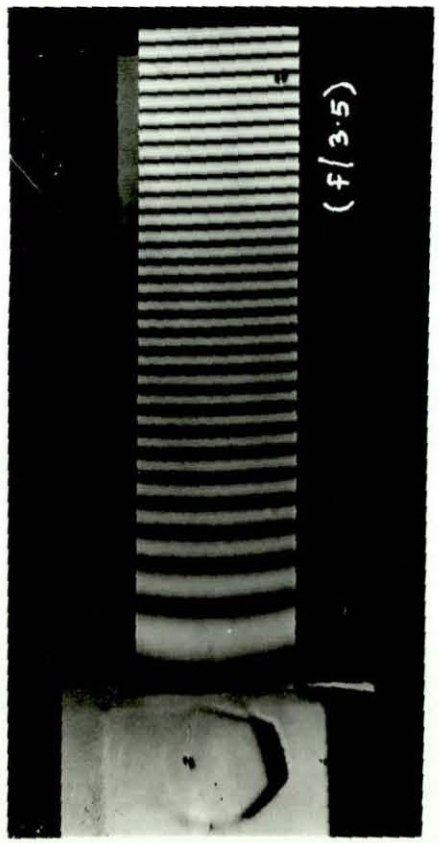

(a)

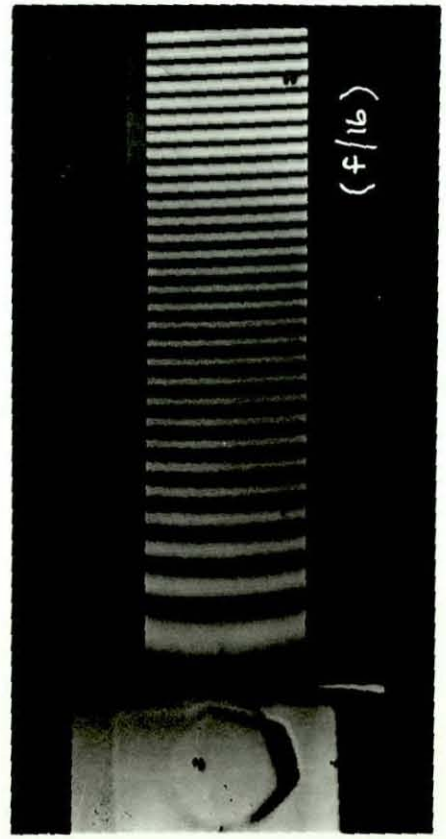

(b)

Fig. 6.4 White light reconstruction from the same FI hologram :-

(a) imaging lens at f/3.5

(b) imaging lens at f/16

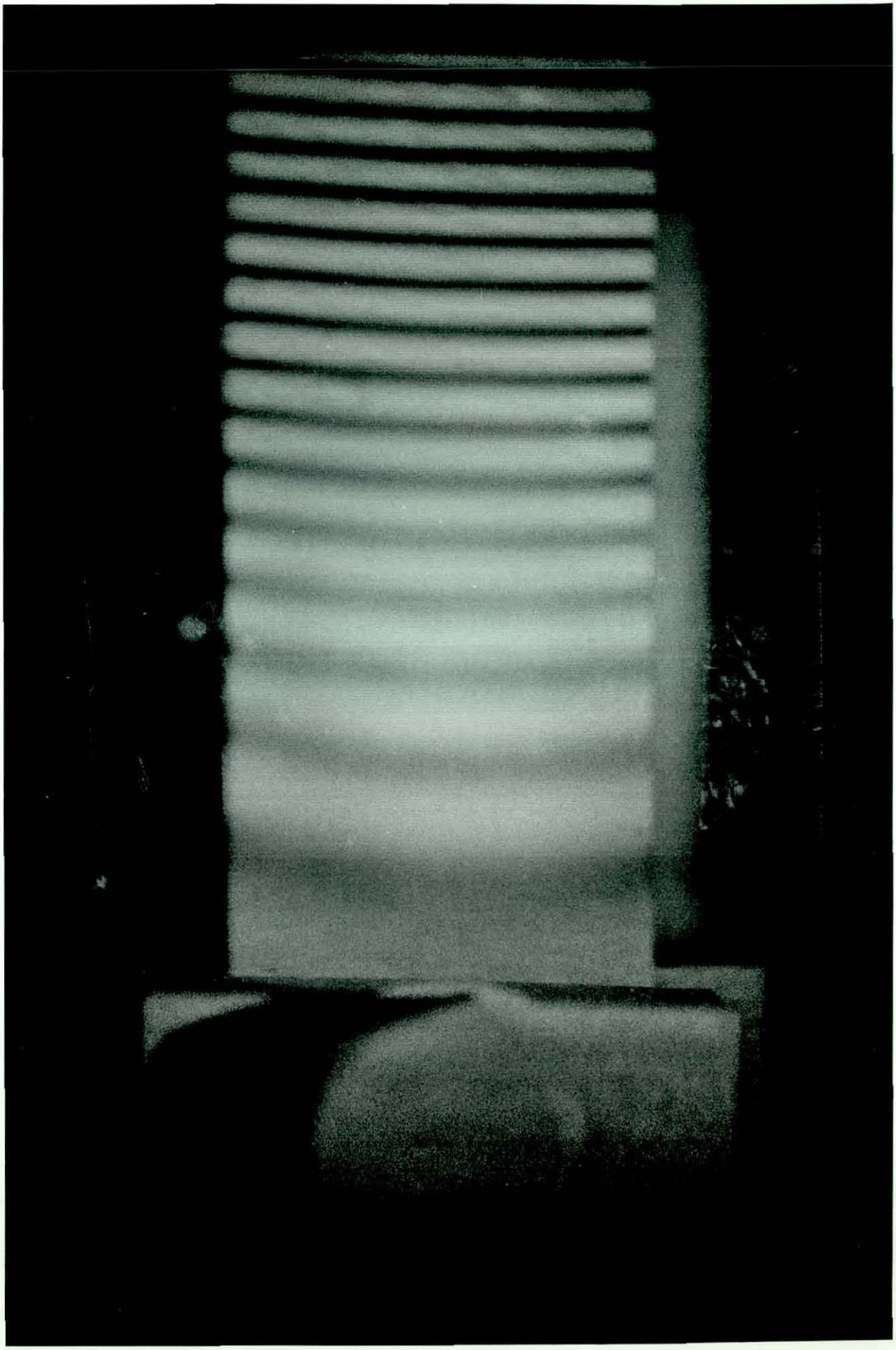

Fig. 6.7 Image by reconstruction from an in-line reference beam FI hologram

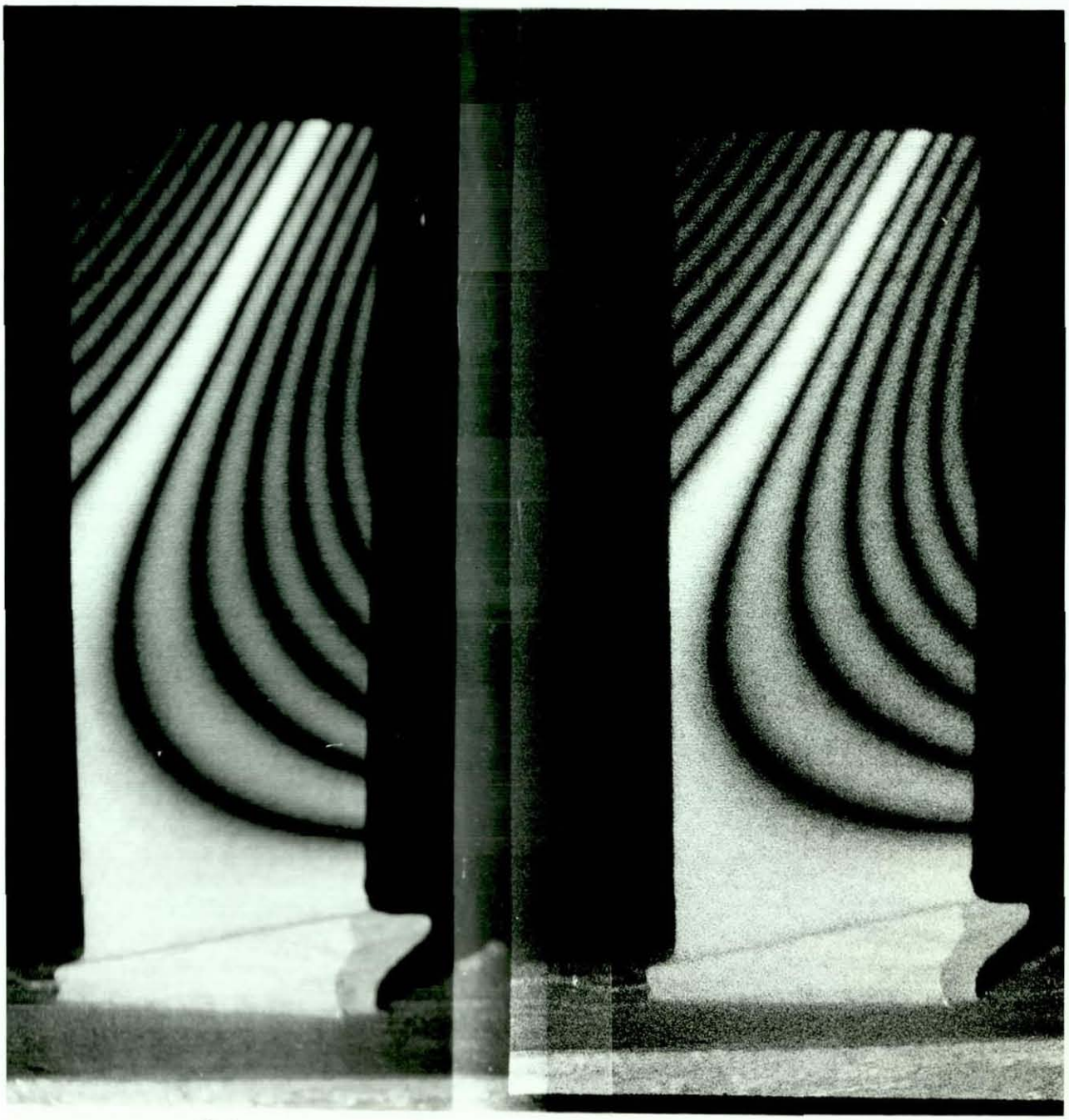

(a) (b)

Fig. 6.9 Photographs of blade resonance at 1647 Hz recorded as in Fig. 6.8 (a) FI hologram; (b) Fresnel hologram (white light reconstruction)

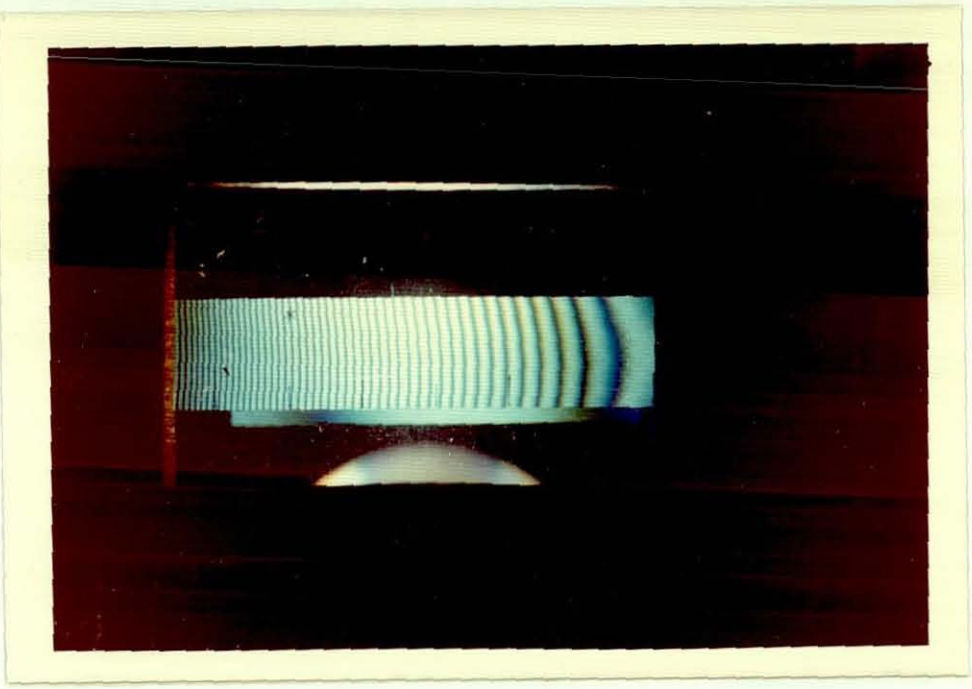

(b)

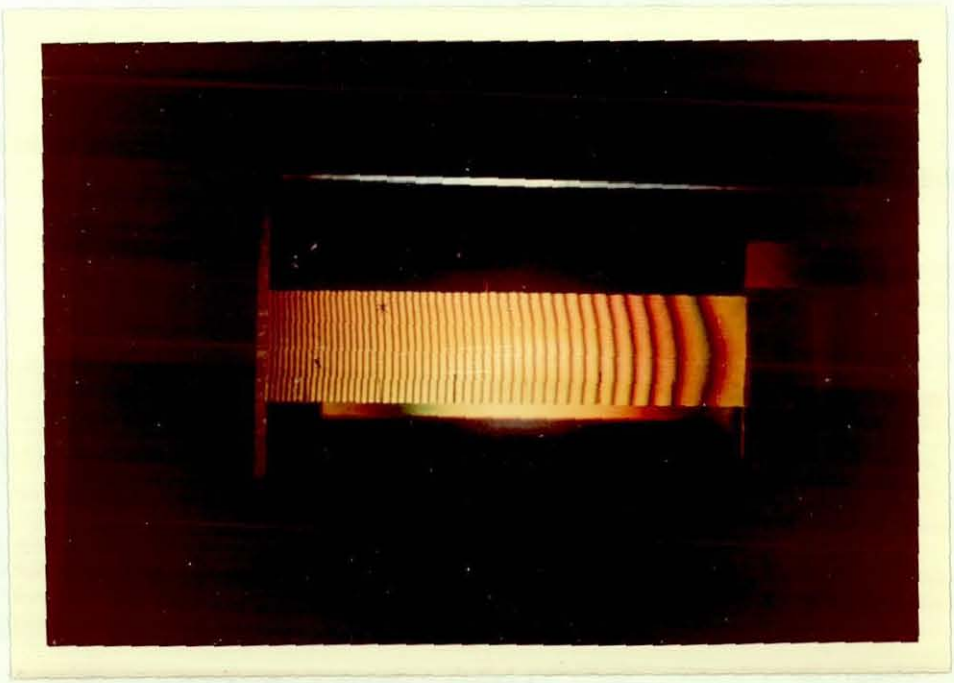

(a)

Fig. 6.10 Interferograms by white light reconstruction from the same F I hologram :-
(a) orange light selected,
(b) blue light selected,
to show fringe colouring and shift.

(a)

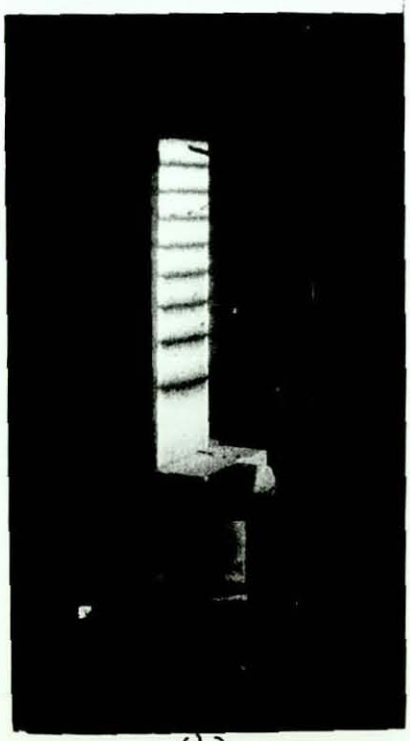

(b)

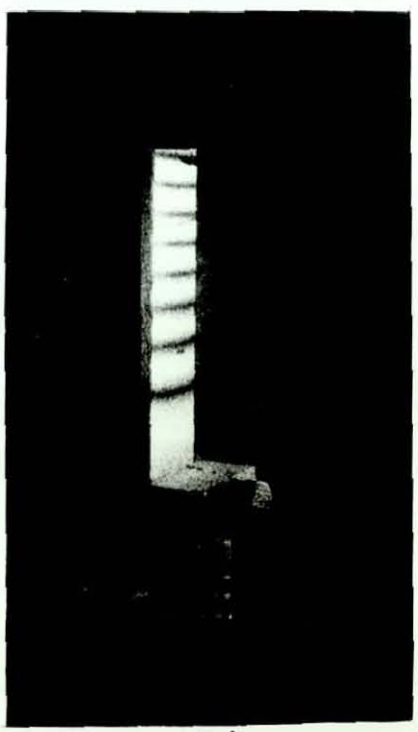

(c)

Fig. 6.13 Laser light reconstruction from a FI hologram recorded at f/3·5 :-

(a) photographed at f/2 ;

(b) }
(c) } ··· at f/16, but each in a different direction

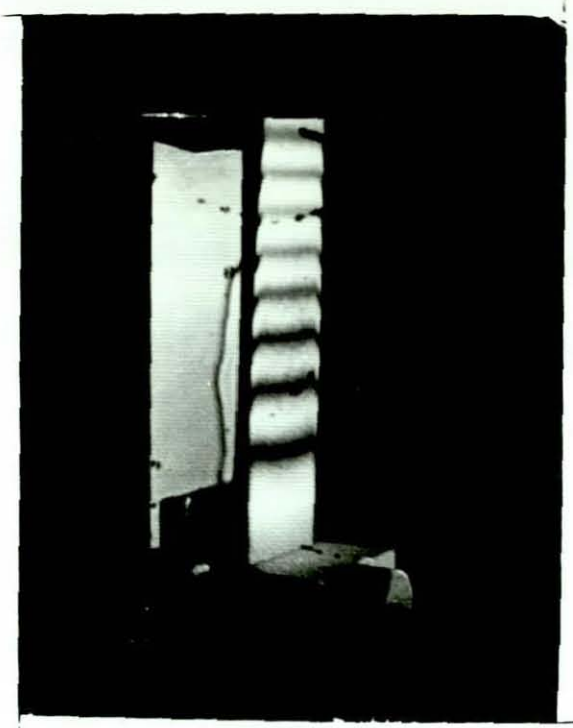

(a)

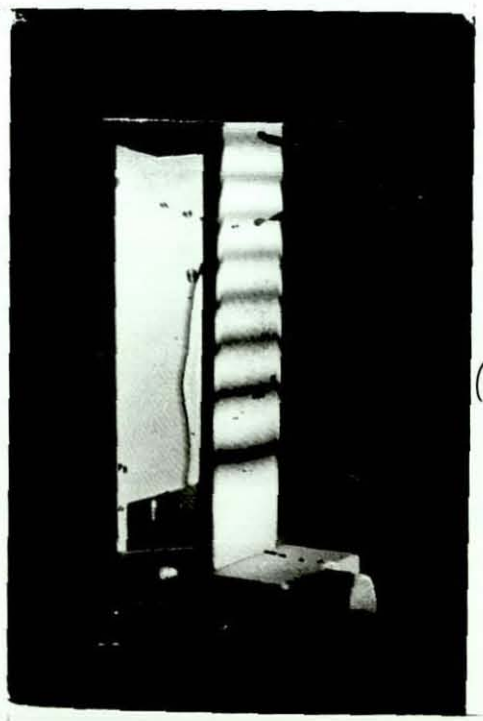

(b)

(c)

Fig. 6.14 White light reconstruction from FI holograms :-

(a) recorded at f/3.5, photographed at f/4;

(b) as (a) but photographed at f/16;

(c) recorded at f/8, photographed at f/4

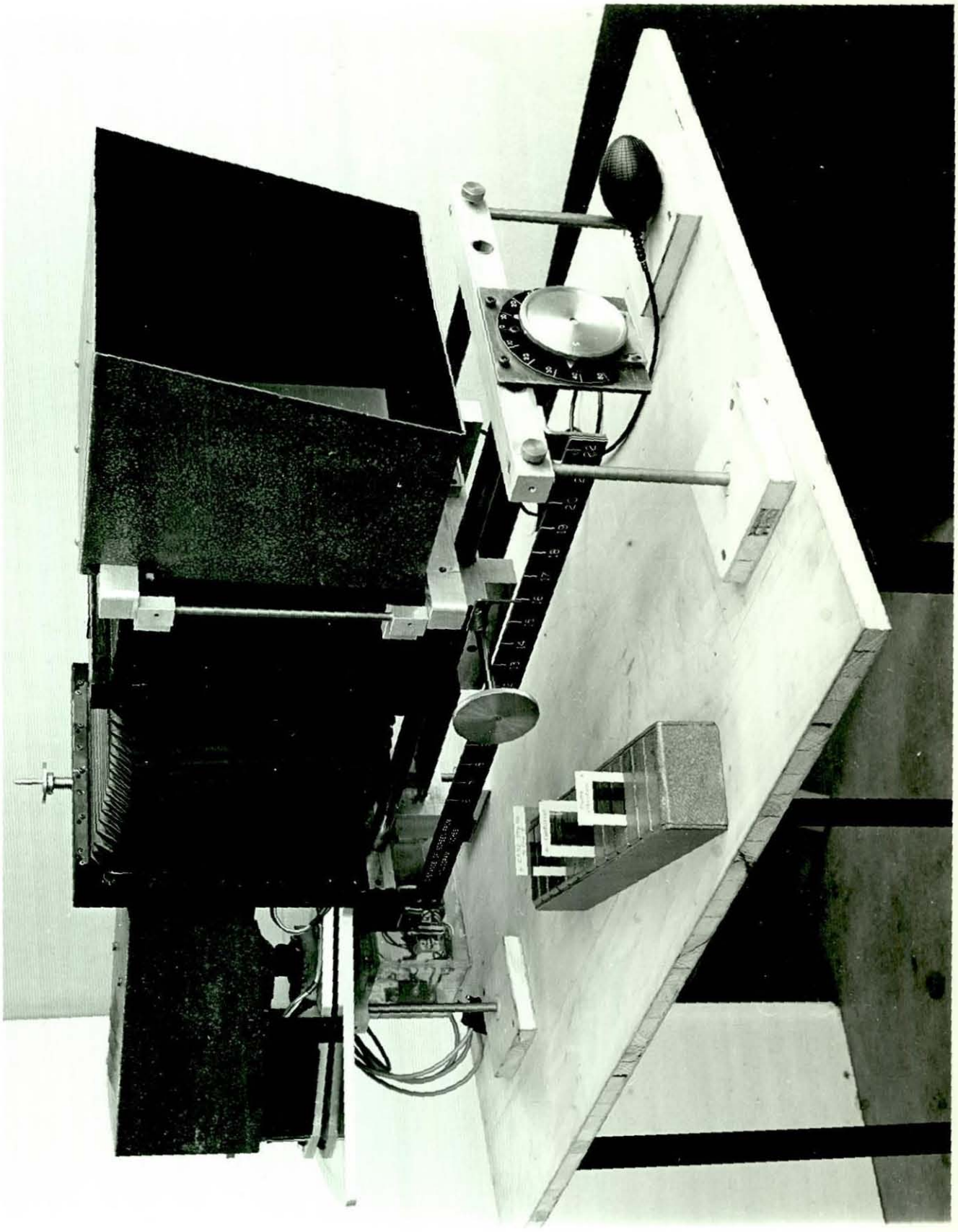

Fig. 6.17 The white light projector for viewing FI holograms

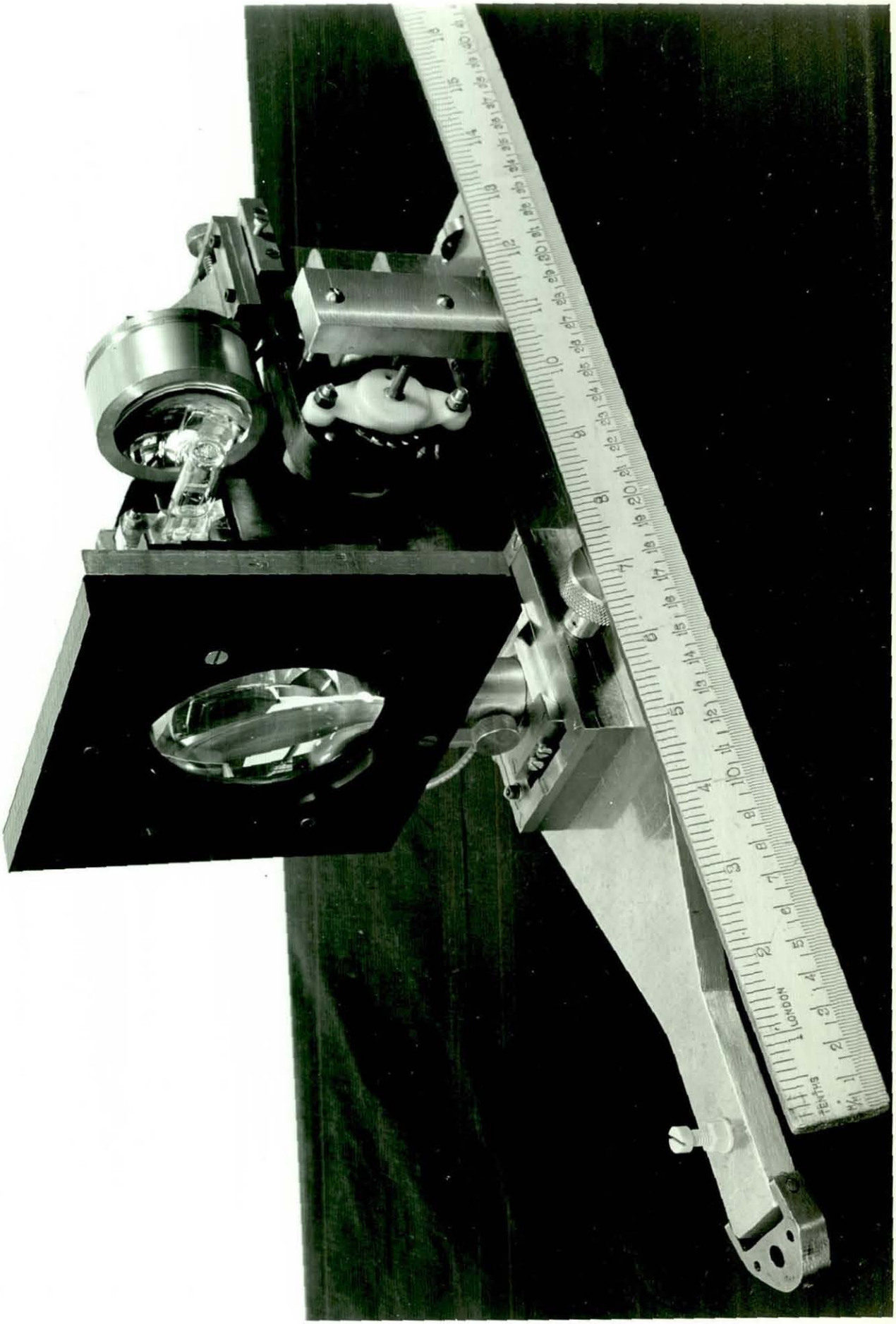

Fig. 6.18 Projector: Beam formation unit on piroted arm

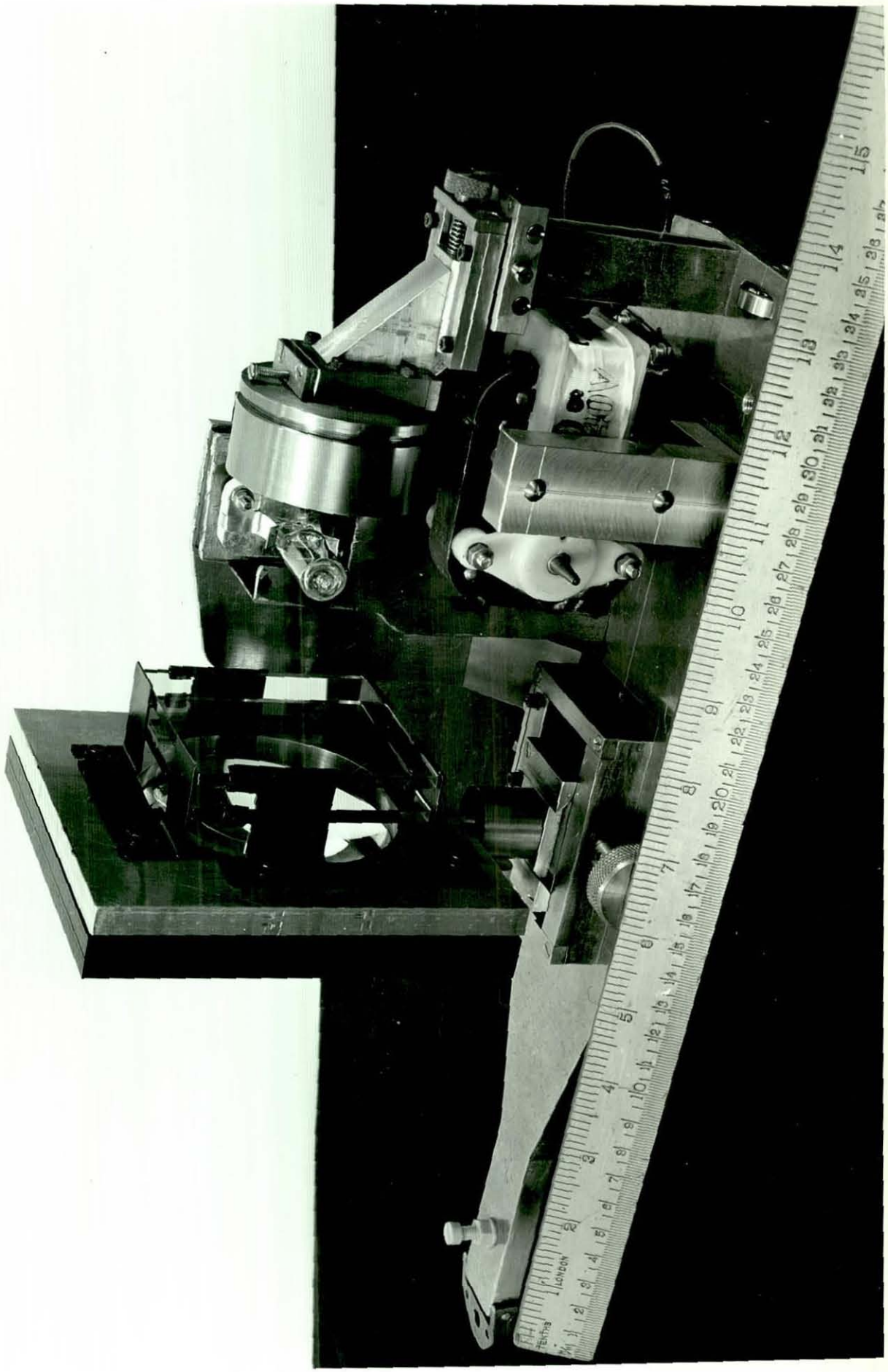

Fig. 6.19 Projector : Beam formation unit on pivoted arm

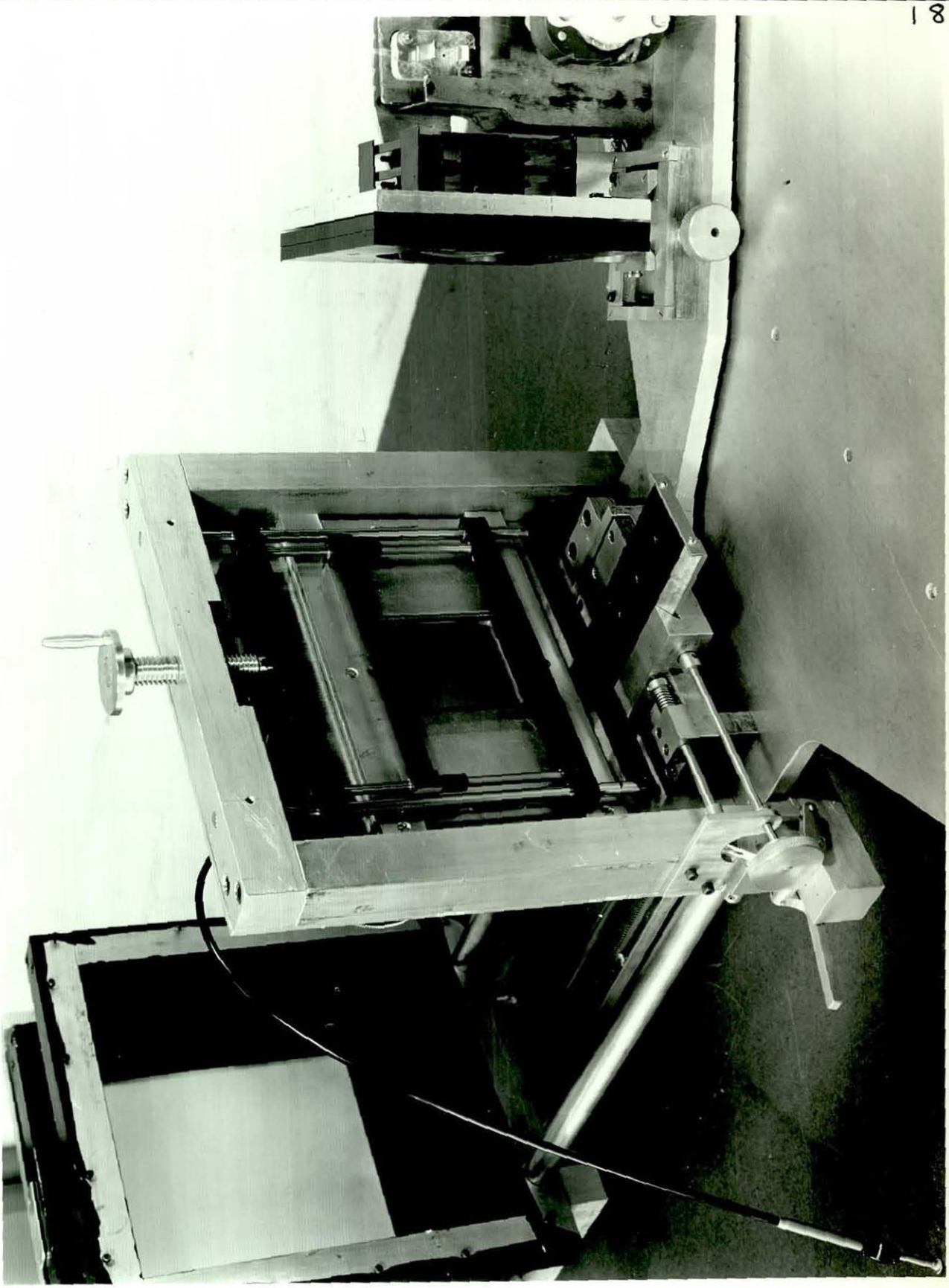

Fig. 6.20 Projector : Hologram mount and means of adjustment

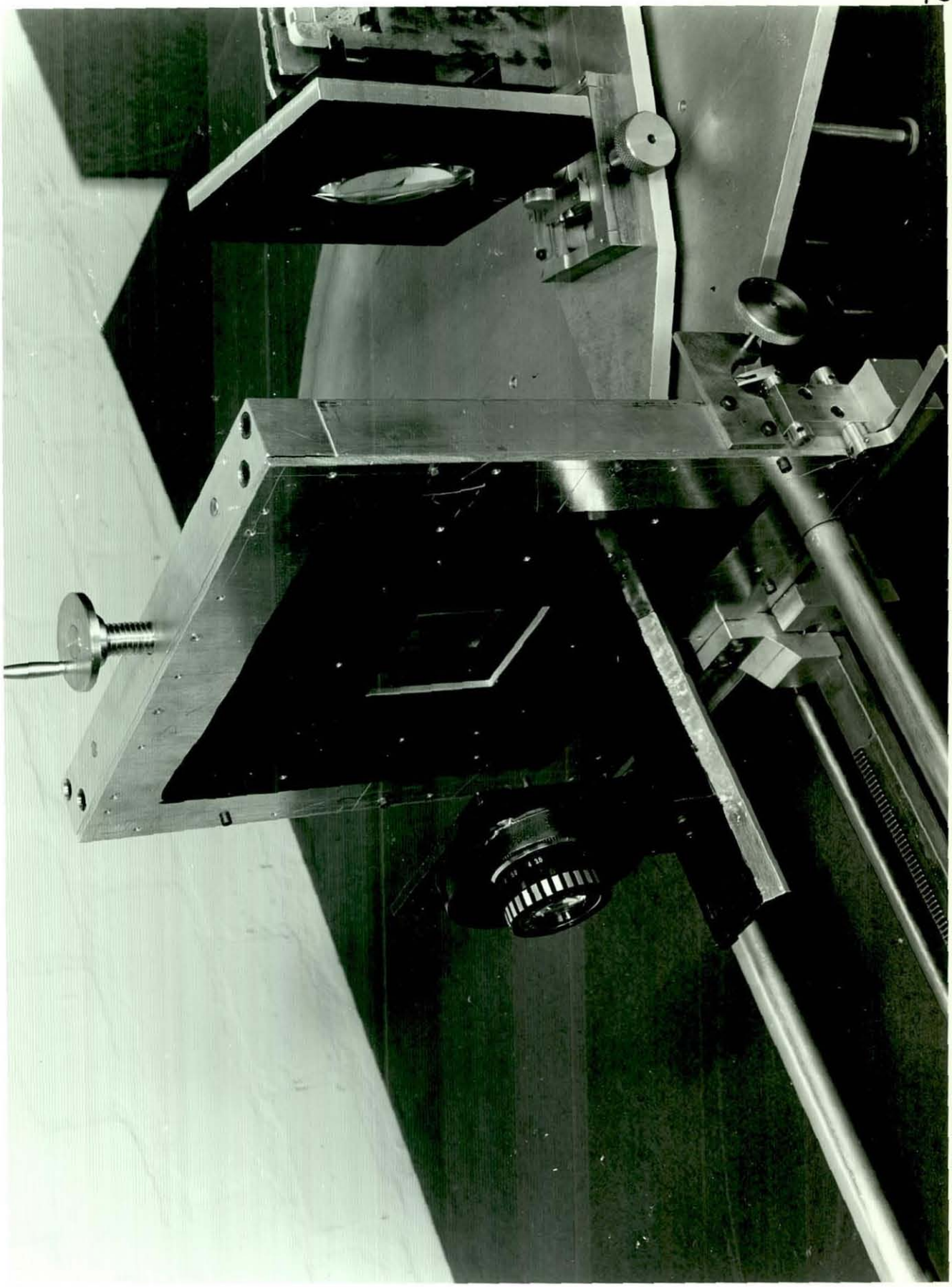

Fig. 6.21 Projector : Axially sliding mount for interchangeable lens

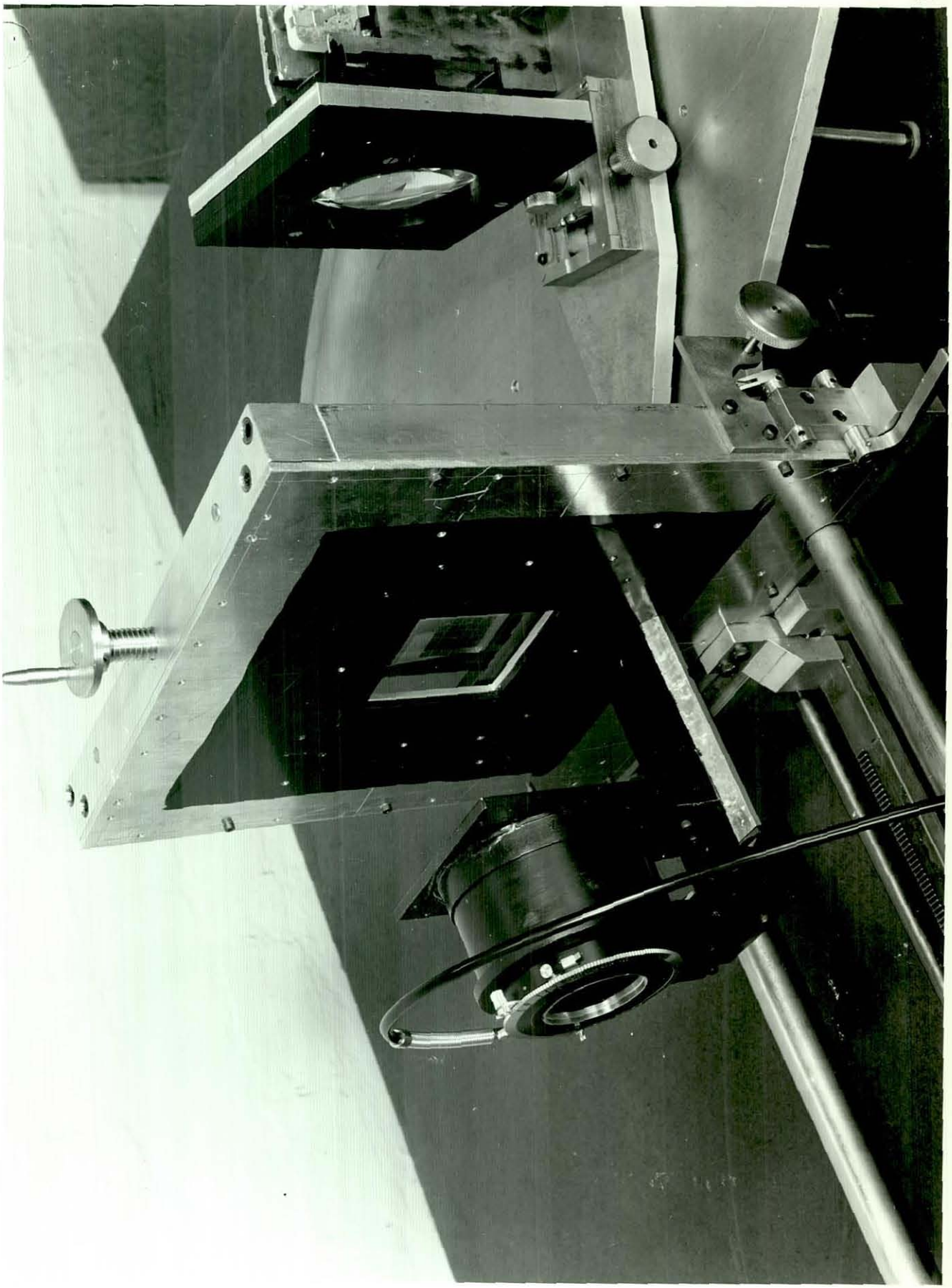

Fig. 6.22 Projector : Showing fitting of shutter up to the imaging lens

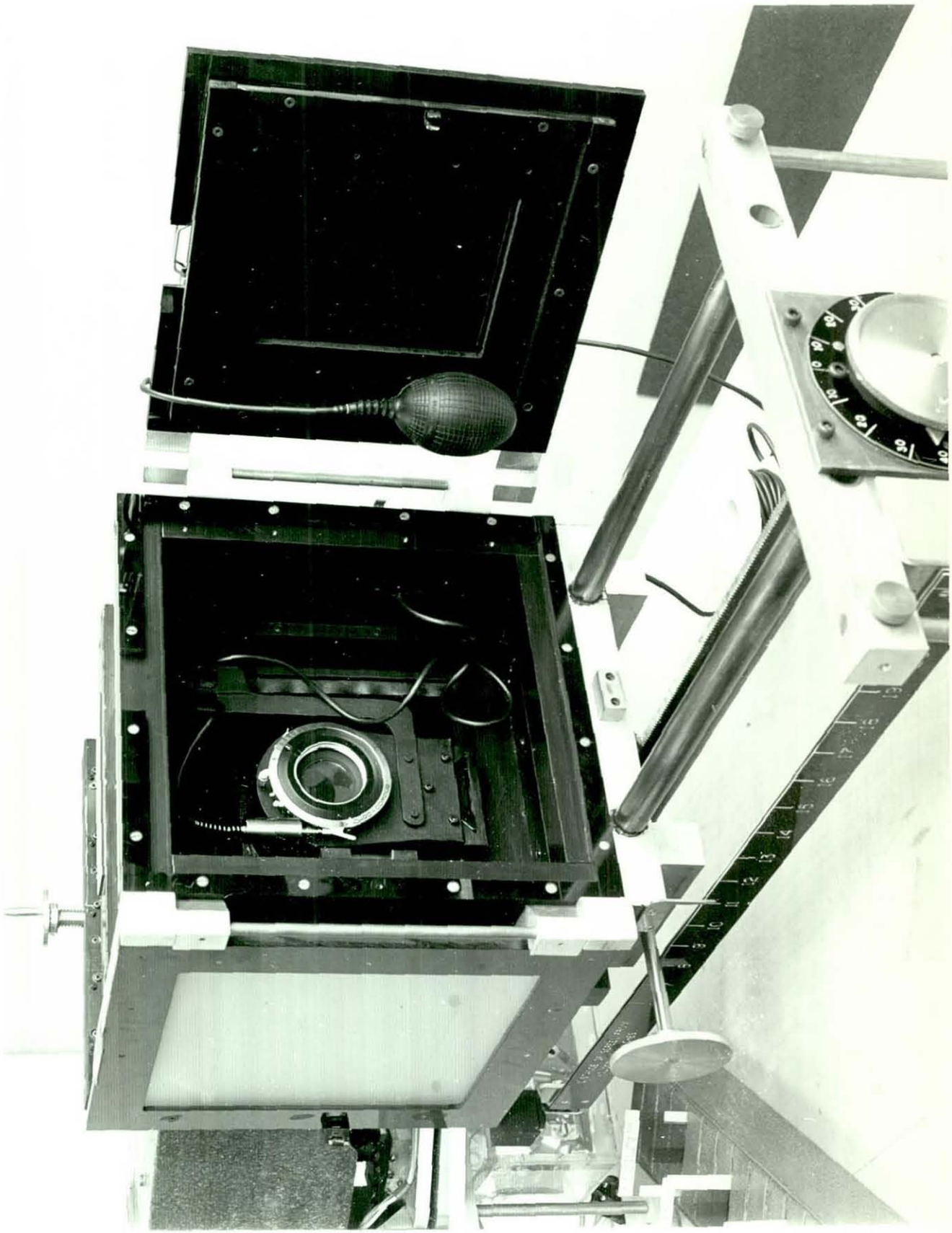

Fig. 6.23 Projector : Screen opened for access to shutter and lens

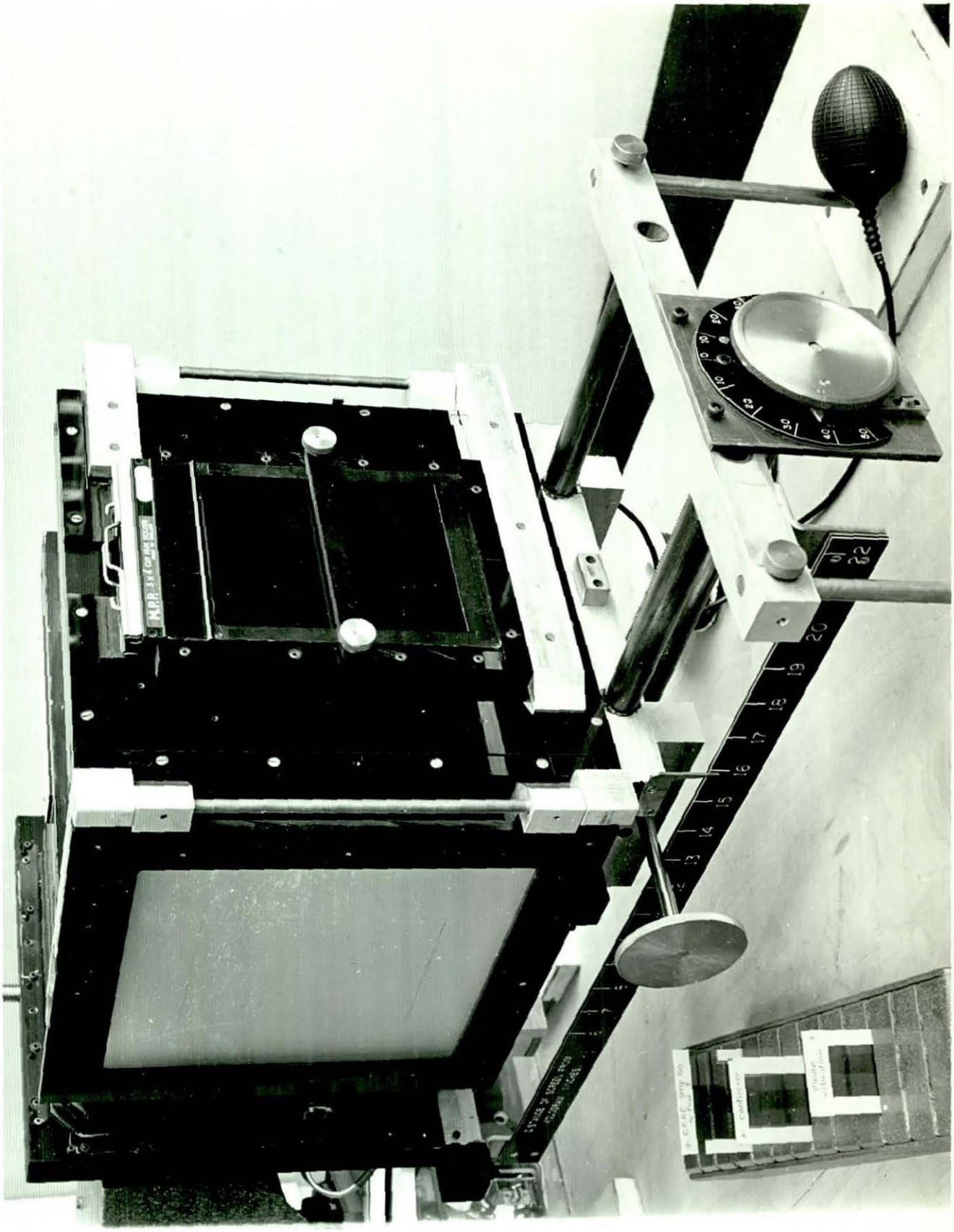

Fig. 6.24 Projector : Operation for photographic recording

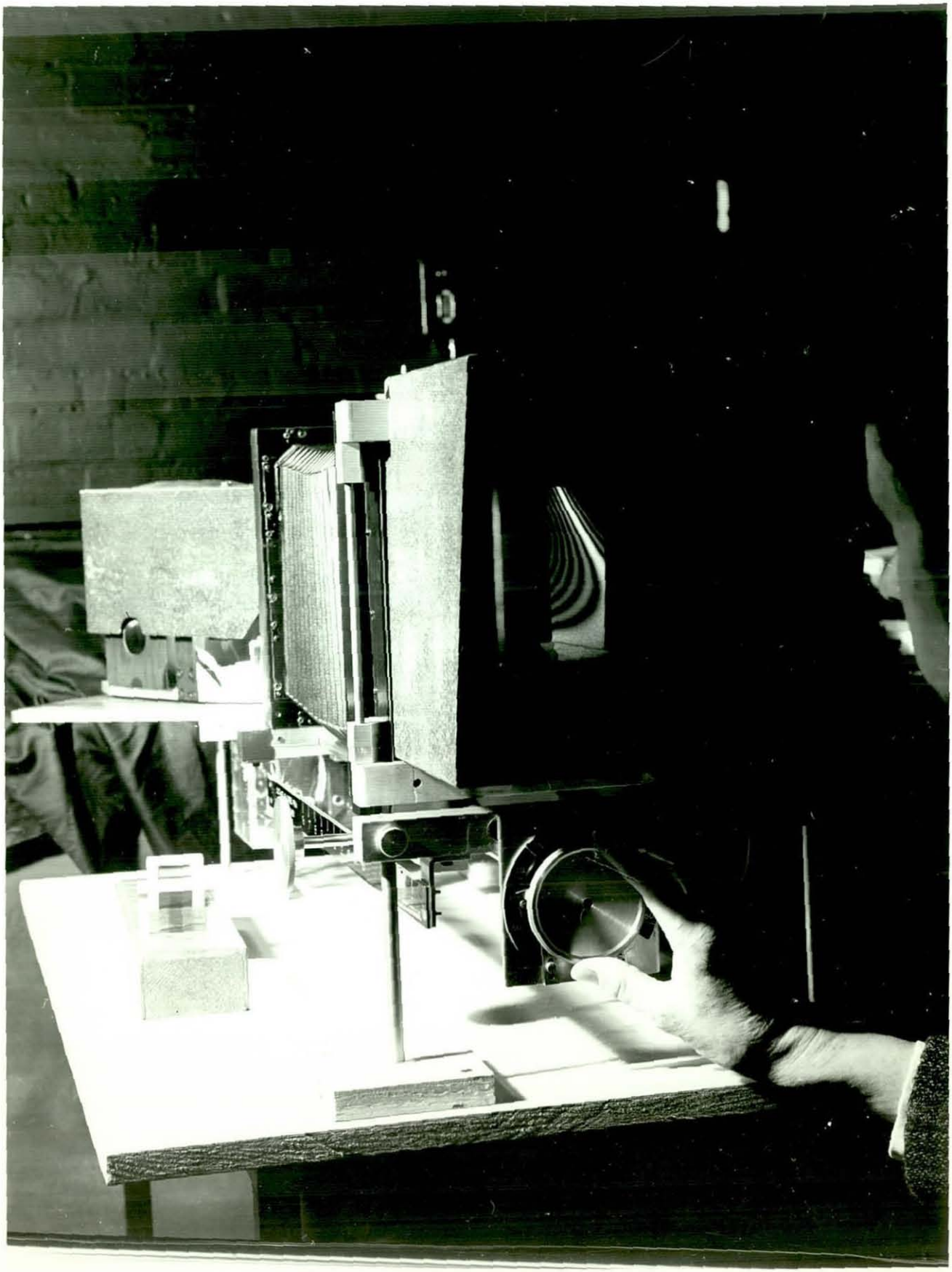

Fig. 6.25 The projector in use, with image on screen

Chapter 7

GENERAL CONCLUSIONS

When commencing this project, the potential benefits of applying holography to interferometric measurement had been demonstrated, but there were practical difficulties and problems of fringe interpretation. Accordingly the aims of this work were:

(i) to investigate fringe interpretation, and to assess accuracy and general feasibility, in relation to engineering measurements;

(ii) to develop apparatus and methods that would simplify procedures and analysis of results.

These have been fulfilled as follows.

Interpretation of holographic interferograms is conveniently divided into two categories: cases in which the direction of surface displacement is independently known, and cases in which it is not. The measurement of surface displacement is possible in both cases, but in the latter the procedure and analysis become relatively elaborate and laborious, and the results are liable to high error. In general, accuracy of measurement is limited by experimental error, (in determining optical path directions and fringe

order numbers), and by environmental effects, (notably temperature change), as in classical interferometry. Sources of error which cannot readily be assessed, including emulsion movement, were shown by experiment to be limited in effect to $\pm$ ¼ fringe in real time work. In a feasibility study of applying HI to an engineering problem, requiring the measurement of surface strain in an engine casing model, the quantitative analysis was slow and inaccurate. However, merits of HI to complement strain gauging, were established, namely, avoidance of surface contact and preparation, and provision of information over the full field of view.

As a consequence of these various investigations, HI is concluded to be more applicable to qualitative analysis, as in much non-destructive testing, and only simple cases of quantitative analysis. Measurement of displacement normal to a flat surface is generally classed as a simple case, whilst in-plane displacement and strain are not.

With regard to methods, double exposure HI producing frozen-fringe holograms is simpler to perform, though less versatile for analysis purposes, than real time HI. Simple methods and apparatus were developed for real time work, to enable good fringe visibility and freedom from initial spurious fringes to be achieved. These procedures are satisfactory in so far as photographic processing is an acceptable procedure.

FI holography is beneficial in HI because white light reconstruction is possible. This provides convenience in examining interferograms, directly from (frozen-fringe)

FI holograms, especially when viewed in the purpose-built projector. The method is most applicable for cases of relatively shallow objects which deform predominantly out of plane. The interpretation of interferograms is based on the same principles as in conventional HI. For future development, a standardized rig for recording FI holograms has been proposed, to be applied in routine testing of vibration modes or static deformations, with a simple form of projector for convenient direct analysis of results.

These various developments have provided improved performance, simplified procedures, and convenience in analysis. Above, appropriate areas for the application of HI have been identified, namely situations requiring qualitative analysis, and the simpler cases of quantitative analysis. Accordingly it is predicted that HI will be used industrially in the fields of non-destructive testing and inspection. Notable examples would be investigations of vibration characteristics, and the detection of imperfect bonds and other 'faults' in laminated materials, structures and components. These applications would allow routine operation, analysis and decision-making to be carried out by staff with only moderate experience in fringe interpretation. At the same time it is anticipated that HI will also contribute to engineering as a sophisticated laboratory technique of measurement, requiring expertise. It would fulfil a supplementary role to other methods of measurement and testing, for example, to supplement information given by photoelasticity and strain gauging in stress and strain analysis. In this role it would serve to solve particular problems and to aid design.

However, at present the application of HI is still restricted by the limitations of:-

(i) slow and inconvenient photographic procedures;

(ii) stability requirements at the recording stage;

(iii) manual analysis of interferograms.

It is concluded that these existing limitations will be overcome, and applications significantly extended, only by effort in the following areas;-

(i) Electronic speckle pattern interferometry (ESPI). Speckle pattern images incorporating a reference beam (or reference speckle pattern) to detect phase changes enable the same measurement operations performed by HI to be carried out. In addition, in-plane displacement can be directly measured from a single interferogram, which is not possible by HI. By means of electronic detection, processing and display, using CCTV equipment, real time interferograms are obtained with rapid 'processing' times, and with practical convenience and versatility, (BUTTERS and LEENDERTZ, 1972). At present, compared with HI, the electronic method requires relatively intense optical images at the detector, resolution in the displayed interferogram is low, parallax is lost, and geometrical errors occur in display. Thus, when these features are critical holography is preferred. Because of similarities between SPI and FI holography, the two methods could with advantage, be combined in one recording rig, especially for non-destructive testing applications. ESPI would be employed first, to rapidly investigate the general behaviour of the object and locate specific areas of interest, to be followed by frozen-fringe FI holograms providing high quality records for detailed analysis.

Other useful developments would be the incorporation of an electronic image intensifier to enable the laser power per unit area of object surface to be reduced, and improved resolution through the use of higher resolution camera tubes (and corresponding higher bandwidth video equipment.)

(ii) Holographic recording materials. A material that could be 'instantly' processed (within one second), and preferably repeatedly used, would certainly provide a breakthrough, in terms of speed, practicability and versatility. A recent survey by TUBBS (1973) indicated that none of the reversible materials under development yet possesses, in combination, the required sensitivity, resolution, and diffraction efficiency in reconstruction, for HI. However, a prototype thermoplastic/photoconductive material, electrically processed and erased, from GEC-Marconi Research laboratories (1973) virtually meets these requirements. If further improved performance is obtained, and forthcoming assessments of this material are favourable, it will be a significant development in holographic practice, and could compete with ESPI.

(iii) Pulsed ruby laser holography. Pulsed ruby laser systems for HI have the potential of overcoming stability problems (always encountered when photographically recording holograms using gas lasers), and of extending applications to dynamic events. HI investigations could then be undertaken in daylight on site, rather than in a darkened laboratory. The development of such lasers is progressing well, but the following proposed specification, as yet unattained, would represent a versatile laser:

a) Mode: TEMoo

b) Energy per pulse : up to 1 J;

c) Pulse duration : 30 ns;

d) Pulse separation : continuously variable from 20 μs to 10 s ;

e) Coherence length (single pulse): 2 m;

f) Change of wavelength between pulses : $\leq$ 0·01 angstrom;

g) Portability.

It is foreseen that modified methods and techniques of analysis would need to be applied when performing HI on site. For example, compensation of the reference beam path to allow for certain bodily movements of an object would be useful. One method, using a very small point of the object surface as the reference source, has been demonstrated for time-averaged steady state vibration (WATERS, 1972). Of course, pulsed laser HI using a new material as in (ii), or combined with ESPI, would be an even more powerful method. In the latter case, the separate recording of two speckle images separated in time by only a millisecond or less, for subsequent subtraction (as part of the ESPI process), could be a formidable problem.

(iv) Automatic fringe scanning and processing. An automatic scanner to determine fringe order numbers (including fractional numbers) at required positions in an interferogram, coupled to a programmed data processor, would be very valuable for quantitative analysis by HI. Not only would this relieve much laborious manual analysis, but could also improve the accuracy of measured displacements and strains. An instrument for scanning moire fringe patterns, using CCTV with electronic computation

of individual fringe separations, or of average fringe separation along a line, has been developed by DAVIES et al (1973). When multiplied by an appropriate scaling factor, the output values are of strain. This instrument could be applied in certain cases to fringe patterns obtained by HI and ESPI. However, considerable development would be needed to contend with the difficult fringe characteristics which can arise in these methods, namely: varying fringe localization, away from the image plane (does not arise in ESPI); varying fringe visibility; and intensity modulation due to speckle (especially in ESPI). Also the detection of a change in the direction of the fringe count would be a formidable problem, requiring electronic logic in addition to extra fringe information.

REFERENCES

ABRAMSON N., 1968, Strathclyde Symposium. *

ALEKSANDROV E.B. & BONCH-BRUEVICH A.M., 1967, Soviet Physics-Technical Physics, 12, 2, pp 258 - 265.

ALEKSOFF C.C.,1969, Applied Physics Letters, 14, 1, pp 23-4

ARCHBOLD E., BURCH J.M. & ENNOS A.E., 1967, Jnl. Phys.E. (Sci. Instruments), 44, pp 489-494.

ARCHBOLD E., & ENNOS A.E., 1968, Nature, 217, pp 942-3.

ARCHBOLD E., BURCH J.M. & ENNOS A.E., 1970, Optica-Acta, 17, 12, pp 883-898.

BARRELL H., 1959, Conference Proceedings "Interferometry" Symposium No. 11, N.P.L., H.M.S.O., 1960.

BARRELL H. & SEARS J.E., 1939, Phil. Trans. Royal Soc. London Series A, 238, 786, pp 1-64.

BEESLEY M.J., Part 3 of "Frequency Conversion 1" by THOMPSON J., TURK W.E. & BEESLEY M.J., 1969, Wykeham Publication Ltd.

BIEDERMANN K. & MOLIN N.E., 1970, Jnl. Phys. E (Sci. Instruments), Series 2, 3, pp 669-680.

BOLSTAD J.O., 1967, Applied Optics, 6, 1, p 170.

BOONE P.M., 1970, Optics Technology, 2, 2, pp 94-8.

BRANDT G.B., 1969, Applied Optics, 8, 7, pp 1421-9.

BROOKS R.E., HEFLINGER L.O. & WUERKER R.F., 1965, Applied Physics Letters, 7, 9, pp 248-9.

BURCH J.M., 1965, Production Engineer, 44, 9, pp 431-449.

BURCH J.M., ENNOS A.E. & WILTON R.J., 1966, Nature, 209, pp 1015-1016.

BURCH J.M., & ENNOS A.E., 1966, Jnl. Opt. Soc.Am., 56, 4.

BUTTERS J.N., 1968, Strathclyde Symposium *

BUTTERS J.N., DENBY D. & LEENDERTZ J.A., 1969, Jnl. Phys. E (Sci. Instruments) Series 2, 2, pp 116-117

BUTTERS J.N. & MIDDLETON T., 1970, Optics & Laser Techn. 2, pp 202-3.

BUTTERS J.N. & LEENDERTZ J.A., 1971, Jnl. Physics E (Sci. Instruments) Series 2, 4 pp 277-9

BUTTERS J.N. & LEENDERTZ J.A., 1972, Applied Optics, 11, 6, pp 1436-7.

CARCEL J.L., RODEMANN A.H., FLORMAN E & DOMESHEK S., 1966 Applied Optics, 5, 7, pp 1199-1201.

CHEN F.S., LaMACCHIA J.T. & FRASER D.B., 1968, Applied Physics Letters 13, 7, pp 223-5

COLLIER R.J., DOHERTY E.T. & PENNINGTON K.S. 1965, Applied Physics Letters, 7, 8, pp 223-5.

DAVIES D.J., EVANS W.A. & LUXMOORE A.R., for publication, (private communication with Luxmoore, 1973).

DENBY D., 1971, Optics and Laser Tech., 3, 4, pp 220-2.

DENBY D. & LEENDERTZ J.A., To be pub. 1974 (Jan), Jnl. Strain Analysis.

ENNOS A.E., 1968, Jnl. Phys.E. (Sci. Instruments), Series 2, 1, pp 731-4.

FOURNEY M.E., 1968, Experimental Mechanics, 8, pp 33-38.

FRIESEM A.A. & WALKER J.L., 1969, Applied Optics, 8, 7, pp 1504 - 1506.

GABOR D., 1948, Nature, 161, pp 777-8.

GEC-Marconi Research Labs. (1973), Information release at the 1973 Physics Exhibition, London.

GOTTENBERG W.G., 1968, Experimental Physics 8, 9, pp 405-410.

GRANT R.M., 1968, Developments by G C Optronics, Inc. in holographic interferometry testing apparatus during the mid 1960's, reported by GRANT at the Strathclyde Symposium, 1968.

HAINES K.A. & HILDEBRAND B.P., 1966A, Applied Optics, 5, 4, pp 595-602.

HAINES K.A. & HILDEBRAND B.P., 1966B, I E E E Transactions, I M-15, 4, pp 149-161.

HEFLINGER L.O., WUERKER R.F. & BROOKS R.E., 1966, Jnl. App. Phys., 37, 2, pp 642-649.

HILDEBRAND B.P. & HAINES K.A., 1967, Jnl. Opt. Soc. Am., 57, 2, pp 155-162.

HILDEBRAND B.P., HAINES K.A. & LARKIN R., 1967, Applied Optics, 6, 7, pp 1267-69.

HOCKLEY B.S., 1969, M. Tech.Thesis, L.U.T., "A holographic method of analysis of compressor, turbine blades and discs."

HORMAN M.H., 1965, Applied Optics, 4, 3, pp 333-336.

HUME K.J., "Engineering Metrology," 3rd Edition, Chap. 2, 1970, Macdonalds technical and scientific.

JENKINS F.A. & WHITE H.E., "Fundamentals of Optics," 3rd. Edition, Chapter 12, 1957, McGraw Hill.

KLIMENKO I.S., MATINYAN E.G. & RUKMAN G.I., 1967 J E T P Letters, 6, 3, pp 57-8.

KLIMENKO I.S., MATINYAN E.G. & RUKMAN G.I. 1970, Optics and Spectroscopy, 29, 1, pp 85-88.

LEENDERTZ J.A., 1970, Jnl. Phys.E. (Sci. Instruments) Series 2, 3, pp 214-8.

LEITH E.N. & UPATNIEKS J., 1962, Jnl. Opt. Soc. Am. 52, 10, pp 1123-1130.

LEITH E.N. & UPATNIEKS J., 1963, Jnl. Opt. Soc. Am., 53 12, pp 1377-1381.

LEITH E.N. & UPATNIEKS J., 1964, Jnl. Opt. Soc. Am., 54, 11, pp 1295-1301.

LIN L.H. & LOBIANCO C.V., 1967, Applied Optics, 6, 7, pp 1255-1258.

LIN L.H. 1969, Applied Optics, 8, 5, pp 963-966.

LURIE M. & ZAMBUTO M., 1968, Applied Optics, 7, 11, pp 2323-5.

MEIER R.W., 1965, Jnl. Opt. Soc. Am., 55, 8, pp 987-992.

MEZRICH R.S., 1969, Applied Physics Letters, 14, 4, pp 132 - 134.

NEUMANN D.B., 1966, Jnl. Opt. Soc. Am., 56, 7, pp 858-861.

NISHIDA N., 1968, Applied Optics, 7, 9, pp 1862-1863.

POWELL R.L. & STETSON K.A., 1965, Jnl. Opt. Soc. Am., 55, 12, pp 1593-1598.

REID C.D. & WALL M.R., 1965, Reference made by Burch J.M., 1965, Production Engineer, 44, 9, pp 431-449.

ROGERS G.L., 1950, Nature, 166, pp 237.

ROGERS G.L., 1952, Proc. Royal Soc. Edinburgh, 63A Part iii (1950-1951) pp 193-221.

ROGERS G.L.? 1966, Jnl. Phys.E. (Sci. Instruments), 43, pp 677 - 684.

SHAJENKO P. & JOHNSON C.D., 1968, Applied Physics, 13, 1, pp 44 - 46.

SMITH H.M., "Principles of Holography", p 157, 1969, Wiley-Interscience.

SOLLID J.E., 1969, Applied Optics, 8, 8, pp 1587-1595.

STETSON K.A. & POWELL R.L., 1965, Jnl. Opt. Soc. Am., 55, 12, pp 1694-1695.

STETSON K.A. & POWELL R.L.? 1966, Jnl. Opt. Soc. Am., 56, 9, pp 1161-6.

STROKE G.W., 1966, Physics Letters, 23, 5, pp 325-7.

TSURUTA T. & SHIOTAKE N., 1967, Japanese Jnl. of App. Phys., 6, pp 661-662.

TUBBS M.R., BEESLEY M.J. & FOSTER H., 1969, Brit. Jnl. App. Phys., Series 2, 2, pp 197-200.

TUBBS M.R., 1973, Optics and Laser Technology, 5, 4, pp 155 - 161.

VIÉNOT J.-CH., 1968, Strathclyde Symposium *

VILKOMERSON D.H.R. & BOSTWICK D., 1967, Applied Optics, 6, 7, pp 1270 - 1272.

WATERS J.P., 1972, Applied Optics, 11, 3, pp 630-6.

WATRASIEWICZ B.M. & SPICER P., 1968, Nature, 217, pp 1142-3.

WELLS D.R., 1969, Materials Evaluation, 27, 11, pp 225-231.

WOLFE R. & DOHERTY E.T., 1966, Jnl. App. Phys., 37, 13, pp 5008 - 9.

WUERKER R.F., 1968, Strathclyde Symposium. *

YAMAGUCHI I, & SAITO H., 1969, Japanese Jnl. App. Phys., 8, 6, pp 768 - 771.

ZELENKA J.S. & VARNER J.R., 1968, Applied Optics, 7, 10, pp 2107 - 2110.

* Published proceedings of Symposium held at the University of Strathclyde, September 1968 :- "The Engineering Uses of Holography", Ed, by Robertson & Harvey, Cambridge University Press, 1970.

Appendix I

SPECIFICATIONS OF EQUIPMENT AND MATERIALS

(i) Lasers The following lasers were used :-

(a) Scientifica and Cook Electronics Ltd., model B18/3.

Type : Helium - neon, continuous wave.

Wavelength : 632·8 nm

Power output : 8 mW approx.

Polarization : linear

Beam diameter : Approximately 2 mm at exit aperture

Tube excitation : hot cathode d.c.

(b) Spectra - Physics Inc., Models 120 and 124 A.

	120 model	124A model
Type	: Helium-neon	Helium-neon
Wavelength	: 632·8 nm	632·8 nm
Power output	: > 5 mW	> 15mW
Transverse mode:	TEM_{oo}	TEM_{oo}
Polarization	: linear to better than 1 part in 1000	
Beam diameter at $1/e^2$ points:	0·65 mm	1·1 mm
Beam divergence at $1/e^2$ points:	1·7 millirad	1 millirad
Tube excitation:	d.c.	

(ii) Photographic emulsions. The following emulsions (on glass plate) were used for recording holograms :-

	Kodak 649 F	Kodak V1043 D	Agfa 8E70	Agfa 10E70
Emulsion thickness produced (μm)	15	7	7	7
Maximum Resolution ,(line pairs/ mm)	>2,000	about 2,000	3,000	2,800
Exposure energy at 632·8 nm ($\mu J/cm^2$)	80-100	40-50	20	5

These data are taken from Kodak and Agfa data sheets. Plates were obtained in sizes of 5 x 4 in and 12 x 9 cm, plate thicknesses of 1 mm (Kodak), and 1·2 - 1·4 mm (Agfa).

Appendix II

GLOSSARY OF TERMS.

In these early years of holography, common terms have not yet been defined and officially accepted, and consequently inconsistencies and confusion of meaning arise. Below is a list of such terms with the author's interpretation of meaning, (referring only to optical holography). In writing this thesis an effort has been made to use accurate terminology. For example wavefronts are "reconstructed", but images, objects and holograms are not.

HOLOGRAPHY A two-step method of imagery in which both amplitude and phase characteristics of wavefronts are recorded, for subsequent reconstruction. These characteristics are preserved by interference with a reference and the physical record of this interference pattern is the HOLOGRAM.

REFERENCE BEAM A beam (usually having a smooth wavefront shape for easy reproduction) incident at the recording plane, firstly for recording a hologram, and subsequently for performing reconstruction.

SIGNAL BEAM Wavefronts from the object to be recorded, incident at the recording plane.

BEAM RATIO Ratio of the intensities of the reference beam to the signal beam, measured at the recording plane.

DESIGN ANGLE The average angle between the directions of the reference and signal beams incident at the recording plane.

COHERENCE LENGTH The difference in path lengths in an interferometer for which the fringe visibility is only just discernible or tolerable.

HOLOGRAPHIC INTERFEROMETRY (HI) Interference of wavefronts, at least one of which is reconstructed from a hologram.

LIVE FRINGES Fringes by HI between a real time wavefront and a reconstructed wavefront.

FROZEN FRINGES Fringes by HI between two (or more) reconstructed wavefronts (usually obtained from a "double exposure hologram").

TIME AVERAGED HOLOGRAM A hologram recorded while the object vibrates with steady amplitude and frequency.

FOCUSED IMAGE HOLOGRAM A hologram of an aerial image of an object, recorded by focusing this image upon the recording material.

Appendix III

PUBLICATIONS

List of publications, solely or jointly by the author, arising from work presented in this thesis, or carried out subsequently :-

'A method for reducing movement in holographic emulsions', Jnl. of Physics E, 1969, Series 2, Vol.2, pp. 116-7 (Jointly with J.N.Butters and J.A.Leendertz). *

'Some practical uses of laser-beam photography in engineering', Jnl. of Photographic Science, 1970, Vol. 78, No.2, pp. 60-67 (Jointly with J.N.Butters).

'Holography as an engineering tool', New Scientist, Feb. 1970, pp. 394-6, (Jointly with J.N.Butters).

'Coherent optics : a new tool in engineering measurement', Physics Bulletin, 1971, Vol. 22, No.7, pp. 393-6, (Jointly with J.N.Butters, P.A.C.Doble, J. A. Leendertz).

'A holographic interferometer comparable with an in-line reference field laser speckle interferometer', Optics and Laser Technology, Vol.3, November 1971, pp. 220-2. *

'Plane surface strain examination by speckle pattern interferometry using electronic processing', To be published January 1974 in Jnl. of Strain Analysis, (Jointly with J.A.Leendertz).

* Reprints are bound in, over page.

Journal of Scientific Instruments (Journal of Physics E)
1969 Series 2 Volume 2

A method for reducing movement in holographic emulsions

J N Butters, D Denby and J A Leendertz
Department of Mechanical Engineering, Loughborough University of Technology
MS *received 27 September 1968*

Abstract Holographically reconstructed wavefronts can be degraded by small local movements of the recording emulsion, during processing. A method of substantially reducing this movement, by releasing strain in the emulsion prior to exposure, is described, together with a simple experimental arrangement to detect the movement. This method is useful in real-time hologram interferometry, to give smoother fringe patterns which can be more easily and accurately interpreted.

In the method of hologram interferometry (Haines and Hildebrand 1966, Aleksandrov and Bonch-Bruevich 1967) the photographic plate is exposed, processed and replaced in its original position to permit comparison between the original and the deformed wavefronts from the object. It has been our experience that small movements of the emulsions, during processing, degrade the fringe patterns obtained.

A simple experimental arrangement which detects this movement clearly is shown in figure 1. A and B are two

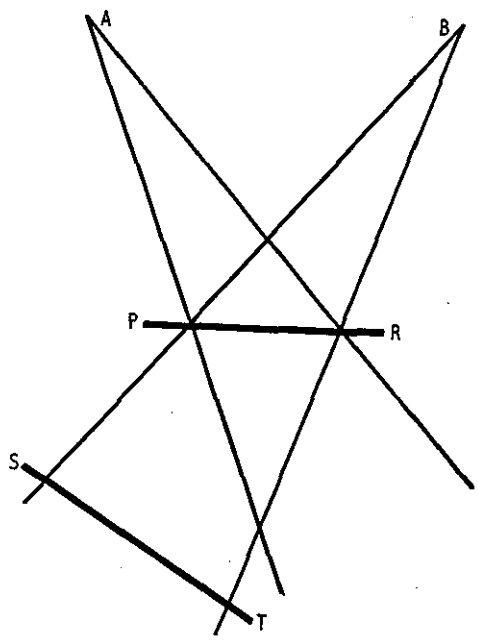

Figure 1 Experimental arrangement to detect emulsion movement

coherent sources obtained from a helium–neon laser, PR is the high resolution photographic plate under investigation and ST is a screen. The plate is exposed to and records the fine interference pattern produced by the sources A and B; after processing it is returned to its original position. The screen then receives light transmitted directly through the plate from B together with light diffracted from A; the latter is the reconstructed wavefront from B. Ideally, the intensities from these two wavefronts would add uniformly across the screen. However, in practice, the emulsion distorts due to

processing (Stevens 1968). Consequently, local distortions occur in the recorded grating spacing of the emulsion, and the reconstructed wavefront suffers local variations in the diffraction angle. This causes interference between the two wavefronts behind the plate. In addition, inexact relocation of the plate after processing contributes further interference.

By using a Kodak 649 F plate in its received condition, and then processed as recommended, the typical fringe pattern shown in figure 2(*a*) was obtained at the screen. The large scale fringes are due to inexact relocation of the plate, while the small scale irregularities are caused by emulsion movement, especially movement in the plane of the emulsion.

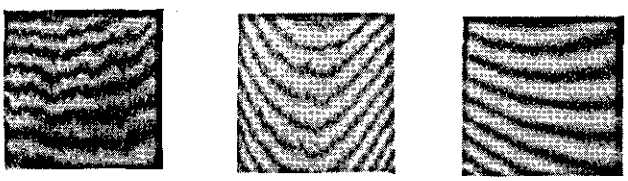

(*a*) (*b*) (*c*)

Figure 2 Fringes obtained at the screen of figure 1

It was considered that this movement could in part be due to the release during processing of production-induced strains 'frozen' in the emulsion. To test this idea, a plate was suspended overnight over a dish of water and allowed to dry for some six hours before exposure. By use of the same arrangement as before, the fringes thus obtained are shown in figure 2(*b*). It is seen that a useful improvement has been obtained. Taking this idea further, a plate from the same batch as the other two was soaked in water for two minutes and dried by washing in industrial methylated spirits and allowed to stand for some ten minutes before exposure. After processing in the usual way the plate was again dried by washing in methylated spirits and draining for ten minutes. Figure 2(*c*) shows the fringes thus obtained. It will be seen that the movement has been greatly reduced in comparison with figure 2(*a*). The use of methylated spirits does not appear to have any adverse effects on the emulsion and it saves considerable drying time.

Figures 3(*a*) and (*b*) show photographs of real-time fringes over an extended object, namely a cantilever strip. In fact, the holograms of this object were recorded on the same plates as were used to produce figures 2(*a*) and (*c*), in order to relate the emulsion distortion fringes to those obtained by hologram interferometry. Again, there is a considerable improvement in the smoothness of the fringes obtained from the treated plate.

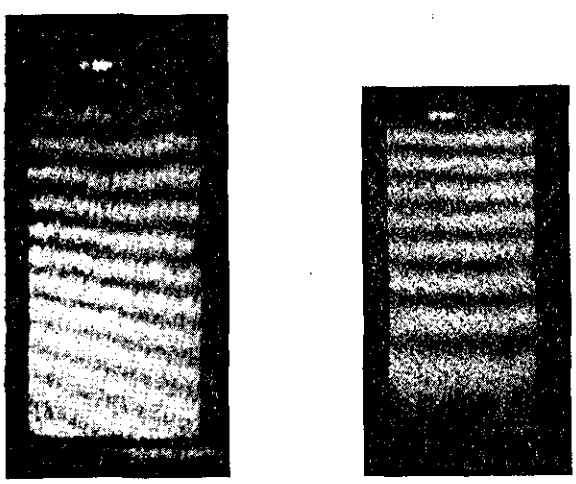

(*a*) (*b*)

Figure 3 Fringes obtained by hologram interferometry

Until now, inexact relocation of the plate and emulsion movement have had the undesired effect in real-time hologram interferometry of producing a coarse fringe pattern, when viewing the object. This problem has been overcome by combining the technique described above with the proposed method of processing the plate *in situ* (Bolstad 1967). A stainless-steel frame with Perspex screws held the plate firmly, the whole being suspended rigidly from an overhead frame. The pre-exposure wash treatment and normal processing were performed by raising beakers so as to submerge the plate in the appropriate solutions. This time the object was a brass plate, 2 in square, silver-spray coated to increase the scattered reflection. So well did the reconstructed wavefront match that from the undisturbed object that not a single fringe was produced over the object. The superposition of the image increased the apparent brightness of the object uniformly all over.

This method is useful in real-time interferometry because the fringe pattern caused by object displacement can be analysed directly; previously, it was necessary to subtract the initial coarse fringe pattern from the observed pattern. In the above case, the interferometer was effectively more sensitive to very slight disturbances than in previous instances, because there was no initial fringe pattern to mask the small variation in intensity. Moreover, by reducing emulsion movement the fringes were very smooth; thus more accurate quantitative analysis is possible.

The pre-exposure strain-relief technique should also be relevant to the application of point holograms for optical elements (Schwar, Pandya and Weinberg 1967). Provided that high quality optical components are used to make such holograms, correspondingly high quality wavefronts should be reconstructed. If emulsion movement occurs, however, these wavefronts will be degraded.

References

Aleksandrov E B and Bonch-Bruevich A M 1967 *Soviet Physics – Technical Physics* **12** 258–65

Bolstad J O 1967 *Appl. Opt.* **6** 170

Haines K A and Hildebrand B P 1966 *Appl. Opt.* **5** 595–602

Schwar M J R Pandya T P and Weinberg F J 1967 *Nature* **215** 239–41

Stevens G W W 1968 *Microphotography* (London: Chapman and Hall) pp. 83–4

A holographic interferometer comparable with an in-line reference field laser speckle interferometer

D. DENBY
Department of Mechanical Engineering, University of Technology, Loughborough, Leicestershire, UK

This article describes the principle of a holographic interferometer, presents experimental results, and draws comparisons with the speckle interferometer of similar optical arrangement.

Over the last two years, various forms of laser speckle interferometer have been devised.[1,2] An improved design for directly observing vibrational modes on a diffusely reflecting surface has recently been reported.[3] Its optical system has a small aperture to form an easily visible speckle pattern, and superimposes a uniform coherent reference field in line with the imaging axis. Vibration of the object is detected by disappearance of the speckle pattern in the vibrating regions, while it remains strong in contrast in the nodal regions. The optical arrangement of this speckle interferometer resembles that of a special form of holographic interferometer that was devised to provide more convenient viewing of holographic interferograms.

It is based on the technique of focused image holography which offers the advantage over normal holography of forming a clear image by reconstruction using a white light source. The purpose in this case was to reduce blur in the image of a deep object, as occurs by white light reconstruction. This article describes the principle of this holographic interferometer, presents experimental results, and draws comparisons with the speckle interferometer of similar optical arrangement.

The feature distinguishing the recording of a focused image hologram from normal off-axis holograms is the use of an imaging lens to image the object surface at the hologram plane. Subsequent reconstruction by white light forms a clear image because the image is in (or close to) the plane where diffraction takes place. A limitation occurs when recording a deep object of which some parts are imaged appreciably out of the hologram plane. White light reconstruction causes these parts to be blurred, image points in different colours being spatially separated, as with normal off-axis holography. In the case where the imaging axis is normal to the hologram plane, and the reference beam is inclined at an angle α to this axis, the amount of lateral blur x of image points at a distance z from the hologram plane due to a wavelength spread $\delta\lambda$ is given to a good approximation by

$$x = z \sin\alpha \, \delta\lambda/\lambda$$

where λ is the recording wavelength. This expression is obtained by treating the hologram as a simple diffraction grating. Thus, blur can be reduced by making α smaller when recording the hologram till in the limit α is zero.

Practical demonstration

In order to demonstrate this reduction of blur, a focused image hologram was made with the reference beam brought in line with the image rays, by means of a prism beam splitter, as sketched in Fig. 1. Strictly, the reference beam was in line with only one out of a range of image ray directions since the imaging lens subtended a cone of rays

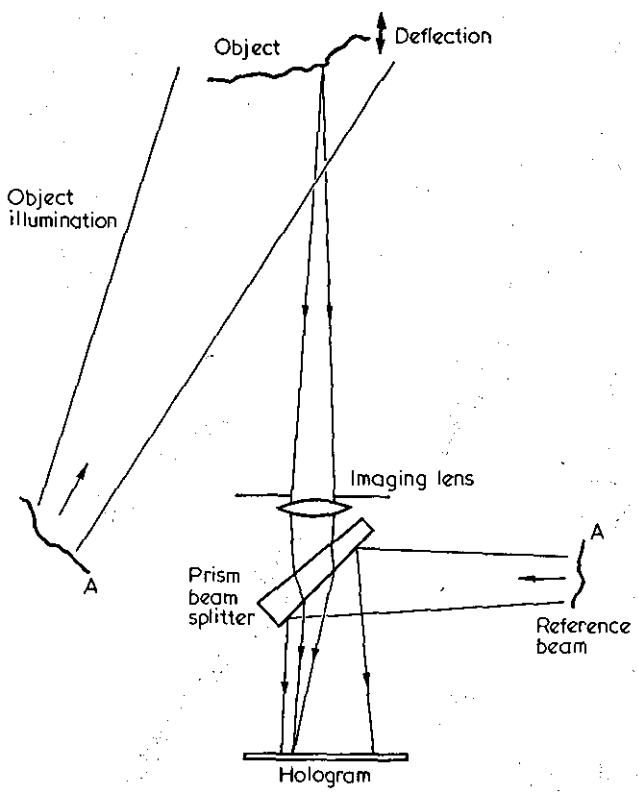

Fig.1 Arrangement for recording an in-line reference beam focused image hologram. Beams 'A' are from the same laser source.

to each image point. The object was a 20-mm wide cantilever with a diffusely reflecting surface, deflected between exposures to produce characteristic 'frozen fringes'. A photographic enlarging lens of 75-mm focal length imaged the surface at the hologram plane, the iris opened to f/3.5 to give a bright image with finely speckled structure. Other parts of the object, including the base clamp and the structure for loading the cantilever, were also imaged forming an overall image depth of 30 mm straddling the hologram plane. Magnification was roughly unity. The reference beam was divergent, from a lens pinhole unit spaced a little over a metre from the hologram plane. A weak prism superimposed the beam in line with the image forming rays, without any overlap at the hologram between the front and rear surface reflections. The intensities of the reference beam and the image were made equal and the double exposure hologram recorded on AGFA 10E70 plate using a 15-mW He-Ne laser.

The processed hologram reveals interesting properties. For reconstruction, a penlight torch is convenient, illuminating the hologram from a distance of about 2/3 metre. Looking at the hologram back along the illumination direction the cantilever image is seen to light up, by diffraction, together with an interferogram representing the cantilever deflection. The orientation of the hologram to the reconstructing source is not critical compared with normal (off-axis) holography. Despite an image depth of 30 mm, straddling the hologram, all parts of the image appear sharp, viewing by eye at the near point of distinct vision. Parallax is evident though to a limited extent predetermined by the aperture of the recording lens. Images are formed, by reconstruction, of the recording lens aperture, one being virtual (the primary image) and the other being real (the conjugate). For the image of the cantilever to be seen at all (by reconstruction), the eye must be positioned within the real image of the lens, or its projection. Turning the hologram round causes the primary image of the lens to become real. Either way round the entire cantilever image can be seen from a single viewing position. (Commonly with off-axis focused image holograms there is a problem in seeing the *entire* image from a single viewing position. Keeping the reconstructing beam divergent, and without using additional optics the only way can be back-projection of the reconstructing beam). The colour dispersion by diffraction from the hologram is so slight that the cantilever image is seen (directly by eye) as a uniform grey. However, if the viewing position is moved off axis, the extremities of the image tend to behave as an off-axis focused image hologram and appear coloured, predominantly red or blue.

A photograph of the cantilever image is shown in Fig. 2. Of course, only one plane is in focus, and the sharpness of image throughout its depth is not demonstrated. The feature of interest concerns the fringes representing the cantilever deflection. It is seen that fringe contrast is good high up the cantilever but decreases towards the base. This is due to the position of the reconstructing source, being in line with the second fringe up from the base. In this region of the image, a considerable amount of scattered light is seen, effectively reducing fringe contrast. When taking the photograph, direct light from the reconstructing source was eliminated by a small stop at its focused image. This filtering would also be appropriate if viewing the image projected on to a diffusing screen.

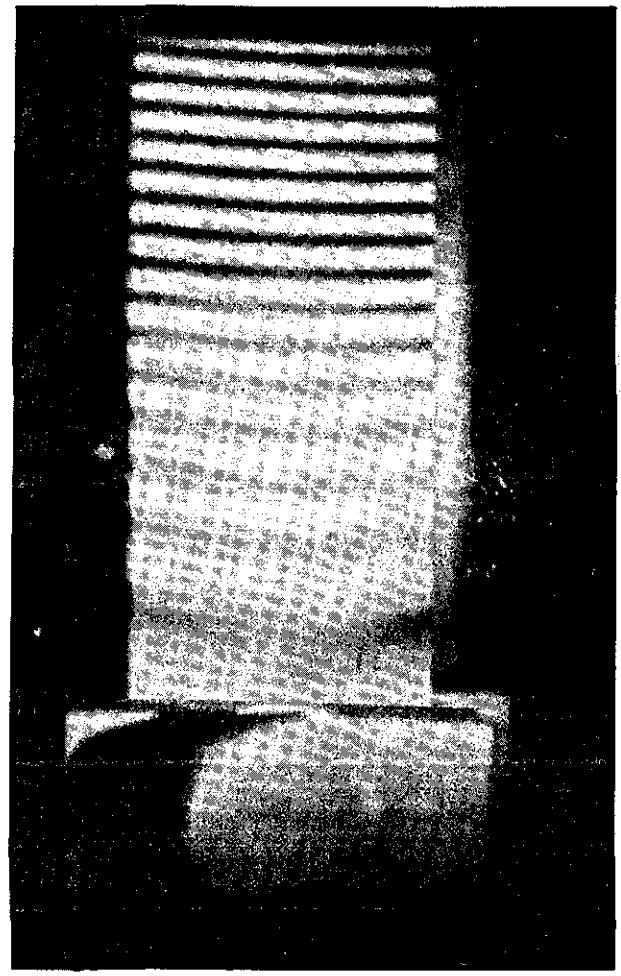

Fig. 2 Interferogram of a deflected cantilever, by in-line reference beam focused image holography.

Comparison of holographic and speckle methods

The described holographic interferometer is an extension of focussed image holography which in interferometry is used primarily for the convenience of examining interferograms by white light reconstruction directly from the hologram. In fact, this form of hologram can be viewed simply by the light of a desk lamp, though the full potential of the technique is realised by projecting the image on to a diffusing screen. A large aperture for the recording lens is used to produce a bright image of finely speckled structure, and to allow appreciable parallax and recognised depth in the image. For the speckle interferometer, the significant difference in the optical arrangement is a much smaller imaging aperture producing a coarsely speckled image. This allows displacements and particularly vibration of the object surface to be observed live, by changes in the speckle pattern, (and without a recording stage). The information content of the image has a low spatial frequency within the resolution capability of a television system, so that for example vibrational modes can be displayed instantaneously on a monitor.[5] Further the use of a small aperture makes component replacement and long term stability much less critical than in holography.

However, the image in a speckle interferometer is not sharp and depth is lost because there is virtually no parallax. Another consequence of a coarsely speckled image is much poorer fringe contrast than obtained with holographic interferograms, though effort is being made to improve

this by electronic processing. For vibration visualisation, the lack of fringe contrast severely limits the amplitude of vibration that can be detected, unless special beam modulation techniques[3] are used. By straight forward holography vibrational fringe order numbers beyond the 100th have been demonstrated.[4] For the speckle interferometer, a uniform reference field is important but is considerably less so in holography since reconstruction operates in spite of the typical dust diffraction patterns recorded on the hologram.

Acknowledgement

I wish to acknowledge helpful discussions with Mr J.A. Leendertz and Mr M.R. Wall.

References

1 Archbold, E., Burch, J.M., Ennos, A.E., Taylor, P.A. (1969) Visual Observation of Surface Vibration Nodal Patterns. Nature. **222**. 263-5.

2 Leendertz, J.A. (1970) Interferometric displacement measurement on scattering surfaces utilising speckle effect. Phys. E: Sci. Instrum. 3. 214-8.

3 Stetson, K.A. (1970) New design for laser image-speckle interferometer. Opt. and Laser Technol. **2** (4). 179-181.

4 Wall, M.R. (1969) Recording high-order holographic vibration fringes. Opt. Technol. 1. 260-270.

5 Butters, J.N. and Leendertz, J.A. (1971) Speckle pattern and holographic techniques in engineering metrology. Opt. Laser Technol. 3. 26-30.